Mathematics of Planet Earth 2

Michael Y. Li

An Introduction to Mathematical Modeling of Infectious Diseases

Springer

Mathematics of Planet Earth

Volume 2

Springer's Mathematics of Planet Earth series provides a variety of well-written books of a variety of levels and styles, highlighting the fundamental role played by mathematics in a huge range of planetary contexts on a global scale. Climate, ecology, sustainability, public health, diseases and epidemics, management of resources and risk analysis are important elements. The mathematical sciences play a key role in these and many other processes relevant to Planet Earth, both as a fundamental discipline and as a key component of cross-disciplinary research. This creates the need, both in education and research, for books that are introductory to and abreast of these developments.

More information about this series at http://www.springer.com/series/13771

Michael Y. Li

An Introduction to Mathematical Modeling of Infectious Diseases

Springer

Michael Y. Li
Mathematical and Statistical Sciences
University of Alberta
Edmonton, AB
Canada

Mathematics of Planet Earth
ISBN 978-3-319-72121-7 ISBN 978-3-319-72122-4 (eBook)
https://doi.org/10.1007/978-3-319-72122-4

Library of Congress Control Number: 2017960197

Mathematics Subject Classification (2010): 34D05, 34D20, 34D23, 92D25, 92D30

Printed on acid-free paper

This Springer imprint is published by Springer Nature
The registered company is Springer International Publishing AG
The registered company address is: Gewerbestrasse 11, 6330 Cham, Switzerland

Preface

Mathematical modeling has been increasingly recognized in the public health community as an important research tool for infectious diseases control. Mathematical models are widely used for evaluating the effectiveness of control strategies for TB, HIV, Influenza, West Nile virus, and the emerging Zika virus, for cost-effect analysis of vaccination programs, and for controlling hospital-acquired infections. Students with modeling skills are finding rewarding careers in public health services and private health industry.

This book is intended to provide its reader with essential modeling skills and methodology for the study of infectious diseases through a one-semester modeling course or directed individual studies. The book is primarily written for upper undergraduate and beginning graduate students in mathematical sciences who have an interest in mathematical modeling of infectious diseases. Mathematical theories and techniques are explained in the context of epidemic models without a sacrifice of mathematical rigor. The basic prerequisites are advanced Calculus and an understanding of matrix theory. Beginning students can learn advanced theory of differential equations in the concrete setting of model analysis. Students who have taken courses in advanced differential equations will be able to see how abstract theories are applied to real-world problems. Materials in the book are also accessible to public health science students with analytical skills. Several graduate students in public health sciences have participated in the

author's modeling courses and went on to write MSc and PhD theses using modeling as the main research tool.

This book has grown from a set of lecture notes the author has been using for a disease modeling course at the University of Alberta. The course was taught in the second semester of the academic year to prepare students for their research on modeling projects during the summer. Each student was given a disease modeling project to work on during the course. Students were required to submit a proposal for their projects by the midterm and complete a written project report at the end of the semester, which comprised the main part of the assessment. Each student also gave a 20-minute oral presentation about the project. Exercises in the book provided students with opportunities to practice modeling skills they learned during the course. Students from public health or biological sciences were each paired with a mathematics student to collaborate on a project for cooperative learning. The highlight of the course has always been the term projects, through which students were able to synthesize the knowledge they gain in the course. In many occasions, term projects were further expanded into a full-fledged MSc thesis or formed the foundation of a PhD dissertation.

The book starts with an introductory chapter (Chapter 1) on the basic process of setting up an epidemic model using differential equations. The chapter contains in-depth discussions of key concepts in infectious disease epidemiology such as the basic reproduction number, incidence rates, latency, immunity, demography, route of transmission, heterogeneity, vaccination, and quarantine. Mathematical descriptions of these key concepts are given and used as building blocks for ever more complex epidemic models. This chapter provides a soft entry into modeling for public health science students and an introductory encounter with infectious disease epidemiology for mathematics students.

Chapter 2 focuses on model analysis with the intention to introduce students to standard mathematical approaches and important mathematical concepts such as stability, bifurcation, and threshold phenomenon, all explained in the context of epidemic models. The author has carefully selected five classic epidemic models to demonstrate five important mathematical approaches

to model analysis: first integrals and level curves, phase-line analysis, phase-plane analysis, reduction of dimension using homogeneity, and monotone dynamical systems.

Chapter 3 contains the abstract theory of differential equations that is used in model analysis in Chapter 2. It provides a rigorous theoretical reference for important concepts and mathematical results used in Chapter 2. It is recommended that the materials in this chapter are explained when they are used in the corresponding sections of Chapter 2.

Chapter 4 deals with the issue of confronting models with data and nonlinear least-squares methods for parameter estimation from data. A detailed presentation of the linear least-squares method and the Gauss–Newton method for nonlinear least squares is given and demonstrated with examples. For practical applications in epidemic models, algorithms for nonlinear least-squares estimation using Matlab routines are described. Matlab codes are included to help students start to use them for their projects.

Chapter 5 provides some special topic for further reading and can be used as additional teaching materials at the instructor's discretion. The first section is a higher dimensional SEIR model with its full analysis. Materials in this section help to reinforce that techniques for the analysis of simple models in Chapter 2 are also equally useful for complex models. The second section covers an in-host model for the viral dynamics of the infection of Human T-cell Lymphotropic Virus Type I (HTLV-I) of $CD4^+$ T cells. Through discussions in this section, students will learn that modeling skills for epidemic models at the population level can be applied to model disease processes at a microbic level. An interesting phenomenon called "backward bifurcation" is introduced in this simple in-host model.

On a personal note, I would like to thank all the students who have participated in my disease modeling course during the past 10 years at the University of Alberta, whose enthusiasm has been the inspiration for writing this book. A special mention is given to my graduate students Hongbin Guo, Rebecca De Boer, Michael Akinwumi, Betsy Varughese, Zhimin Su, Alison Muscat, Kim Simmons, Lordlin Owusu, Weston Roda, Jeanette Amissah,

and Frank Lee, whose feedbacks really helped with the development of materials in the book. Many of these students are working as modelers in public health services and private sectors. A special thanks to Rebecca De Boer and Weston Roda for their assistance with Matlab codes and for teaching Matlab tutorials in my modeling classes.

I want to express my deep gratitude to my family for their unwavering support of my work, especially to my wife Audrey for her constant encouragement, and to my daughter Jessica for proof reading the manuscripts. I wish to thank many of my mentors, James Muldowney, Paul Waltman, Fred Brauer, Pauline van den Driessche, and Gail Wolkowicz, for their guidance and support for my research.

A special thanks to Donna Chernyk of Springer for all her work and help during the publication process of the book.

Michael Y. Li
Edmonton, Alberta
October 15, 2017

Contents

Chapter 1

Important Concepts in Mathematical Modeling of Infectious Diseases

1.1 Mathematical Modeling of Infectious Diseases: Issues and Approaches

A disease is *infectious* if the causative agent, whether a virus, bacterium, protozoa, or toxin, can be passed from one host to another through modes of transmission such as direct physical contact, airborne droplets, water or food, disease vectors, or mother to newborn.

The objective of a mathematical model of an infectious disease is to describe the *transmission process* of the disease, which can be defined generally as follows: when infectious individuals are introduced into a population of susceptibles, the disease is passed to other individuals through its modes of transmission thus spreading in the population. An infected individual may remain asymptomatic at the early stage of infection, only later developing clinical symptoms and being diagnosed as a *disease case*. If the number of cases rises above the usual average within a short period of time, a *disease outbreak* occurs. When the disease spreads quickly to many people, it is an *epidemic*. Infected individuals recover from infection, either through treatment or due to the action of the immune system, and gain various degrees of acquired immunity against reinfection. When the pool of susceptible individuals is sufficiently depleted, new infections will cease

M. Y. Li, *An Introduction to Mathematical Modeling of Infectious Diseases*, Mathematics of Planet Earth 2,
https://doi.org/10.1007/978-3-319-72122-4_1

and the epidemic slows down and stops. If fresh susceptibles are added to the population, either from birth or migration, or if reinfection occurs easily, the epidemic may persist and the infection may remain in the population over a long period of time. In this case, the disease is said to be *endemic* in the population. If the disease spreads spatially on a global scale to many countries and continents, a *pandemic* occurs. The 1918 Spanish flu that spread to all continents and killed over 50 million people is a classic example of a global pandemic. With modern air travel, many emerging and reemerging infectious diseases have an increasing potential to cause a global pandemic.

Facing an imminent epidemic, public health authorities will be looking for answers to the following important questions:

(1) How severe will the epidemic be? The severity can be measured in two different ways:
   (a) Total number of infected people who may require medical care.
   (b) Maximum number of infected people at any given time.
(2) How long will it last? When will it peak? What will be its time course?
(3) How effective will quarantine or vaccination be?
(4) What quantity of vaccine or anti-viral drugs should be stockpiled?
(5) What are effective measures to contain, control, and eradicate an endemic disease?

Partial answers may be obtained using a variety of approaches. Mathematical modeling has proven to be an important tool in assisting public health authorities to make informed decisions.

This brings us to the obvious question: why is mathematical modeling of infectious diseases useful? Part of the answer is that traditional methods using experimental and statistical approaches may not be adequate for various reasons:

(1) Infectious diseases often affect a large population of individuals over a large geographic area. Experiments conducted in laboratories are often inadequate simply because of the huge difference in scale.
(2) For infectious diseases in humans, large-scale experiments may be impossible or unethical.
(3) Existing data sets about the disease may not be complete or accurate enough for the statistical analysis to be reliable. For instance, there will be little or no disease surveillance data available on infected people who are asymptomatic.
(4) Since repeated experiments of disease outbreaks in a population are rarely possible, disease surveillance data often represents a single outbreak (sample) with a large amount of information. Statistical analysis of high-dimensional data from small samples is a challenge since statistics theory relies on large samples.

Mathematical modeling can provide an understanding of the underlying mechanisms of disease transmission and spread, help to pinpoint key factors in the disease transmission process, suggest effective control and preventive measures, and provide an estimate for the severity and potential scale of the epidemic. Put it simply, mathematical modeling should become part of the toolbox of public health research and decision-making.

The next question we would like to answer is: what is the general process of mathematical modeling? Generally speaking, the modeling process involves the following six stages:

(1) Make assumptions about the disease transmission process based on the best available biological knowledge on the pathogenesis of the infection and epidemiology of the disease.
(2) Set up mathematical models for the transmission process based on these assumptions. This usually starts from drawing the transfer diagram and then deriving the mathematical equations.
(3) Perform mathematical analysis on the model to understand all possible qualitatively distinct model outcomes. This is

typically done by applying existing mathematical theories on stability and bifurcations in conjunction with numerical simulations.

(4) Interpret the mathematical findings within the modeling context. These interpretations form our understanding of the disease transmission process entailed by the set of assumptions made in Step (1).

(5) Collect available disease data from public health agencies and from research publications. Validate the model using data.

(6) Improve the model by modifying the earlier assumptions in Step (1), and produce a more accurate understanding of the disease process.

It is important to keep in mind that a mathematical model is an approximation of the real disease process. It is a mathematical translation of our hypotheses about disease transmission. Another important role for mathematical models is hypothesis testing: by comparing the model outcomes with existing knowledge or data of the disease, we can use the model to test various hypotheses about the disease. Compared to experimental approaches, the modeling approach has the advantage of saving enormous amounts of time and resources.

We should caution that a mathematical model is not a magic bullet. There are often many difficulties associated with mathematical modeling. The following is a list of important issues involved in the mathematical modeling process:

(1) Due to our limited knowledge about an infectious disease, realistic assumptions about its transmission process are not always possible. Various degrees of simplification need to be made. Very often, our assumptions are simply hypotheses. When interpreting findings from the model, we always need to keep these limitations in mind.

(2) Model validation using disease data is important because it provides a test of our modeling hypotheses. This may not always be possible or may be difficult to do depending on the availability and quality of data.

(3) Mathematical analysis of the model may be limited by existing mathematical theory.

There is always a trade-off in mathematical modeling between more realistic and therefore more complex models and our ability to analyze the model mathematically and obtain useful information for interpretation. Advancement in mathematical theory and methodology often allows us to successfully use more realistic models. When using mathematical models to analyze or interpret disease data, it is not always true that a more realistic model will do better. Part of the reason is that more realistic models incorporate a greater degree of biological complexity and hence introduce more model parameters. With the same dataset, it may be more difficult to estimate all the parameter values for a more complex model compared to a simpler model. The result might be a greater degree of uncertainty in model outcomes.

There are three general approaches to mathematical modeling of infectious diseases:

(1) Statistical models. These models are very data oriented and are constructed to deal with a specific set of data.

- Advantages: statistical models are widely used in epidemiology and public health research.
- Drawbacks: statistical models require large samples of data.

(2) Deterministic models. These are typically models using differential and difference equations of various forms. The key assumption is that the sizes of the susceptible and infectious populations are continuous functions of time. The models describe the dynamic interrelations among the rates of change and population sizes.

- Advantages: mathematical theories for this type of model are more mature in comparison to stochastic models; the derivation of mathematical models are less data dependent in comparison to statistical models; and mathematical models are suited for making predictions.

- Drawbacks: these models are not expected to be valid if the population sizes are very small, in which case stochastic disturbances become non-negligible.

(3) Stochastic models. In this type of model, disease infection is treated as a stochastic process. The models describe dynamic interrelations of its probability distributions.

- Advantages: stochastic models are suitable to deal with small population groups such as a small community or a single hospital, or where a few infected individuals are highly active and have a high number of infectious contacts.
- Drawbacks: mathematical analysis of stochastic models is difficult due to a lack of mathematical machinery; model analysis largely relies on observations from a huge number of numerical simulations.

This book is an introduction to deterministic models of infectious diseases, their mathematical analysis, and model calibration from disease data.

1.2 Deterministic Epidemic Models: Compartmental Approach

In this section, we explain how to set up a mathematical model for the transmission process of an infectious disease using a compartmental approach. We first partition the host population into mutually exclusive groups – compartments – according to the natural history of the disease. For a simple infectious disease, possible compartments may be:

S : susceptible hosts, I : infectious hosts, R : recovered hosts.

Then, we illustrate the transmission process schematically in a carton, called a *transfer diagram*, shown in Figure 1.1. In the transfer diagram, the arrows indicate movements of individuals among

compartments. The term "removal" includes loss of individuals through death or out-migration.

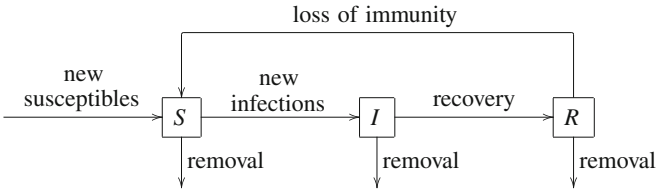

Figure 1.1: Transfer diagram for an SIR compartment model.

The goal of modeling is to track the number of hosts in each of the three compartments at any given time t, and we denote these numbers by $S(t), I(t)$, and $R(t)$ accordingly. To set up the compartmental model, we consider a small time interval $[t, t + \Delta t]$ and the net change in the number of individuals in each compartment. In the transfer diagram, the arrows indicate the direction of individual movement. The net change of the number of hosts in a compartment is the number coming into the compartment minus the number leaving the compartment during the time interval. Applying this principle to each compartment, we arrive at the following equations:

$$\begin{aligned}
\Delta S(t) &= \boxed{\text{new susceptibles}} + \boxed{\text{transfer from } R} - \boxed{\text{new infections}} \\
&\quad - \boxed{\text{removal from } S} \\
\Delta I(t) &= \boxed{\text{new infections}} - \boxed{\text{transfer into } R} - \boxed{\text{removal from } I} \\
\Delta R(t) &= \boxed{\text{transfer from } I} - \boxed{\text{transfer into } S} - \boxed{\text{removal from } R}.
\end{aligned} \tag{1.1}$$

If we divide both sides of these equations by Δt and let $\Delta t \to 0$, then the left-hand side will be the derivatives $S'(t), I'(t)$, and $R'(t)$, since

$$\frac{\Delta S(t)}{\Delta t} = \frac{S(t + \Delta t) - S(t)}{\Delta t} \to S'(t), \quad \text{as } \Delta t \to 0,$$

and similar relations hold for $I'(t)$ and $R'(t)$. The terms on the right-hand side will become instantaneous rates of incidence,

recovery, and removal. We thus have the following differential equations:

$$\begin{aligned} S'(t) &= \boxed{\text{influx of new susceptibles}} + \boxed{\text{transfer rate from } R} - \boxed{\text{incidence rate}} \\ &\quad - \boxed{\text{removal rate from } S} \\ I'(t) &= \boxed{\text{incidence rate}} - \boxed{\text{transfer rate into } R} - \boxed{\text{removal rate from } I} \\ R'(t) &= \boxed{\text{transfer rate from } I} - \boxed{\text{transfer rate into } S} - \boxed{\text{removal rate from } R}. \end{aligned} \tag{1.2}$$

If we express all the terms on the right-hand side as functions of $S(t), I(t)$, and $R(t)$, we will obtain a system of differential equations for $S(t), I(t)$, and $R(t)$, which will form our mathematical model. It is important to note that how these terms are expressed as functions of $S(t), I(t)$, and $R(t)$ is based on our hypotheses regarding the biological processes of disease transmission and population transfer among compartments. Therefore, different hypotheses will give rise to different forms of the model, and may lead to different model outcomes. If data is available to verify our model outcomes, then the model can be used to test the validity of our hypotheses about the disease transmission process. In the next section, we will see how basic hypotheses can be made in order to derive one of the classic epidemic models.

1.3 An Example: Kermack–McKendrick Model

To demonstrate how various rates in equation (1.2) may depend on $S(t), I(t)$, and $R(t)$, we make the following hypotheses about the transmission process of an infectious disease and its host population:

(1) Transmission occurs horizontally through direct contact between hosts.
(2) Mixing of individual hosts is homogeneous and thus the *Law of Mass Action* holds: the number of contacts between hosts from different compartments depends only on the number

of hosts in each compartment. In particular, the *incidence rate* – number of new infections per unit time – can be expressed as $\lambda I(t)S(t)$, where λ is called the *transmission coefficient*.

(3) Rate of transfer from a compartment is proportional to the population size of the compartment. For instance, the rate of transfer from I to R, the *recovery rate*, can be written as $\gamma I(t)$, for some rate constant γ.

(4) Infected individuals become infectious upon infection with no latency period.

(5) There is no loss of immunity and no possibility of reinfection. This implies that the transfer rate from R back to S is zero.

(6) There is no input of new susceptibles and no removal from any compartments. The influx of new susceptibles is zero, and so are the removal rates from all compartments.

(7) The total host population remains a constant. This is a direct result of the previous assumption, but we state it here explicitly to emphasize the fact. The dynamics of epidemic models can be more complicated if the total population varies with time.

Although they may appear very restrictive, these assumptions are quite plausible for a disease spread within the student population on a campus, where mixing occurs mainly in classes, cafeterias, libraries, and other public places. Based on these assumptions, the transfer diagram for a conceptual model shown in Figure 1.1 can be translated into an explicit model as shown in Figure 1.2.

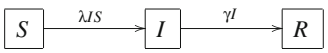

Figure 1.2: Transfer diagram for an simple SIR model.

Substituting all terms in (1.2) by our mathematical descriptions, we obtain the following system of differential equations:

$$\frac{dS}{dt} = -\lambda IS \tag{1.3}$$

$$\frac{dI}{dt} = \lambda IS - \gamma I \tag{1.4}$$

$$\frac{dR}{dt} = \gamma I, \tag{1.5}$$

with initial conditions

$$S(0) = S_0 > 0, \quad I(0) = I_0 > 0, \quad R(0) = 0.$$

In the model, functions $S(t), I(t)$, and $R(t)$ are *variables*. Since they denote the number of people, they are expected to take nonnegative values. Constants λ and γ are model *parameters*, and they are assumed to be nonnegative since they denote rate constants. If the values of model parameters λ and γ are known, then for each set of initial conditions S_0 and I_0, model (1.3)–(1.5) has a unique solution $(S(t), I(t), R(t))$ that produces a prediction for the time course of the epidemic for $t > 0$. Here $t = 0$ marks the beginning of the epidemic.

Even when the values of parameters are not known, some simple observations about the solutions to system (1.3)–(1.5) can be made that hold for all or a large set of possible parameter values.

1. Let $N(t) = S(t) + I(t) + R(t)$ denote the total host population. Then, by adding equations (1.3)–(1.5), we have

   $$\frac{dN}{dt} = 0,$$

   and thus the total population $N(t) = N_0 = S_0 + I_0$ remains a constant.
2. From equation (1.3) we obtain

   $$\frac{dS}{dt} \leq 0.$$

   Therefore, $S(t)$ is always decreasing. In particular, $S(t) \leq S_0$.

3. Rewrite equation (1.4) as

$$\frac{dI}{dt} = (\lambda S - \gamma)I.$$

Then, we have the following two cases:

(1) If $S_0 < \frac{\gamma}{\lambda}$, then $\frac{dI}{dt}\Big|_{t=0} < 0$. Since $S(t) \leq S_0 < \frac{\gamma}{\lambda}$, we know $I'(t) < 0$ for all $t \geq 0$, and thus $I(t)$ strictly decreases. As a result, no epidemics can occur in this case.

(2) If $S_0 > \frac{\gamma}{\lambda}$, then $S(t) > \frac{\gamma}{\lambda}$ for $t \in [0, \bar{t})$ for some $\bar{t} > 0$. This implies $I'(t) > 0$ and thus $I(t)$ strictly increases for $t \in [0, \bar{t})$. As a result, an epidemic happens.

This demonstrates the well-known *threshold phenomenon*: there is a threshold value $\frac{\gamma}{\lambda}$, which S_0 must exceed for an epidemic to occur. This threshold value is often called the *critical community size* for an epidemic.

We see that it is possible to derive properties of solutions without knowing specific values of model parameters. Our analysis can identify parameter regions for distinct model outcomes. This is the power and often the objective of mathematical analysis. We will revisit this model in greater detail in the next chapter.

1.4 Important Concepts in Compartmental Epidemic Models

In this section, we discuss some important epidemiological concepts used in compartmental modeling, demonstrate how to describe them in mathematical terms, and explore the assumptions used for deriving a specific mathematical term, such as the disease incidence $\lambda I(t)S(t)$ introduced in the previous section. Through these discussions, students in mathematics can learn how mathematical terms in a model correspond to epidemiological concepts, and students in public health sciences can learn how mathematics is used to quantify epidemiological concepts.

An understanding of the assumptions behind the mathematical terms in the model can help students consider alternative ways to describe them and learn how to generalize a model.

1.4.1 Transfer Rates

For the simple Kermack–McKendrick model described in the previous section, we assumed that the recovery rate, or the rate of transfer from compartment I to R, is given by γI. This is equivalent to assuming the following:

(**H**) the fraction of the infectious population that recovers per unit time is a constant γ.

Proportional transfer rates as assumed in (**H**) are often used for transfers between compartments in simple compartmental models. However, we need to understand that this is only one of the many assumptions we can make about population transfers. In fact, our assumption that recovery rate is in proportion to the size of the infectious population is by no means universal. In the following, we develop a better mathematical understanding of the proportional transfer rate and consider other possible alternatives.

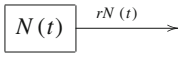

Figure 1.3: A compartment C.

Consider a general compartment C of total population size $N(t)$, where individuals leave the compartment at a rate $rN(t)$ $(r > 0)$. Then the size $N(t)$ satisfies

$$\frac{dN(t)}{dt} = -rN(t), \qquad r > 0,$$

and thus $N(t) = N_0 e^{-rt}$, or

$$\frac{N(t)}{N_0} = e^{-rt}. \tag{1.6}$$

Therefore, e^{-rt} gives the fraction of the population that remains in the compartment C. In probability terms, e^{-rt} is the probabil-

ity of an individual entering C at time $t = 0$ and remaining in C at time $t > 0$. Since we are interested in the population transfer out of C, we consider

$$F(t) = \begin{cases} 1 - e^{-rt}, & t \geq 0, \\ 0, & t < 0, \end{cases} \tag{1.7}$$

which gives the fraction of the population that has left C during the time period $[0, t)$, or the probability of an individual who has left C during $[0, t)$. Here we see that $F(t)$ has the characteristics of a probability distribution. In fact, if we let X denote the random variable of the *residence time* of an individual in compartment C, i.e., the time period from entrance to exit, we see that

$$F(t) = \text{Prob}\,[\,X \leq t\,]. \tag{1.8}$$

In other words, $F(t)$ is the *probability distribution function* of the individual residence time in C, and it satisfies the standard properties of a probability distribution function:

(1) $F(t) \geq 0$

(2) $F(t) \to 0$, as $t \to -\infty$

(3) $F(t) \to 1$, as $t \to +\infty$.

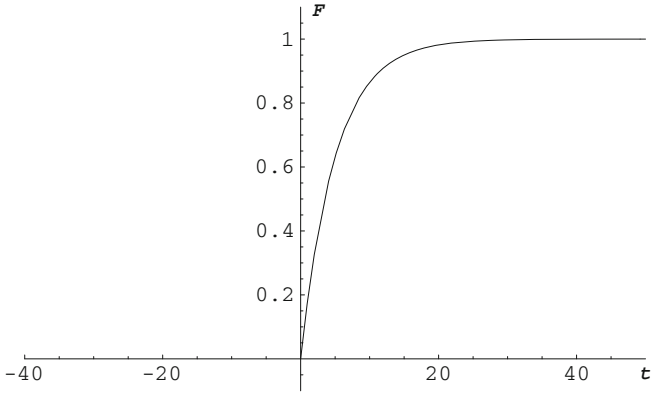

Figure 1.4: A probability distribution function.

Now we see that the assumption of proportional exit rate is the same as the following:

(**H′**) the residence time of an individual in compartment C has an exponential distribution.

We can also describe the random variable X in terms of the probability density function $f(t) = \frac{d}{dt}F(t)$, namely:

$$f(t) = \begin{cases} re^{-rt}, & t \geq 0, \\ 0, & t < 0, \end{cases} \tag{1.9}$$

which has the following properties:

(1) $f(t) \geq 0$

(2) $\int_{-\infty}^{\infty} f(t)dt = 1$

(3) $F(t) = \text{Prob}\,[\,X \leq t\,] = \int_{-\infty}^{t} f(s)ds.$

An example of a probability density function with an exponential distribution is shown in Figure 1.5. The probability density $f(t)$ gives the proportion of individuals with residence time t. We see from the graph of $f(t)$ in Figure 1.5 that a larger proportion of individuals have a small residence time and hence exit the compartment shortly after entry, while a smaller proportion of individuals exit after a longer time. This is the hallmark of the exponential distribution.

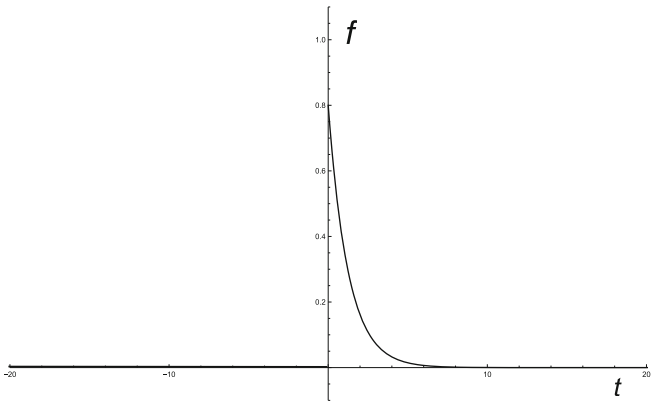

Figure 1.5: A probability density function.

The expected value, also called the *mean value*, of X is

$$E[X] = \int_{-\infty}^{\infty} tf(t)dt = \frac{1}{r}. \tag{1.10}$$

Therefore, the mean residence time, under the proportional exit rate assumption, is $\frac{1}{r}$.

For transfers from compartment I to R, the residence time is the period between time of infection and time of recovery, which is the *infectious period*. The following transfer diagram:

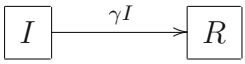

is equivalent to assuming that the infectious period of individuals has an exponential distribution

$$F(t) = \begin{cases} 1 - e^{-\gamma t}, & t \geq 0, \\ 0, & t < 0, \end{cases}$$

and $\frac{1}{\gamma}$ is the mean infectious period. Similarly, in the transfer diagram

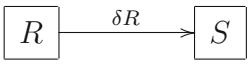

the residence time is the *immune period* – the period recovered individuals are protected from reinfection – and proportionate rate δR assumes that the immune periods of individuals have an exponential distribution

$$F_1(t) = \begin{cases} 1 - e^{-\delta t}, & t \geq 0, \\ 0, & t < 0, \end{cases}$$

and the mean immune period is $\frac{1}{\delta}$.

A natural question is: how do we derive the model equations if individual infectious periods have a general probability distribution function $F(t)$?

We will revisit the SIR model (1.3)–(1.5) with this general assumption. We see that the change in assumption for the infectious period does not impact the S equation (1.3). We need to re-derive equations for $I(t)$ and $R(t)$ based on this new assumption. Let the residence time X have the probability distribution function $F(t) = \text{Prob}[X \leq t]$ as defined in (1.8). We consider the associated *survival function*

$$G(t) = 1 - F(t) = \text{Prob}[X > t].$$

For any given time $\tau > 0$, $G(t - \tau)$ is the fraction of individuals who become infected at time $\tau > 0$ and are still infectious at time t $(t > \tau)$. Therefore, the number of individuals who are infected at time τ and remain infectious at time t is given by

$$\lambda I(\tau)S(\tau)G(t - \tau).$$

Therefore, at time t, the number of individuals who have accumulated in the I compartment since $\tau = 0$ is

$$I(t) = I_0(t) + \int_0^t \lambda I(\tau)S(\tau)G(t - \tau)\, d\tau, \tag{1.11}$$

where $I_0(t)$ is the cumulative number of individuals who are already infected at $\tau = 0$ and remain infectious at time $t > 0$. Similarly, the R equation is given by

$$R(t) = R_0(t) + \int_0^t \lambda I(\tau)S(\tau)(1 - G(t - \tau))\, d\tau. \tag{1.12}$$

We see that our new SIR model (1.3), (1.11) and (1.12) with generally distributed infectious periods is a system of differential-integral equations.

In the special case when $F(t) = 1 - e^{-\gamma t}$ is an exponential distribution, we have $G(t) = e^{-\gamma t}$, and from (1.11)

$$I(t) = I_0(t) + \int_0^t \lambda I(\tau)S(\tau)e^{-\gamma(t-\tau)}\, d\tau,$$

and $I_0(t) = I(0)e^{-\gamma t}$ by (1.6). Therefore,

$$\begin{aligned} I'(t) &= I_0'(t) + \lambda I(t)S(t) - \gamma \int_0^t \lambda I(\tau)S(\tau)e^{-\gamma\tau}\, d\tau \\ &= I_0'(t) + \lambda I(t)S(t) - \gamma(I(t) - I_0(t)). \end{aligned}$$

Since $I_0'(t) = -\gamma I_0(t)$, we obtain the original equation (1.3)

$$I'(t) = \lambda I(t)S(t) - \gamma I(t).$$

Similarly, we have from (1.12)

$$R'(t) = \gamma I(t).$$

This confirms our claim that the SIR model in the form of ODE (1.3)–(1.5) assumes an exponentially distributed infectious period.

Let us take another special case when infectious periods have the following survival function:

$$G(t) = \begin{cases} 1 & \text{if } -\infty < t < \omega, \\ 0 & \text{otherwise.} \end{cases} \tag{1.13}$$

Correspondingly, $F(t) = 1 - G(t)$ is the Heaviside function at $t = \omega$, for some constant $\omega > 0$. Then, the equation for $I(t)$ becomes

$$I(t) = I_0(t) + \int_{t-\omega}^t \lambda I(\tau)S(\tau)\, d\tau,$$

and thus, for $t > \omega$,

$$I'(t) = I_0'(t) + \lambda I(t)S(t) - \lambda I(t-\omega)S(t-\omega).$$

Since $I_0(t) = 0$ for $t > \omega$, we arrive at a differential equation with a time delay ω,

$$I'(t) = \lambda I(t)S(t) - \lambda I(t-\omega)S(t-\omega). \tag{1.14}$$

Similarly, for $t > \omega$,

$$R(t) = R_0(t) + \int_0^{t-\omega} \lambda I(\tau)S(\tau)\, d\tau,$$

and

$$R'(t) = \lambda I(t-\omega)S(t-\omega). \tag{1.15}$$

Here we have used the fact that $R_0(t) = 1$ for $t > \omega$. We see here that the delayed differential equation model (1.3), (1.14) and (1.15) is the result of assuming that the infectious periods have a Heaviside distribution function, or Dirac delta density function, at $t = \omega$.

Exercises.

(1) Show that

$$f(t) = \begin{cases} 0 & t < 0 \\ \gamma e^{-\gamma t} & t \geq 0 \end{cases}$$

is a probability density function on $(-\infty, \infty)$, and that the probability mean of an exponentially distributed random variable $X \geq 0$ is given by

$$E[X] = \gamma \int_0^\infty t e^{-\gamma t} dt = \frac{1}{\gamma}.$$

(2) Compute the probability mean for the distribution function given in (1.13).

(3) For the transfer diagram in Figure 1.2, derive the equations for $I(t)$ and $R(t)$ when the infectious period has a general distribution function $P(t)$. Prove that, when $P(t) = 1 - e^{-\gamma t}$ for $t \geq 0$ and $P(t) = 0$ for $t < 0$, the equations become differential equations (1.4)–(1.5).

1.4.2 Modeling Disease Incidence

Disease *incidence* is the rate at which new infections occur; namely, the number of newly infected individuals (both reported cases and asymptomatic individuals) per unit time. This should be distinguished from disease *prevalence*, which measures the number of infected individuals at time t.

1. Simple incidence forms.

The incidence term in the Kermack–McKendrick model in Section 1.3 is given by βIS, which is often called simple mass-action incidence, or *bilinear incidence*. It is based on the Law of Mass Action, first derived for chemical kinetics in 1864 by Waage and Guldberg [1, 41, 59], which states that the rate of chemical reaction is proportional to the density of the reactants:

$$\begin{aligned} A + B &\Longleftrightarrow AB \\ \text{rate} &= k\,[A]\,[B]. \end{aligned}$$

The underlying assumptions of the Law of Mass Action are:

(1) Homogeneous mixing so that contact rate only depends on the density of reactants.
(2) Conservation of total mass.
(3) Low reactant densities.

We see that, for contacts among individuals (human, animals, or cells), these assumptions are at best crude approximations. Modification of any of these assumptions will lead to different incidence forms.

2. The effects of saturation.

If a host population is saturated with infectious individuals, the rate of new infections will only be determined by the number of susceptibles S, and homogeneous mixing is no longer valid. To describe incidence rate in this situation, we can learn from standard theory of enzyme kinetics. The reaction rate v_0 has a nonlinear dependence on the concentration $[A]$ of the substrate A given by the Michaelis–Menten equation:

$$v_0 = \frac{v_{\max}\,[A]}{K + [A]}. \tag{1.16}$$

In this equation, $v_{\max}$ is the maximum reaction rate, and K is the Michaelis–Menten constant [44, 48].

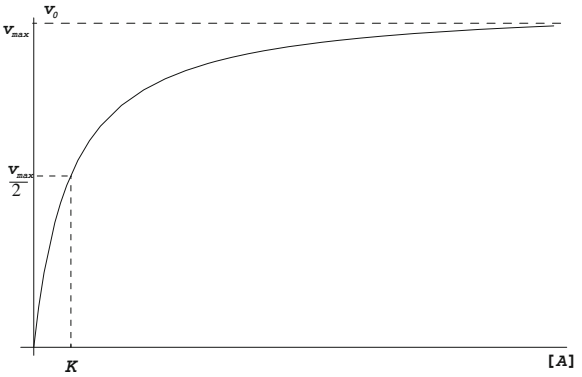

Figure 1.6: Michaelis–Menten reaction curve.

We see from the graph of the Michaelis–Menten reaction that when substrate concentration $[A]$ is large, reaction rate v_0 saturates at the constant $V_{\max}$.

The function

$$f(x) = \frac{a\,x}{K + x} \tag{1.17}$$

is often called the Monod function, or Holling's type II function in ecology literature [5, 45, 48, 55]. The saturation effect on the disease incidence can be modeled using the Monod function to give

$$\frac{\beta I S}{K + I}, \tag{1.18}$$

so that when the population of I is large, the incidence rate is approximately βS. Other incidence forms can be

$$\frac{\beta I^m S}{K + I^m}, \quad m > 0. \tag{1.19}$$

Similarly, saturation of susceptibles may be modeled by

$$\frac{\beta I S^n}{K + S^n}, \quad n > 0. \tag{1.20}$$

3. Varying total population size.

Another way to derive disease incidence is the following: let $S(t), I(t), R(t),$ and $N(t) = S(t) + I(t) + R(t)$ denote the sizes

of the susceptible, infectious, recovered, and total population, respectively. Let λ be the average per capita contact number among individuals per unit time, and p the probability that a contact will produce an infection. Then the incidence is given by

$$p\lambda \cdot \frac{S(t)}{N(t)} \cdot I(t),$$

which can be interpreted as

average number of effective contacts produced by each infectious individual	·	probability that a contact is made with a susceptible individual	·	total number of infectious individuals

If we combine the probability p with the contact number λ, so that λ is the per capita effective contact number, then the incidence is given by

$$\frac{\lambda}{N} IS. \tag{1.21}$$

When the total population size N is a constant, then the incidence form in (1.21) is the same as the simple mass-action incidence form with $\beta = \lambda/N$. However, when $N(t)$ varies with t, things become more complicated. We consider the following two simple cases:

Case 1. The effective contact number λ is independent of the total population size. In this case, the incidence is given by

$$\frac{\lambda I(t)S(t)}{N(t)}, \tag{1.22}$$

where λ is a constant. This form is called the proportionate incidence or *standard incidence*.

Case 2. The effective contact number is proportional to the total population size, namely

$$\lambda(N) = \beta N$$

for a constant β. Then the incidence is again of the simple mass-action form

$$\beta I(t)S(t). \tag{1.23}$$

Suitability of these different incidence forms has been discussed in many research articles [6, 13, 26, 27, 66].

We examine the different assumptions behind these two incidence forms. The difference lies in the assumption on how contact rate varies with the total population size. It is reasonable to assume that the contact rate is in proportion to the total population density. Therefore, the difference between incidence forms (1.22) and (1.23) lies in the assumption on how total population density changes as the total population size varies.

Assumption 1: population density is independent of population size. This is likely the case in a rural population; as population size increases, rural towns tend to expand to maintain a constant population density.

Assumption 2: population density is in proportion to population size. This is likely the case for a large urban population where the city is confined in space; an increase in population size will proportionally increase the population density.

In this sense, proportionate incidence (1.22) is more suitable for a population in a rural setting, whereas the bilinear incidence (1.23) is suitable for a large urban population.

Above discussions are applicable to diseases such as influenza and tuberculosis, for which the transmission occurs through airborne droplets from coughing. We note that an exception is sexually transmitted diseases in which the transmission occurs between sexual partners. In this case, the contact number may not vary with the population density. The standard incidence $\frac{\lambda IS}{N}$ is commonly used for sexually transmitted diseases.

1.4.3 Demography: Birth, Death, and Population Growth

To incorporate demographic factors into the Kermack–McKendrick models (1.3)–(1.5), we need to make various assumptions on the birth, death, and growth of the host population, the simplest of which is the proportional rate assumption that the

birth or death rate is proportional to the population size. A model that incorporates these assumptions is depicted in the diagram in Figure 1.7 with the corresponding system of differential equations (1.24)

$$\begin{aligned} S'(t) &= bN(t) - \lambda I(t)S(t) - d_1 S(t) \\ I'(t) &= \lambda I(t)S(t) - (\gamma + d_2)I(t) \\ R'(t) &= \gamma I(t) - d_3 R(t) \\ N(t) &= S(t) + I(t) + R(t) \end{aligned} \tag{1.24}$$

Here b is the natural birth rate constant, and d_1, d_2, and d_3 are death rate constants for compartments S, I, and R, respectively. Rate constant d_2 may include both natural and disease-caused death. If we add the first three equations in (1.24), we obtain

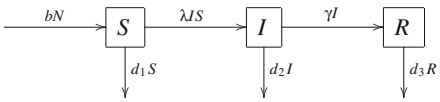

Figure 1.7: Transfer diagram for an SIR model with birth and death.

$$N'(t) = bN(t) - d_1 S(t) - d_2 I(t) - d_3 R(t).$$

In general, when d_i are different, this implies that $N(t)$ will vary with time. In the special case when $d_1 = d_2 = d_3 = d$, we have

$$N'(t) = (b - d)N(t),$$

and thus

$$N(t) = N_0 e^{(b-d)t}.$$

If $b > d$, $N(t) \to \infty$ exponentially as $t \to \infty$; if $b < d$, $N(t) \to 0$ exponentially as $t \to \infty$; and if $b = d$, $N(t) \equiv N_0$, a constant.

Exponential growth and decay of the total population are often modified by the logistic growth,

$$N'(t) = (b - d)N(t) - \frac{N^2(t)}{K}, \tag{1.25}$$

where b, d are natural birth and death rates, respectively, and $(b-d)K$ is the carrying capacity for the population. The logistic growth can be incorporated into the Kermack–McKendrick model as follows:

$$\begin{aligned} S'(t) &= bN(t) - \frac{N^2(t)}{K} - \lambda I(t)S(t) - dS(t) \\ I'(t) &= \lambda I(t)S(t) - (\gamma + d)I(t) \\ R'(t) &= \gamma I(t) - dR(t). \end{aligned} \tag{1.26}$$

For more discussions on epidemic models with density-dependent demographics, we refer the reader to [18].

Another source of new susceptible individuals is migration or immigration. A simple way of incorporating the immigration into a model is to assume that the number of new immigrants is a constant A per unit time. For instance, we may have the transfer diagram with immigration as shown in Figure 1.8, and derive the corresponding differential equations as before. We also note that, rates d_1S, d_2I, and d_3R can also be interpreted as removal rates, which can include removal of individuals from a compartment due to death and out-migration.

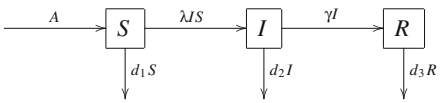

Figure 1.8: Transfer diagram for an SIR model with migration/immigration and removal.

Exercises.

(1) Derive the system of differential equations for the model with transfer diagram in Figure 1.8.
(2) Consider the case that new migrants into the population consist of both susceptible and infectious individuals. Draw a transfer diagram that represents this situation and derive the corresponding differential equations.

1.4.4 Disease Latency: Latent and Incubation Periods

Disease infection begins with the transmission of the pathogen from one host to another. After pathogens invade the host body, they need to be able to evade or overcome the host immune response and be able to multiply or replicate. When the pathogens accumulate sufficiently in large numbers and reach the target organs, they begin to cause sufficient damage to the host body so that the host becomes symptomatic and the host is capable of transmitting the pathogens to others. For some infections, the symptoms may appear after the host becomes contagious. The period from time of infection to time of onset of symptoms is called the *incubation period*. The period from time of infection to time of being contagious or infectious is called the *latent period*. The period during which the host is infectious is called the *infectious period*. See the illustration in Figure 1.9 for an example of relations between these periods. During the latent period, a host may or may not show symptoms, but the host is not capable of transmitting pathogens to other hosts. In Figure 1.9, the onset of the symptoms is shown to occur after the host becomes infectious. We note that the reverse could also happen, and the incubation period can be shorter than the latent period for certain diseases.

To incorporate the disease latency in a mathematical model, we need to make some basic assumptions about the latency of the disease. The simplest is to divide the infected compartment into two compartments: a latent compartment E and an infectious compartment I, and assume that the transfer from E to I satisfies the proportional rate assumption, namely, given by ϵE with rate constant ϵ. From our discussions in Section 1.4.1, we know that this is equivalent to assuming that individual latency has an exponential distribution, and $1/\epsilon$ is the mean latent period. We have a new transfer diagram as shown in Figure 1.10, which leads to a system of differential equations (1.27).

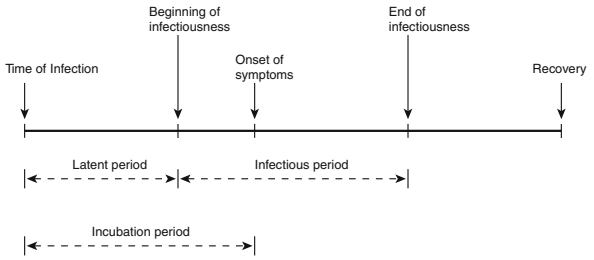

Figure 1.9: A graphical illustration of incubation, latent and infectious periods.

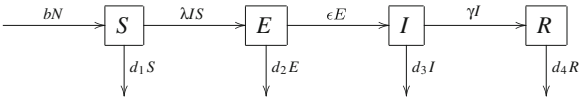

Figure 1.10: Transfer diagram for an SEIR model.

$$\begin{aligned} S'(t) &= bN(t) - \lambda I(t)S(t) - d_1 S(t) \\ E'(t) &= \lambda I(t)S(t) - (\epsilon + d_2)E(t) \\ I'(t) &= \epsilon E(t) - (\gamma + d_3)I(t) \\ R'(t) &= \gamma I(t) - d_4 R(t) \\ N(t) &= S(t) + E(t) + I(t) + R(t). \end{aligned} \tag{1.27}$$

This is an SEIR model. Variations of the model can be derived when different incidence and demographic terms are used.

1.4.5 Acquired Immunity

When an infected host recovers from an infection, it usually maintains a certain degree of immunity against reinfection from the same strain of pathogen. If the infection has caused a humoral immune response, antibodies produced by the host usually remain in the body for a period of time and guard the body from the same antigens. Memory T lymphocytes in the immune system have the ability to recognize the specific antigen against which they are specifically created, and persist long past the primary infection for the purpose of mounting a much quicker immune response when the same pathogenic antigen is recognized. Mild immune

responses can also be induced by inoculation or immunization so that the body is pre-stocked with the correct antibodies or memory T cells to fight the infection when it occurs.

Without exposure to reinfection, immunity against a specific disease will wane and eventually disappear. Certain diseases such as measles are known to cause permanent immunity in humans so that no reinfection occurs after recovery. In terms of compartmental models, loss of immunity results in a transfer of recovered individuals back to the susceptible compartment, as illustrated in Figure 1.11. We assume that the transfer rate is proportional to the size of the compartment. Other assumptions on the rate of transfer can be made according to our discussions in Section 1.4.1.

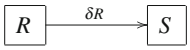

Figure 1.11: Loss of immunity resulting in individuals in compartment R moving into S.

Exercise. Draw the transfer diagram for an SEIRS model with disease latency and temporary immunity. Derive the differential equations. You may want to consider different incidence forms.

1.4.6 Routes of Transmission: Horizontal and Vertical

In the Kermack–McKendrick model, the infection is assumed to occur by direct contact of an infectious and a susceptible host. This is often called *horizontal transmission*. Other routes of transmissions exist for many diseases. One example is *vertical transmission*, in which the pathogens are passed to a newborn directly from an infected mother. Example of diseases that can be transmitted vertically include HIV/AIDS, Chagas disease, and Hepatitis B. To model vertical transmission, we assume that a fraction p of newborns from the infected population becomes infected at birth, and the remaining fraction $(1-p)$ are susceptible. The transfer diagram in Figure 1.12 illustrates a disease spread with both horizontal and vertical transmissions.

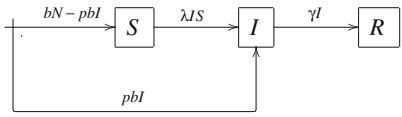

Figure 1.12: Transfer diagram for an SIR model with vertical transmission.

In Figure 1.12, bN is the total number of newborns with natural birth rate b, pbI is the number of newborns who are infected at birth, $bN - pbI$ is the number of healthy but susceptible newborns. The resulting model is described by the following system of differential equations:

$$\begin{aligned} S'(t) &= bN(t) - pbI(t) - \lambda I(t)S(t) \\ I'(t) &= pbI(t) + \lambda I(t)S(t) - \gamma I(t) \\ R'(t) &= \gamma I(t). \end{aligned} \tag{1.28}$$

A good reference for mathematical modeling of vertically transmitted diseases is the book by Busenberg and Cooke [8].

Exercise. Consider an SEIR model with both horizontal and vertical transmission. What assumptions can one make about the newborns of mothers from the E and I compartments? Should the infected newborns enter the E compartment or the I compartment, or both? Think of the possibilities. Draw transfer diagrams according to different assumptions you make, and derive the corresponding differential equations.

1.4.7 Heterogeneity: Age and Social Groups, Differential Infectivity, Multiple Hosts, and Disease Vectors

The Kermack–McKendrick model considers a single homogeneous host population. In reality, host populations are far from homogeneous. Many characteristics of the host population can contribute to heterogeneity. Age is an important source of heterogeneity; mixing is often preferential to individuals in the same age group,

vulnerability to a particular disease and the case fatality rate generally vary greatly across different age groups. Certain social groups may have much higher incidence of sexually transmitted diseases than the general population. Different ethnic groups may have different susceptibilities to certain diseases. Another important factor for heterogeneity in disease transmission is the spatial spread; an infectious disease typically starts from an outbreak at one location and spreads elsewhere. For vector-borne diseases and diseases that involve several hosts, there exists heterogeneity among the disease vectors, intermediate hosts and human hosts. These factors need to be incorporated into a mathematical model to represent realistically the disease transmission process. In this section, we will discuss how to incorporate age structures into our basic model.

Let $S(a,t), I(a,t)$, and $R(a,t)$ be the number of individuals who are susceptible, infectious, and recovered at age a and time t, respectively. Here a, t are considered as independent variables. The rate of change of the population in each compartment should account for changes due to time, as we have seen in Section 1.2, and changes due to aging, which are described as partial derivatives with respect to a: $\frac{\partial S(a,t)}{\partial a}$, $\frac{\partial I(a,t)}{\partial a}$, and $\frac{\partial R(a,t)}{\partial a}$, respectively. The Kermack–McKendrick model with age structure becomes a system of integral partial differential equations:

$$\begin{aligned}
\frac{\partial S(a,t)}{\partial t} + \frac{\partial S(a,t)}{\partial a} &= -S(a,t)\int_0^\infty \lambda(a,b)I(b,t)db \\
\frac{\partial I(a,t)}{\partial t} + \frac{\partial I(a,t)}{\partial a} &= S(a,t)\int_0^\infty \lambda(a,b)I(b,t)db - \gamma(a)I(a,t) \\
\frac{\partial R(a,t)}{\partial t} + \frac{\partial R(a,t)}{\partial a} &= \gamma(a)I(a,t).
\end{aligned} \tag{1.29}$$

Birth terms will appear as boundary conditions at $a = 0$:

$$\begin{aligned}
S(0,t) &= \int_{a_0}^\infty [b(a)N(t,a) - p(a)b(a)I(t,a)]da, & S(a,0) &= \psi(a), \\
I(0,t) &= \int_{a_0}^\infty p(a)b(a)I(t,a)\,da, & I(a,0) &= \phi(a), \\
R(0,t) &= 0, & R(0,a) &= \xi(a).
\end{aligned} \tag{1.30}$$

Here, parameter $b(a)$ denotes the birth rate for populations at age a, and $p(a)$ is the fraction of infectious newborns from populations at age a. The individuals are assumed to become child-bearing at age a_0. The term $p(a)b(a)I(t,a)$ in the boundary conditions is due to vertical transmission, and $(\psi(a), \phi(a), \xi(a))$ denotes the initial age distribution. The age-dependent force of infection is given by

$$\lambda(a,t) = \int_0^\infty \lambda(a,b)I(b,t)db,$$

where $\lambda(a,b)$ is the transmission coefficients from the subpopulation at age b to the subpopulation at age a.

For discussions and analysis of age-structured epidemic models, see [32, 33, 63].

1.4.8 Disease Control and Prevention Measures: Immunization and Quarantine

Apart from medical treatment, two of the most effective and widely used prevention and control measures for infectious diseases are immunization and quarantine.

An effective vaccine can protect an otherwise susceptible host against possible infection. By immunizing a large portion of the susceptible host population before or at the early phase of a disease outbreak, we can reduce the initial number S_0 of susceptibles to a level that is below the threshold $\frac{\gamma}{\beta}$, and by our threshold result in Section 1.3, a full-blown epidemic can be prevented. From a compartmental modeling viewpoint, vaccination moves susceptible hosts directly to the recovered compartment without going through the I compartment. If we assume that a fraction p of all susceptibles is vaccinated per unit time, then we arrive at the transfer diagram in Figure 1.13 and a system of differential equations (1.31).

$$\begin{aligned} S' &= bN - \lambda IS - dS - pS \\ I' &= \lambda IS - (d+\gamma)I \\ R' &= pS + \gamma I - dR \\ N &= S + I + R. \end{aligned} \tag{1.31}$$

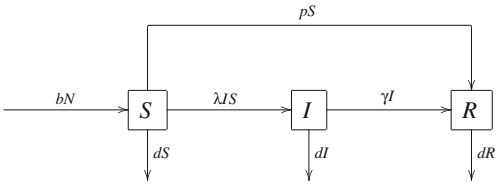

Figure 1.13: Transfer diagram for an SIR model with vaccination.

One of the issues with vaccination is that some vaccines can be "leaky" or imperfect; namely, the immune protection of hosts is not perfect and immunized hosts can still get infected, albeit with a smaller probability than unvaccinated hosts. To model a leaky vaccine, we add a new compartment V of vaccinated hosts and an additional incidence term $\alpha\lambda VS$ due to the infection of vaccinated individuals. We obtain the transfer diagram in Figure 1.14.

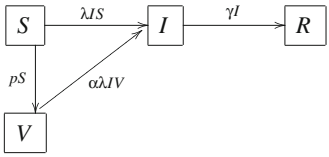

Figure 1.14: A vaccination model with a leaky vaccine.

In Figure 1.14, $0 < \alpha \leq 1$ denotes the reduced probability of transmission due to immune protection from the imperfect vaccine. A set of differential equations can be readily derived based on the transfer diagram.

Quarantine is a measure that isolates infectious individuals and hence prevents them from infecting others. Through quarantine, we can slow down and even stop the transmission process. We introduce a new compartment Q for the quarantined individuals,

and assume that quarantine is carried out in such a way that a fraction $0 < p \leq 1$ of infectious individuals will be isolated. A simple transfer diagram is depicted in Figure 1.15, where δ is the rate constant for the recovery of quarantined individuals.

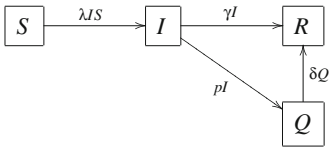

Figure 1.15: An SIR model with quarantine.

Exercise. Derive systems of differential equations according to transfer diagrams depicted in Figure 1.14 and Figure 1.15.

1.4.9 The Basic Reproduction Number $\mathcal{R}_0$

The basic reproduction number $\mathcal{R}_0$, also called the basic reproductive number or the basic reproductive ratio, is the single most important parameter in epidemic modeling. It measures the average number of secondary infections caused by a single infectious individual in an entirely susceptible population during the mean infectious period.

In the context of the Kermack–McKendrick model, $\mathcal{R}_0$ can be expressed as

$$\lambda \cdot S_0 \cdot \frac{1}{\gamma}$$

which can be interpreted as

average number of effective contacts of a single infectious host	$\cdot$	initial susceptible population	$\cdot$	mean infectious period

Using $\mathcal{R}_0$, the threshold phenomenon described in Section 1.3 can be expressed as follows:

If $\mathcal{R}_0 < 1$, then an epidemic will not occur;
If $\mathcal{R}_0 > 1$, an epidemic will occur.

We will see in later chapters that threshold results in this form occur even in more complex epidemic models.

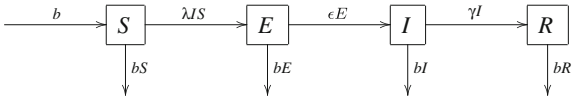

Figure 1.16: Transfer diagram for an SEIR model.

For the SEIR model with the transfer diagram in Figure 1.16, the basic reproduction number is given by

$$\mathcal{R}_0 = \lambda \cdot \frac{\epsilon}{\epsilon + b} \cdot \frac{1}{\gamma + b},$$

which can be interpreted as

average number of effective contacts of a single infectious host	·	probability of a newly infected host surviving the latent period	·	mean infectious period	.

Note that the mean infectious period $\frac{1}{\gamma+b}$ is understood as the mean period an individual remains alive and infectious. We also note that the initial susceptible population does not appear in $\mathcal{R}_0$ in this case. The reason is that, in this model, the constant total population $N = S + E + I + R$ is scaled to 1.

When models get more complex, $\mathcal{R}_0$ may be harder to derive directly from the transfer diagram. Other methods for deriving $\mathcal{R}_0$ exist. Most of them are based on the stability analysis of the disease-free equilibrium. In the later chapters, we will illustrate various ways to derive and interpret $\mathcal{R}_0$.

For more detailed description and discussions on the basic reproduction number for epidemic models, we refer the reader to [2, 7, 14, 15, 27, 57, 60]. A practical approach to the computation of $\mathcal{R}_0$ for complex epidemic models is given in [64].

Chapter 2

Five Classic Epidemic Models and Their Analysis

In this chapter, we present some standard mathematical methods for the analysis of compartmental epidemic models. We have chosen five classic epidemic models to demonstrate these methods. We start from the basic Kermack–McKendrick model and progressively expand it to a model with demography, and then introduce the Ross–MacDonald model for malaria. Each model is chosen to illustrate a specific mathematical approach for model analysis: the method of first integrals and level curves, the phase-line analysis, phase-plane analysis, reduction of dimension using homogeneity, and monotone dynamical systems. The general mathematical theories applied in this chapter are provided in Chapter 3 for reference and in-depth learning. Students in mathematics have a chance to learn these general theories in the setting of epidemic models and see how abstract theories of differential equations are applied to real-world problems. Students in public health and biological sciences will be able to learn the basic model analysis and gain exposure to some abstract mathematical concepts such as stability and bifurcations explained in the context of epidemiology, as well as to the theory of modern differential equations.

Section 2.1 contains analysis of the Kermack–McKendrick model introduced in Section 1.3. The main mathematical technique presented is the method of first integrals and how to obtain

M. Y. Li, *An Introduction to Mathematical Modeling of Infectious Diseases*, Mathematics of Planet Earth 2,
https://doi.org/10.1007/978-3-319-72122-4_2

orbits of solutions from level curves of first integrals. Epidemiological concepts discussed include the basic reproduction number, final size formula, and threshold phenomenon for epidemics.

Section 2.2 discusses a simple model for diseases without immunity. The resulting model equation is a 1-dimensional differential equation. We present the method of phase-line analysis to illustrate important concepts of equilibria, stability, bifurcation, and bifurcation diagrams.

Section 2.3 deals with a model with demography which leads to a 2-dimensional system of ordinary differential equations. We present the standard phase-plane analysis, which is based on the classical Poincaré–Bendixson theory, one of the most beautiful theories in differential equations. The techniques used include local stability analysis by linearization, global stability using the method of Lyapunov functions, and global convergence using the Bendixson–Dulac criteria and the Poincaré–Bendixson Theorem.

Section 2.4 investigates a model with the proportionate incidence term and exponential birth and death terms. The resulting system of equations is 3-dimensional and does not allow us to apply the phase-plane analysis directly. The homogeneous property satisfied by the model system can be used to reduce the dimension by one. We show how to derive a system of equations for the fractional variables that becomes 2-dimensional. Mathematically, this amounts to projecting the original system onto a hyperplane or sphere. We show how a complete understanding of the projected system can help us to analyze the original 3-dimensional system.

Section 2.5 deals with the classic Ross–MacDonald model for malaria. We will show how to derive a model for vector-borne diseases. The mathematical techniques used in this section are part of the monotone dynamical systems theory.

The models discussed in this chapter are kept simple and analysis mostly elementary. Some of the same mathematical approaches demonstrated using these simple models are used for analysis of more complex models in Chapter 5.

2.1 Kermack–McKendrick Model

In this section we carry out detailed mathematical analysis and derive important properties of solutions to the Kermack–McKendrick model,

$$\begin{aligned} \frac{dS}{dt} &= -\beta IS \\ \frac{dI}{dt} &= \beta IS - \gamma I \\ \frac{dR}{dt} &= \gamma I, \end{aligned} \tag{2.1}$$

with initial conditions $S(0) = S_0 > 0, I(0) = I_0 > 0$, and $R(0) = R_0 \geq 0$.

2.1.1 Simple Properties of Solutions

Property 1. Model (2.1) is well posed.

By well-posedness we mean that nonnegative initial conditions lead to nonnegative solutions, namely, $S_0 \geq 0, I_0 \geq 0$, and $R_0 \geq 0$ imply $S(t) \geq 0, I(t) \geq 0$, and $R(t) \geq 0$ for $t \geq 0$. Another way to describe this is that the nonnegative cone of $\mathbb{R}^3$,

$$\mathbb{R}^3_+ = \{\, (S, I, R) \in \mathbb{R}^3 \mid S \geq 0, I \geq 0, R \geq 0 \,\}, \tag{2.2}$$

is positively invariant with respect to (2.1).

Positive invariance of $\mathbb{R}^3_+$ can be verified by examining the direction of the vector field $(-\beta IS, \beta IS - \gamma I, \gamma I)^T$ of (2.1) on each coordinate plane. We want to show the vector field is either tangent to the coordinate or pointing to the interior of $\mathbb{R}^3_+$.

(1) On the SR-plane: $I = 0$ on this plane, and

$$\left.\frac{dI}{dt}\right|_{I=0} = 0.$$

This shows that the vector field on the SR-plane is tangent to the SR-plane. This tangency also implies that the SR-plane itself is invariant – solutions starting on the SR-plane remain on the

same plane. Biologically, this says that if there is no infection at the beginning, there remains no infection.

(2) On the IR-plane: $S = 0$ on this plane, and

$$\left.\frac{dS}{dt}\right|_{S=0} = 0.$$

Therefore, the IR-plane is also invariant. No solutions in the interior of $\mathbb{R}^3_+$ can escape through the IR-plane or the SR-plane.

(3) On the SI-plane: $R = 0$ on this plane, and

$$\left.\frac{dR}{dt}\right|_{R=0} = \gamma I \geq 0.$$

Therefore, the vector field on the SI-plane points to the interior of $\mathbb{R}^3_+$. No solutions can escape the interior through the SI-plane. We thus have shown that all solutions starting in $\mathbb{R}^3_+$ remain in $\mathbb{R}^3_+$ for $t > 0$.

Property 2. Total population is constant.

Let $N(t) = S(t) + I(t) + R(t)$, $N_0 = S_0 + I_0 + R_0$. Adding all three equations in (2.1) we obtain

$$N'(t) = 0 \quad \text{for all } t \geq 0,$$

which implies $N(t) = N_0$ for all $t \geq 0$.

Property 3. Solutions to (2.1) exist for $t \in [0, +\infty)$.

From Properties 1 and 2 we know that solutions $(S(t), I(t), R(t))$ are bounded in their maximal interval of existence. Fundamental theory of differential equations tells us that solutions can be extended for all positive time.

Property 4. Limit $\lim_{t\to\infty}(S(t), I(t), R(t)) = (S(\infty), I(\infty), R(\infty))$ exists.

From (2.1) we know

$$S'(t) = -\beta I(t)S(t) \leq 0.$$

Therefore, $S(t)$ is decreasing and bounded below by 0, and thus $S(\infty) \geq 0$ exists. Similarly,

$$R'(t) = \gamma I(t) \geq 0$$

and $R(t)$ is increasing and bounded above by N_0. Therefore, $R(\infty) \geq 0$ exists. From

$$I(t) = N_0 - S(t) - R(t)$$

we know that $I(\infty) = N_0 - S(\infty) - R(\infty) \geq 0$ exists.

Property 5. $S_0 > 0$ and $I_0 > 0$ imply $0 < S(\infty) < S_0$ and $I(\infty) = 0$.

Without loss of generality we may assume that $R_0 = 0$, since otherwise, we may choose $\bar{N}_0 = N_0 - R_0$. Then $S(t) > 0, I(t) > 0$, and $R(t) > 0$ for $t > 0$. Dividing the equations for S and R, we have

$$\frac{dS}{dR} = -\frac{\beta}{\gamma} S.$$

Solving this equation for S we obtain

$$S(R) = S_0 e^{-\frac{\beta}{\gamma} R} \geq S_0 e^{-\frac{\beta}{\gamma} N_0} > 0. \tag{2.3}$$

Therefore, $0 < S(\infty) < S_0$.

From the S equation and the fact that $S(\infty)$ and $I(\infty)$ exist, we know that

$$\lim_{t \to \infty} S'(t) = -\beta I(\infty)\, S(\infty) \quad \text{exists.}$$

Furthermore, $\lim_{t\to\infty} S'(t) = 0$. Otherwise, if $\lim_{t\to\infty} S'(t) = \alpha < 0$, then $S'(t) < \alpha/2$ for $t \geq T$, for sufficiently large time T, and thus

$$S(t) < S(T) + \frac{\alpha}{2}(t - T) < 0 \quad \text{for } t > T - \frac{2S(T)}{\alpha}.$$

This contradicts $S(t) > 0$ for all $t > 0$. Therefore, $S(\infty)I(\infty) = 0$. Since $S(\infty) > 0$, we know $I(\infty) = 0$.

We can draw two important biological conclusions based on these properties:

(1) The disease eventually dies out ($I(\infty) = 0$). The model describes an epidemic disease.

(2) There is always a positive fraction $S(\infty)/S_0$ of susceptibles that escape infection at the end of the epidemic. The epidemic does not stop because of complete exhaustion of susceptibles.

The second conclusion begs the question: why does an epidemic first rise, peak, and then decline? We address this question in the next subsection.

2.1.2 Phase Portrait in the *SI*-Plane: Epidemic Curves

For a better understanding of the behaviors of solutions, we try to view their orbits in the SI-plane. Consider only the S, I equations:

$$\begin{aligned} \frac{dS}{dt} &= -\beta IS \\ \frac{dI}{dt} &= \beta IS - \gamma I \end{aligned} \tag{2.4}$$

in the first quadrant of the SI-plane. Dividing the two equations we obtain

$$\frac{dI}{dS} = -1 + \frac{\gamma}{\beta S} = -1 + \frac{\rho}{S}, \tag{2.5}$$

where $\rho = \gamma/\beta$ is the threshold number for S_0. Integrating (2.5) we obtain

$$\phi(S, I) = I + S - \rho \log S = C, \tag{2.6}$$

where C is an integration constant and can be determined from S_0 and I_0. The function $\phi(S, I) = I + S - \rho \log S$ is called a *first integral* of system (2.4), since it satisfies

$$\frac{d}{dt}\phi(S(t), I(t)) = I'(t) + S'(t) - \rho\frac{S'(t)}{S(t)} = -\gamma I(t) + \rho\beta I(t) = 0$$

for all t. Therefore, function $\phi(S, I)$ remains a constant along a solution $(S(t), I(t))$ of (2.4). This implies that trajectories $(S(t), I(t))$ of system (2.4) are given by the family of level curves $\phi(S, I) = C$ of the first integral $\phi(S, I)$, or equivalently defined by equation (2.6). This gives us a way to plot trajectories of (2.4) by

plotting level curves of a first integral $\phi(S, I)$ for different values of C. These curves are depicted in Figure 2.1.

We can observe several characteristics of the phase trajectories.

(1) The maximum value $I_{\max}$ of I is achieved when $S = \rho$, the threshold value. This fact is also clear from the equation of I, since $I' = 0$ if and only if $S = \rho$, and $S = \rho$ is a critical point for I.

(2) If $S_0 < \rho$, then $I(t)$ decreases monotonically as t increases and the epidemic declines and no new outbreaks occur.

(3) If $S_0 > \rho$, then $I(t)$ initially increases monotonically while $S(t)$ decreases, $I(t)$ peaks when $S = \rho$, and then as $S(t)$ decreases below ρ, $I(t)$ decreases to 0. This gives the rise–peak–decline cycle of an epidemic.

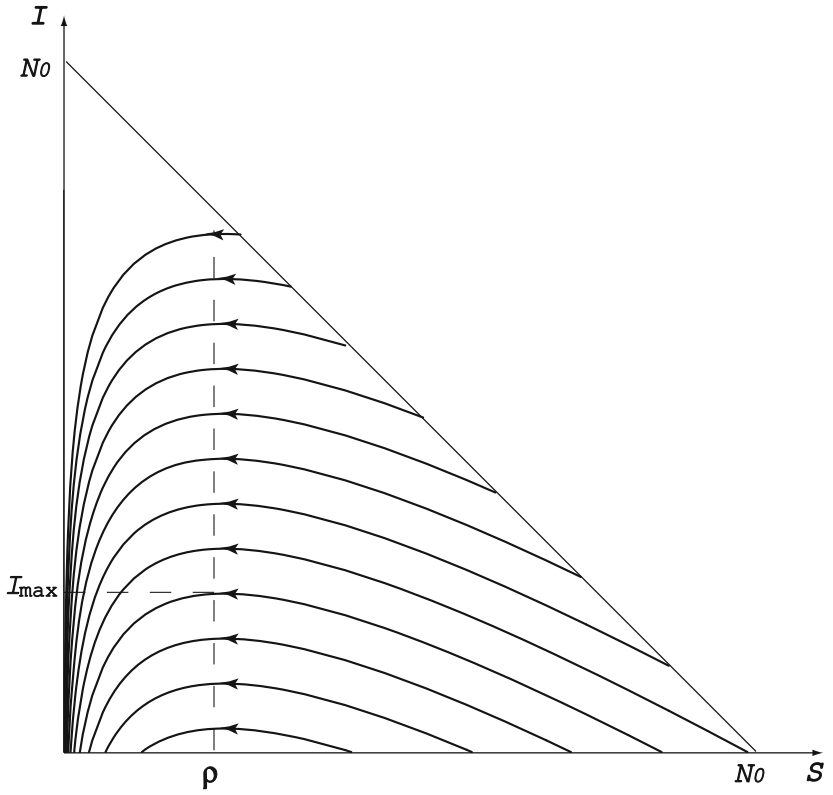

Figure 2.1: Family of epidemic curves.

Clearly, cases (2) and (3) confirm the threshold phenomenon we have observed in Section 1.3 and demonstrate the important role threshold parameter $\rho = \gamma/\beta$ plays in determining the fate of an epidemic.

The threshold condition $S_0 > \rho$ can also be interpreted in the equivalent form $S_0/\rho > 1$, or

$$\frac{\beta}{\gamma} S_0 > 1.$$

From Section 1.4.9, we know that the expression $\beta\, S_0/\gamma$ represents the average number of secondary infections during an mean infectious period in an initially susceptible population S_0, which is the *basic reproduction number* $\mathcal{R}_0$. Therefore, the conclusions in (2) and (3) can be restated as the following threshold result: no outbreaks will occur if the basic reproduction number $\mathcal{R}_0 < 1$; and an initial case will lead to an outbreak if $\mathcal{R}_0 > 1$.

An important epidemiological message from the mathematical theory is that, in the natural history of an epidemic, the decline after peak happens when the available susceptible population declines below the threshold value $\rho = \gamma/\beta$. Interventions that decrease the transmission coefficient β by reducing chances of contact or increase γ by shortening the infectious period will impact the threshold value, and in turn change the timing of the peak.

2.1.3 Final Size Formula and the Severity of an Epidemic

Recall equation (2.6)

$$\phi(S, I) = S + I - \rho \log S = C.$$

Assume that $I_0 \approx 0$. From

$$\phi(S_0, 0) = \phi(S_\infty, 0),$$

we obtain

$$S_0 - S_\infty = \rho(\log S_0 - \log S_\infty), \tag{2.7}$$

and

$$\rho = \frac{S_0 - S_\infty}{\log S_0 - \log S_\infty}. \tag{2.8}$$

Note that S_∞ gives the number of susceptible individuals who escape the epidemic and can be used as an indicator of the severity of the epidemic. Equation (2.7) is often called the *final size equation*. If the basic reproduction number $\mathcal{R}_0 = \frac{S_0}{\rho} = \frac{\beta}{\gamma} S_0$ is known for a disease, then equation (2.7) can be used to estimate the final size S_∞. On the other hand, after an epidemic, the final size S_∞ is known, and equation (2.8) can be used to estimate the basic reproduction number $\mathcal{R}_0$, which can give an estimate of the transmission rate β.

The severity of an epidemic can also be measured in terms of the cumulative number of infected individuals, also called the size of an epidemic:

$$\text{size of epidemic} = S_0 - S_\infty. \tag{2.9}$$

If we know that $R(0) = 0$ and $I(0) \approx 0$, then we have

$$S_0 - S_\infty = R_\infty. \tag{2.10}$$

This relation is clear from biological interpretation. It can also be derived mathematically. Dividing the equations for S and R in (2.1) we have

$$-\rho \frac{dS}{S} = dR.$$

Integrating both sides and using the final size formula (2.7) we obtain

$$\rho(\log S_0 - \log S_\infty) = R_\infty = S_0 - S_\infty.$$

The third way to measure the severity of an epidemic is the maximum number of infected individuals, $I_{\max}$, which can be used to predict whether there will be sufficient hospital capacity. From relation (2.6) we obtain

$$C = I_0 + S_0 - \rho \log S_0 = N_0 - \rho \log S_0,$$

and thus

$$I = -S + \rho \log S + N_0 - \rho \log S_0. \tag{2.11}$$

Since $\frac{dI}{dS} = 0 \iff S = \rho$, we can derive

$$I_{\max} = I(\rho) = -\rho + \rho \log \rho + N_0 - \rho \log S_0. \tag{2.12}$$

Once the basic reproduction number $\mathcal{R}_0 = \frac{S_0}{\rho}$ is estimated, $I_{\max}$ can be estimated from this relation.

2.1.4 Kermack–McKendrick Threshold Theorem

To arrive at their now famous threshold theorem, Kermack and McKendrick obtained approximate solutions of model (2.1). Using $S + I + R = N_0$, the R equation in (2.1) can be rewritten as

$$\frac{dR}{dt} = \gamma(N_0 - R - S).$$

Using relation (2.3), $S(R) = S_0 e^{-R/\rho}$, we obtain

$$\frac{dR}{dt} = \gamma(N_0 - R - S_0 e^{-\frac{R}{\rho}}). \tag{2.13}$$

To obtain an approximation solution to (2.13), we use Taylor expansion of $e^{-R/\rho}$ at $R = 0$ up to the second order and obtain an approximation of equation (2.13):

$$\frac{dR}{dt} = \gamma\left[N_0 - S_0 + \left(\frac{S_0}{\rho} - 1\right)R - \frac{S_0}{2\rho^2}R^2\right]. \tag{2.14}$$

Solving this equation we obtain

$$R(t) = \frac{\rho^2}{S_0}\left[\frac{S_0}{\rho} - 1 + \alpha \tanh\left(\frac{1}{2}\alpha\gamma t - \phi\right)\right], \tag{2.15}$$

where

$$\begin{aligned} \alpha &= \left[\left(\frac{S_0}{\rho} - 1\right)^2 + \frac{2S_0 I_0}{\rho^2}\right]^{\frac{1}{2}}, \\ \phi &= \tanh^{-1}\frac{1}{\alpha}\left(\frac{S_0}{\rho} - 1\right). \end{aligned} \tag{2.16}$$

Therefore

$$\frac{dR}{dt} = \frac{\gamma\alpha^2\rho^2}{2S_0}\operatorname{sech}^2\left(\frac{1}{2}\alpha\gamma t - \phi\right). \tag{2.17}$$

If $I_0 \approx 0$ and $S_0 > \rho$, then we have from (2.16), $\alpha = \frac{S_0}{\rho} - 1$, and from (2.15)

$$R(t) = \frac{\rho^2}{S_0}\left(\frac{S_0}{\rho} - 1\right)\left[1 + \tanh\left(\frac{\gamma}{2}(\frac{S_0}{\rho} - 1)t - \phi\right)\right]. \tag{2.18}$$

Letting $t \to \infty$ and using $\lim_{t\to\infty}\tanh(at+b) = 1$, we obtain an approximate value for the size $R_\infty = S_0 - S_\infty$ of the epidemic

$$R_\infty = 2\rho\left(1 - \frac{\rho}{S_0}\right). \tag{2.19}$$

If we write $S_0 = \rho + \nu$ for $\nu > 0$, then

$$\begin{aligned} R_\infty &= 2\rho\left(1 - \frac{\rho}{\rho+\nu}\right) = 2\rho\frac{\nu}{\rho+\nu} \\ &= 2\nu\frac{\rho}{\rho+\nu} \approx 2\nu. \end{aligned}$$

Namely, the size of the epidemic is roughly 2ν. Therefore,

$$S_\infty = S_0 - R_\infty = \rho + \nu - 2\nu = \rho - \nu.$$

This relation leads to the threshold theorem of Kermack–McKendrick.

Theorem 2.1.1 (Threshold Theorem)

(1) *An epidemic occurs if and only if S_0 exceeds the threshold ρ.*

(2) *If $S_0 = \rho + \nu$, $\nu > 0$, then after the epidemic, the number of susceptible individuals is reduced by an amount approximately 2ν, namely, $S_\infty \approx \rho - \nu$.*

If all cases in an epidemic terminate in death, then R can be considered the removed class, and $\frac{dR}{dt}$ will be the rate for disease death. This can be fitted to the weekly death register data. Kermack and McKendrick used relation (2.17) to fit the data from the Bubonic plague in Bombay in 1905–06 and obtained a very good fit using a simple model. See [48], page 325, for a demonstration of the fitting.

Exact solutions to (2.13) were obtained by Kendall in 1956. In present days, numerical solutions can be easily obtained using a computer software and are used to fit data.

Exercises.

(1) Solve equation (2.13) and find its exact solutions (hint: try separation of variables).

(2) Numerically solve equation (2.13) and its second-order approximation (2.14) using a mathematical software package. Compare solutions of the two equations that originate from the same initial point. Describe what you observe about the differences of the two solutions. Can you explain the differences you observed? Based on these numerical simulations, what conclusions can you draw regarding the accuracy of the second-order approximation of equations (2.13)? Based on your observations, what can you say about the validity of statement (2) of Theorem 2.1.1?

2.2 A Model for Diseases with No Immunity

Consider an infectious disease that confers no immunity. Ignoring demography and latency, we have the transfer diagram in Figure 2.2.

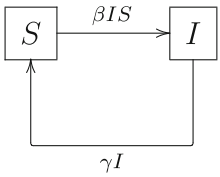

Figure 2.2: Transfer diagram for an SIS model.

Infected individuals return to the susceptible compartment upon recovery, and the natural history of the infection can be illustrated as $S \to I \to S$. This type of model is called an SIS model. The model equations are:

$$\begin{aligned} S'(t) &= -\beta IS + \gamma I \\ I'(t) &= \beta IS - \gamma I. \end{aligned} \tag{2.20}$$

Initial conditions are $S(0) = S_0$ and $I(0) = I_0$. As we have seen in previous sections, $N = S + I = N_0 = S_0 + I_0$. In this model, there will be two possible outcomes for an initial outbreak: either the outbreak terminates or the disease becomes endemic. To see this, we replace $S = N_0 - I$ in the second equation and obtain

$$I' = \beta I(N_0 - I) - \gamma I = (\beta N_0 - \gamma - \beta I)I,$$

or

$$I' = (\beta N_0 - \gamma)I\left(1 - \frac{I}{N_0 - \frac{\gamma}{\beta}}\right). \tag{2.21}$$

Let

$$f(I) = (\beta N_0 - \gamma)I\left(1 - \frac{I}{N_0 - \frac{\gamma}{\beta}}\right). \tag{2.22}$$

Then the differential equation (2.21) can be written as

$$I' = f(I). \tag{2.23}$$

Properties of solutions to (2.23) can be largely determined from the graph of $f(I)$, which is depicted in Figure 2.3, using a procedure called *phase-line analysis*. The basic ideas of phase-line analysis are as follows: since solutions of equation (2.23) can only

move along a straight line and cannot self-intersect, we know that $I(t)$ is either monotonically increasing ($I'(t) > 0$) or monotonically decreasing ($I'(t) < 0$). From (2.23) we also know that the sign of $I'(t)$ can be determined from the graph of f: in an interval on the I-axis where $f(I) > 0$, we know that $I'(t) > 0$ and that $I(t)$ is increasing, and solutions move to the right; in an interval where $f(I) < 0$, $I(t)$ is decreasing and solutions move to the left. These situations are depicted in Figure 2.3 in which the arrows on the I-axis denote the direction solutions are moving. Equilibria of (2.23) are solutions that do not depend on t ($I'(t) = 0$), and hence are points where $f(I) = 0$, or where the graph of f intersects the I-axis. If the arrows on either side of an equilibrium I^* are moving toward I^*, then solutions near I^* are convergent to I^*. In this case, the equilibrium I^* is said to be *asymptotically stable*. On the other hand, if the arrows are moving away from I^*, then I^* is an *unstable* equilibrium.

Applying the phase-line analysis to (2.21) with $f(I)$ given in (2.22), we see that (2.21) has two equilibria: $I_1^* = 0$ and $I_2^* = N_0 - \frac{\gamma}{\beta} = N_0 - \rho$. Whether I_2^* is positive depends on the sign of $N_0 - \frac{\gamma}{\beta}$. If $N_0 < \frac{\gamma}{\beta}$, then the equation only has one equilibrium $I^* = 0$ in the nonnegative I-axis and it is asymptotically stable. If $N_0 > \frac{\gamma}{\beta}$, both equilibria I_1^* and I_2^* exist in the nonnegative I-axis. Equilibrium $I_1^* = 0$ is unstable and I_2^* is asymptotically stable. See Figure 2.3 (a) and (b). We summarize these results in the next proposition.

Proposition 2.2.1

(1) *If* $\frac{\beta N_0}{\gamma} < 1$, *then, for any* $0 < I_0 < N_0$, $I(t) \to 0$ *monotonically as* $t \to \infty$.

(2) *If* $\frac{\beta N_0}{\gamma} > 1$, *then, for any* $0 < I_0 < N_0$, $I(t) \to N_0 - \frac{\gamma}{\beta}$ *monotonically as* $t \to \infty$.

Proof is left as an exercise.

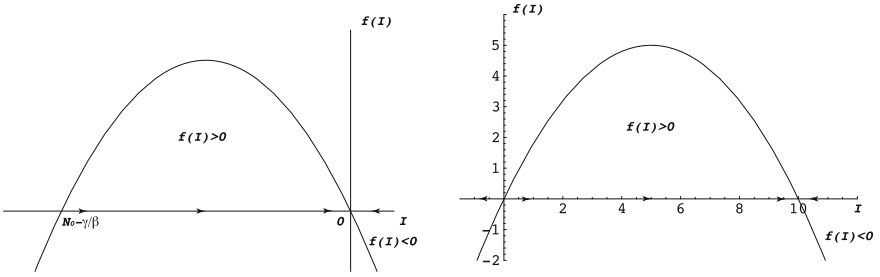

(a) $N_0 < \frac{\gamma}{\beta}$ (b) $N_0 > \frac{\gamma}{\beta}$

Figure 2.3: Graphical demonstration of phase-line analysis.

Recall that $\mathcal{R}_0 = \frac{\beta N_0}{\gamma}$ denotes the basic reproduction number. Proposition 2.2.1 can be reinterpreted as follows for solutions $(S(t), I(t))$ of (2.20):

(1) If $\mathcal{R}_0 < 1$, then $(S(t), I(t)) \to (N_0, 0)$ as $t \to \infty$.

(2) If $\mathcal{R}_0 > 1$, then $(S(t), I(t)) \to (\frac{\gamma}{\beta}, N_0 - \frac{\gamma}{\beta})$ as $t \to \infty$.

The equilibria $P_0 = (N_0, 0)$ and $P^* = (\frac{\gamma}{\beta}, N_0 - \frac{\gamma}{\beta})$ of model (2.20) are called the *disease-free equilibrium* and the *endemic equilibrium*, respectively. Let

$$\Gamma = \{(S, I) \in \mathbb{R}^2_+ \mid S + I = N_0\}$$

be the feasible region for model (2.20). Summarizing the preceding discussions, we arrive at the next threshold theorem.

Theorem 2.2.2

(1) *For each $N_0 > 0$, there are two possible equilibria in the feasible region Γ: the disease-free equilibrium $P_0 = (N_0, 0)$ and the endemic equilibrium $P^* = (\frac{\gamma}{\beta}, N_0 - \frac{\gamma}{\beta})$.*

(2) *If $\mathcal{R}_0 < 1$, then all solutions in Γ converge to P_0.*

(3) *If $\mathcal{R}_0 > 1$, then all solutions with $I_0 > 0$ converge to P^*.*

Biological interpretations:

(1) The basic reproduction number $\mathcal{R}_0$ serves as a threshold parameter that determines the outcome of an initial outbreak.

(2) For the same value of $\mathcal{R}_0$, the outcomes are qualitatively the same for all initial conditions.

(3) When $\mathcal{R}_0 < 1$, the disease dies out. From the monotonicity of $S(t)$ and $I(t)$, we know that no epidemic will develop.

(4) Because $(\frac{\gamma}{\beta}, N_0 - \frac{\gamma}{\beta})$ is an equilibrium, $S(t)$ stays only on one side of $\frac{\gamma}{\beta}$, and thus $I'(t) = I(t)(\beta S(t) - \gamma)$ does not change sign. As a consequence, $I(t)$ is monotone. See Figure 2.4. This indicates that an SIS model is not capable to catch the rise and fall pattern of a typical disease outbreak.

In the preceding discussions, we notice that, when the value of $\mathcal{R}_0$ increases from $\mathcal{R}_0 < 1$ to $\mathcal{R}_0 > 1$, behaviors of solutions to system (2.20) in the feasible region undergo qualitative changes in both the number of equilibria and their stability. We say that system (2.20) undergoes a *bifurcation* and $\mathcal{R} = 1$ is the bifurcation value.

A simple geometric mechanism for this bifurcation can be seen by observing the changes in the parabola defined in (2.22) as we vary N_0 from $N_0 < \rho/\beta$ ($\mathcal{R}_0 < 1$) to $N_0 > \rho/\beta$ ($\mathcal{R}_0 > 1$), and how the equilibrium $I_2^* = N_0 - \rho/\beta$ increases from left of the origin when $N_0 < \rho/\beta$ ($\mathcal{R}_0 < 1$), merges with $I_1^* = 0$ when $N_0 = \rho/\beta$ ($\mathcal{R}_0 = 1$), and then emerges right of the origin when $N_0 > \rho/\beta$ ($\mathcal{R}_0 > 1$). The graph of $f(I)$ also explains the changes in stability that accompany the changes in the number of equilibria.

In the next section, we continue the discussion of bifurcation and show how to represent it graphically in a bifurcation diagram.

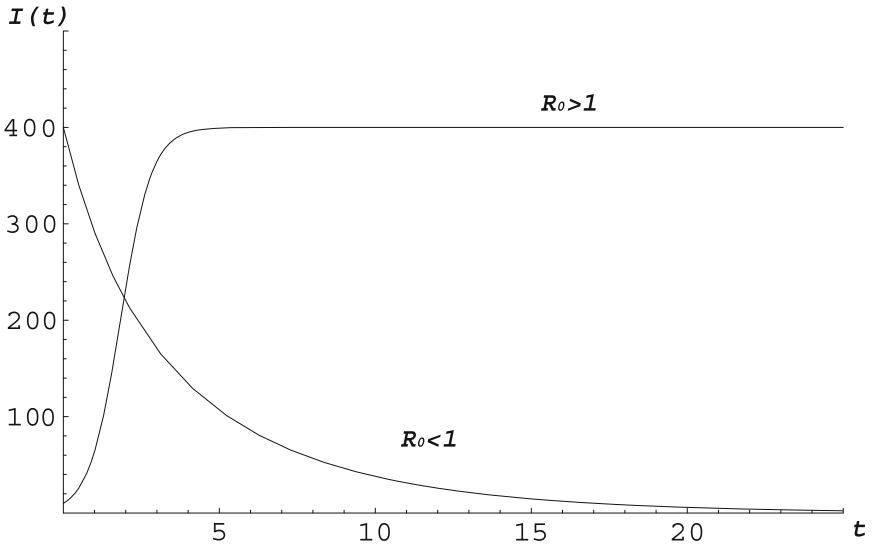

Figure 2.4: Time plots of $I(t)$.

Exercises.

(1) Prove the results in Proposition 2.2.1.

(2) Consider an ODE in $\mathbb{R}^n$,

$$x' = f(x)$$

and assume that f is a C^1 function. Suppose a solution $x(t) \to \bar{x}$ as $t \to \infty$. Show that $\bar{x}$ is an equilibrium, namely, $f(\bar{x}) = 0$.

(3) Vary N_0 from $N_0 < \rho/\beta$ to $N_0 > \rho/\beta$ and observe the changes in the parabola defined in (2.22). In the process, determine changes to the equilibrium $I_2^* = N_0 - \rho/\beta$ and to the stability of both $I_1^* = 0$ and I_2^*.

(4) Apply the phase-line analysis to an SIS with demography as depicted in Figure 2.5.

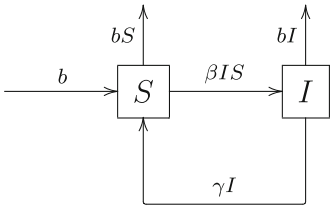

Figure 2.5: Transfer diagram for an SIS model with demography.

2.3 A Model with Demography

Consider the following modified Kermack–McKendrick model with demography:

Here, the birth and death processes are assumed to have the same rate constant b, and the disease is not fatal. The total population is kept as a constant, which is already scaled to 1. The differential equations for the model are:

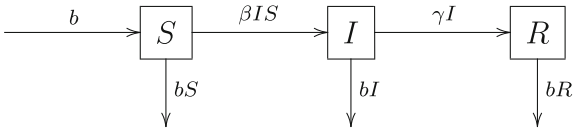

Figure 2.6: Transfer diagram for a model with demography.

$$\begin{aligned} S' &= b - \beta IS - bS \\ I' &= \beta IS - \gamma I - bI \\ R' &= \gamma I - bR. \end{aligned} \tag{2.24}$$

The feasible region for model (2.24) is:

$$G = \{(S, I, R) \in \mathbb{R}^3_+ \mid S + I + R = 1\}.$$

We would like to know if the threshold theorem in the previous section still holds for this model with the basic reproduction number $\mathcal{R}_0 = \frac{\beta}{\gamma+b}$ (see Section 1.4.9). Because of the conservation law $S + I + R = 1$, we will be able to reduce the number of equations by 1. System (2.24) is in fact a 2-dimensional system. To

simplify our analysis, we can ignore the R equation since the first two equations in (2.24) do not contain R. Once behaviors of $(S(t), I(t))$ are known, those of $R(t)$ can be readily obtained from $R = 1 - S - I$. For this reason, we can consider the following equivalent system:

$$\begin{aligned} S' &= b - \beta IS - bS \\ I' &= \beta IS - \gamma I - bI \end{aligned} \tag{2.25}$$

in a 2-dimensional feasible region

$$\Gamma = \{(S, I) \in \mathbb{R}^2_+ \mid 0 \le S + I \le 1\}.$$

2.3.1 Disease-Free and Endemic Equilibria

Based on our experience in Section 2.3, longtime outcomes of the disease are manifested in the form of equilibria, or solutions that do not change in time. To find equilibria of (2.25), we set $S' = I' = 0$ and obtain a system of algebraic equations

$$\begin{aligned} b - \beta IS - bS &= 0 \\ \beta IS - \gamma I - bI &= 0. \end{aligned} \tag{2.26}$$

Solving these equations, we obtain two possible equilibria: $P_0 = (1, 0)$, the disease-free equilibrium, and $P^* = (S^*, I^*)$, the endemic equilibrium, where

$$S^* = \frac{b + \gamma}{\beta}, \quad I^* = \frac{b[\beta - (b + \gamma)]}{\beta(b + \gamma)}.$$

Note that P^* falls outside of the feasible region Γ if $\mathcal{R}_0 = \frac{\beta}{b+\gamma} < 1$, and coincides with P_0 when $\mathcal{R}_0 = 1$.

Proposition 2.3.1 *System (2.25) has two possible equilibria.*

(1) *If $\mathcal{R}_0 \le 1$, then $P_0 = (1, 0)$ is the only equilibrium in Γ.*

(2) *If $\mathcal{R}_0 > 1$, then both P_0 and the endemic equilibrium P^* exist in Γ.*

2.3.2 Local Stability Analysis of Equilibria

Local stabilities of P_0 and P^* determine the disease outcomes when initial conditions are close to those at the equilibrium. A standard method for investigating local stability is by the method of linearization, as explained in Section 3.2 of Chapter 3.

1. Stability of P_0. The Jacobian matrix of (2.25) at P_0 is

$$J(P_0) = \begin{bmatrix} -b & -\beta \\ 0 & \beta - (b+\gamma) \end{bmatrix}.$$

Because of the upper triangularity of the matrix, its eigenvalues are the same as the diagonal elements, $\lambda_1 = -b, \lambda_2 = \beta - (b+\gamma)$. Therefore, P_0 is locally asymptotically stable if $\lambda_2 < 0$, or if $\mathcal{R}_0 < 1$, and P_0 is a saddle (unstable) if $\mathcal{R}_0 > 1$. When $\mathcal{R}_0 = 1$, $\lambda_2 = 0$. In this case, P_0 is no longer a hyperbolic equilibrium, and the method of linearization is not applicable. The stability of P_0 when $\mathcal{R}_0 = 1$ will be dealt with using the method of Lyapunov functions in Section 3.3.

2. Stability of P^*. The Jacobian matrix at $P^* = (S^*, I^*)$ is

$$J(P^*) = \begin{bmatrix} -\beta I^* - b & -\beta S^* \\ \beta I^* & 0 \end{bmatrix}.$$

Finding eigenvalues of this matrix is more involved than that of $J(P_0)$. We will use the Routh–Hurwitz conditions in Section 3.2 to determine the stability. Straightforward calculation leads to

$$\operatorname{tr}(J(P^*)) = -\beta I^* - b = -\frac{b}{S^*} < 0, \tag{2.27}$$

$$\det(J(P^*)) = \beta I^* S^* > 0, \quad \text{if } \mathcal{R}_0 > 1. \tag{2.28}$$

By the Routh–Hurwitz criteria, we know that P^* is locally asymptotically stable if and only if $\mathcal{R}_0 > 1$, or as long as it exists in Γ.

2.3.3 Bifurcation Digram

We see in Sections 2.3.1 and 2.3.2 that the number of equilibria in Γ, together with their local stability, is determined by the values

of $\mathcal{R}_0$. The model (2.25) undergoes a bifurcation at $\mathcal{R}_0 = 1$, as we have seen in Section 2.2. This bifurcation can be depicted graphically in a bifurcation diagram, as shown in Figure 2.7. In the bifurcation diagram, the horizontal axis is the values of the bifurcation parameter $\mathcal{R}_0$, with the bifurcation value $\mathcal{R}_0 = 1$ marked, and the vertical axis is for values of I^* at an equilibrium. A stable equilibrium is represented by a solid line and an unstable one by a dashed line.

We make the following observations about the bifurcation diagram:

(1) For $0 < \mathcal{R}_0 < 1$, there is only one equilibrium, P_0, and it is asymptotically stable. We mark P_0 by a solid line.

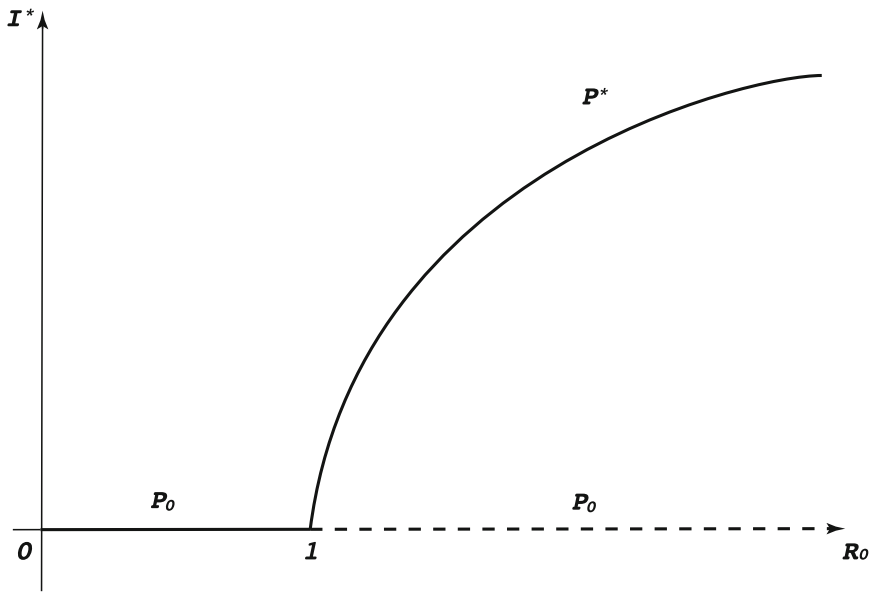

Figure 2.7: Bifurcation diagram for a model with demography.

(2) $\mathcal{R}_0 = 1$ is a bifurcation value; as $\mathcal{R}_0$ increases across 1, P_0 continues to exist and a new equilibrium P^* comes to existence in the feasible region Γ. Furthermore, P_0 loses its stability when $\mathcal{R}_0 > 1$ and P^* gains stability as it comes into

existence. We mark P_0 by a dashed line and P^* by a solid curve.

The type of bifurcation shown in Figure 2.7 is called a *transcritical* bifurcation, a very common bifurcation that occurs in many epidemic models.

2.3.4 Establishing the Global Stability of P_0: the Method of Lyapunov–LaSalle

As we have seen in Section 2.2, when $\mathcal{R}_0 < 1$, all solutions converge to the disease-free equilibrium P_0. We show that the same result holds for model (2.25). In this case, we say that P_0 is *globally stable* in the feasible region Γ. The method we use to show the global stability is the method of Lyapunov–LaSalle. Consider a Lyapunov function

$$L(S, I) = I.$$

Its derivative along a solution $(S(t), I(t))$ is

$$\begin{aligned} \frac{dL}{dt} = \frac{dI}{dt} &= I(\beta S - \gamma - b) \leq I(\beta - \gamma - b) \\ &\leq 0, \quad \text{if } \mathcal{R}_0 \leq 1. \end{aligned} \tag{2.29}$$

Therefore, LaSalle's Invariance Principle (Theorem 3.3.4, Section 3.3) implies that all limit points of solutions to (2.25) belong to the largest invariance set in

$$K = \{(S, I) \in \Gamma \ \mid \ \frac{dL}{dt} = 0\}.$$

From (2.29) we know that $\frac{dL}{dt} = 0$ if and only if either (1) $I = 0$ or (2) $\mathcal{R}_0 = 1$ and $S = \frac{\gamma+b}{\beta}$. In case (2), we necessarily have $S = \frac{\gamma+b}{\beta}, I = I^*$. In case (1), any solution of (2.25) staying in the set where $I = 0$ will satisfy $S' = b - bS$, and thus $S(t) \to 1$ as $t \to \infty$. In both cases, the only compact invariant set in the set K is the singleton $\{P_0\}$. This implies that all solutions in Γ converge to P_0. We can also show that the existence of the Lyapunov function L and the global convergence imply the local stability of

P_0. Therefore, we have shown that P_0 is globally stable in Γ when $\mathcal{R}_0 \leq 1$.

2.3.5 Establishing the Global Stability of P^*: Phase-Plane Analysis

Assuming that $\mathcal{R}_0 > 1$, we will show that all solutions with $I_0 > 0$ converge to the endemic equilibrium P^*. For this goal, we will use the Poincaré–Bendixson theory through the following steps:

Step 1. Show that system (2.25) has no nonconstant periodic solutions using the Bendixson–Dulac criteria (Theorem 3.6.5, Section 3.6).

Step 2. By the Poincaré–Bendixson Theorem (Theorem 3.6.2, Section 3.6) and the fact that P^* is the only equilibrium in the interior $\overset{\circ}{\Gamma}$ of Γ, all solutions with $I_0 > 0$ must have P^* as an omega limit point, and thus can get arbitrarily close to P^*.

Step 3. Since P^* is locally asymptotically stable, any solution that gets sufficiently close to P^* must converge to P^*. Therefore, all solutions with $I_0 > 0$ converge to P^*, and P^* is globally stable in $\overset{\circ}{\Gamma}$.

It only remains to show that (2.25) has no nonconstant periodic solutions. Write (2.25) as

$$\begin{aligned} S' &= P(S, I) \\ I' &= Q(S, I). \end{aligned} \tag{2.30}$$

Let $\alpha(S, I) = \frac{1}{I}$ be a Dulac multiplier. Then

$$\begin{aligned} \frac{\partial}{\partial S}(\alpha P) + \frac{\partial}{\partial I}(\alpha Q) &= \frac{\partial}{\partial S}\left(\frac{b}{I} - \beta S - \frac{bS}{I}\right) + \frac{\partial}{\partial I}(\beta S - b - \gamma) \\ &= -\beta - \frac{b}{I} < 0, \quad \text{in } \overset{\circ}{\Gamma}. \end{aligned}$$

Therefore, the Bendixson–Dulac condition holds in $\overset{\circ}{\Gamma}$ and no non-constant periodic solutions exist in $\overset{\circ}{\Gamma}$.

Summarizing the analyses in previous sections, we obtain a threshold theorem.

Theorem 2.3.2

(1) *If* $\mathcal{R}_0 \leq 1$, *the disease-free equilibrium is the only equilibrium in the feasible region* Γ, *and it is globally stable in* Γ.

(2) *If* $\mathcal{R}_0 > 1$, *then* P_0 *is unstable, and the unique endemic equilibrium* P^* *is globally stable in the interior* $\overset{\circ}{\Gamma}$.

Behaviors of solutions can be shown graphically in the SI-space, where each solution $(S(t), I(t))$ can be regarded as a parametric curve, called an *orbit*, starting from its initial point $(S(0), I(0))$. When the limiting behaviors of all orbits are shown, we obtain the *phase portrait* of system (2.24). The phase portraits of system (2.24) in both cases (a) and (b), as established in Theorem 2.3.2, are depicted in Figure 2.8. The type of analysis employed in this section to establish the phase portraits is called *phase-plane analysis*.

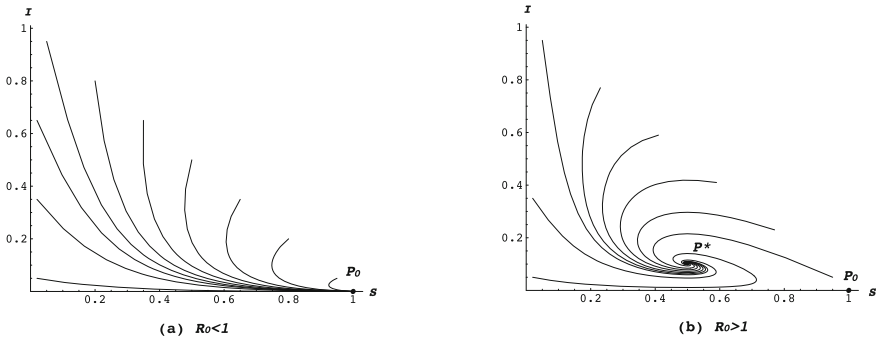

Figure 2.8: Phase portraits of an SIR model.

Exercises.

(1) Derive the characteristic equations for the eigenvalues of the Jacobian matrix $J(P^*)$ in Section 2.3.3, and use the quadratic formula to show that both eigenvalues are either negative real numbers or complex eigenvalues with negative real parts. This is a direct method to show asymptotic stability without using the Routh–Hurwitz conditions.

(2) In general, convergence of all solutions to an equilibrium does not necessarily imply local stability of the equilibrium. Show that, for model (2.24) when $\mathcal{R}_0 = 1$, the facts that $I'(t) \leq 0$ along all solutions and that all solutions converge to as $t \to \infty$ imply the local stability of the disease-free equilibrium P_0.

(3) Apply the phase-plane analysis to prove a threshold theorem for the SIRS model depicted in the transfer diagram in Figure 2.9, and draw the bifurcation diagram. Compare the basic reproduction number for this model that is derived in this section.

(4) Apply the phase-plane analysis to prove a threshold theorem for the SIR model with a nonlinear incidence as shown in the transfer diagram in Figure 2.10. Note that, because of the $\sqrt{I}$ term, the partial derivatives of the vector field are not continuous at $I = 0$, and the linearization at the disease-free equilibrium P_0 is not well defined. What other methods beside the linearization can you use to establish the local stability of P_0?

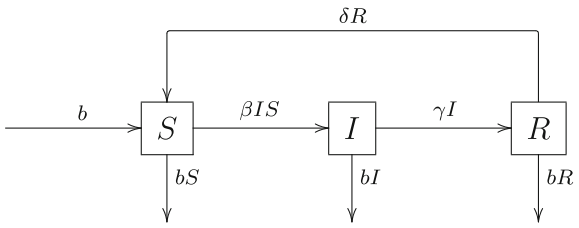

Figure 2.9: Transfer diagram for an SIRS model.

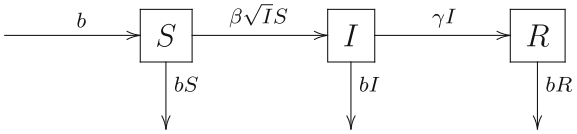

Figure 2.10: Transfer diagram for an SIR model with nonlinear incidence.

2.4 An SIR Model with Varying Total Population: Homogeneous Systems

Consider an SIR model whose transfer diagram is depicted in Figure 2.11.

In the model, $N = S + I + R$ denotes the total population. We assume that the birth process is in the form bN and the incidence is the standard incidence $\frac{\lambda IS}{N}$. The modeling equations are:

$$\begin{aligned} S' &= bN - \frac{\lambda IS}{N} - dS \\ I' &= \frac{\lambda IS}{N} - \gamma I - dI \\ R' &= \gamma I - dR. \end{aligned} \tag{2.31}$$

The total population N satisfies

$$N' = (b - d)N. \tag{2.32}$$

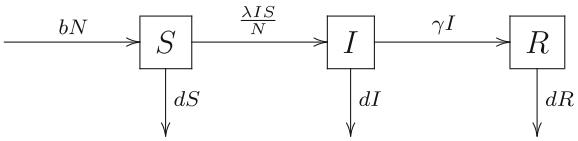

Figure 2.11: Transfer diagram for an SIR model.

If $b \neq d$, then $N(t)$ varies with time t. Thus (2.31), unlike (2.24), cannot be directly reduced to a 2-dimensional system. However, (2.31) is a homogeneous system of degree 1. This property allows us to transform it into a system that is reducible to 2 dimensions and can be analyzed using the phase-plane analysis in Section 2.3. We first establish a general framework for homogeneous systems.

A system of differential equations

$$x' = f(x), \quad x \in \mathbb{R}^n, \tag{2.33}$$

is said to be *homogeneous of degree* 1 if $f(x)$ satisfies

$$f(\lambda x) = \lambda f(x), \quad \lambda > 0, \ x \in \mathbb{R}^n. \tag{2.34}$$

Functions that satisfy (2.34) are called homogeneous of degree 1, and examples of this type of function include

$$f(x) = Ax, \quad \text{where } A \text{ is an } n \times n \text{ matrix} \tag{2.35}$$

$$f(x_1, x_2) = \frac{x_1 x_2}{x_1 + x_2}, \quad (x_1, x_2) \in \mathbb{R}^2. \tag{2.36}$$

Proposition 2.4.1 (Euler Identity) *Suppose that $f(x)$ is homogeneous of degree* 1*, namely, $f(x)$ satisfies (2.34). Then*

$$\sum_{i=1}^{n} \frac{\partial f(x)}{\partial x_i} x_i = f(x), \quad \textit{for } x \in \mathbb{R}^n. \tag{2.37}$$

Proof. Differentiating (2.34) with respect to λ we obtain

$$\sum_{i=1}^{n} \frac{\partial f(\lambda x)}{\partial x_i} x_i = f(x).$$

Setting $\lambda = 1$ we obtain the Euler Identity.

Suppose that (2.33) represents a biological model for which the nonnegative cone $\mathbb{R}^n_+$ is positively invariant. Then the homogeneity of f allows us to introduce a set of new variables

$$y_i = \frac{x_i}{N}, \quad i = 1, 2, \cdots, n,$$

where $N = x_1 + x_2 + \cdots + x_n \neq 0$, and $x_i \geq 0$. Then $y = (y_1, \cdots, y_n) \in \mathbb{R}^n_+ \setminus \{0\}$ satisfies

$$\begin{aligned} y' &= \frac{x'}{N} - \frac{x}{N^2} N' = \frac{1}{N} f(x) - \frac{x}{N^2} \sum_{i=1}^{n} f_i(x) \\ &= f\Big(\frac{x}{N}\Big) - \frac{x}{N} \sum_{i=1}^{n} f_i\Big(\frac{x}{N}\Big) \quad \text{(by (2.34))} \\ &= f(y) - y \sum_{i=1}^{n} f_i(y). \end{aligned}$$

Namely,

$$y' = f(y) - y \sum_{i=1}^{n} f_i(y), \tag{2.38}$$

and

$$\sum_{i=1}^{n} y_i = 1. \tag{2.39}$$

System (2.38) is the projection of (2.33) onto the hyperplane (simplex) $\sum_{i=1}^{n} y_i = 1$, so it is of dimension $n-1$.

Back to our model (2.31). It is straightforward to verify that function

$$f(S, I, R) = \Big(bN - \frac{\lambda IS}{N} - dS,\ \frac{\lambda IS}{N} - (d+\gamma)I,\ \gamma I - dR\Big)^T,$$

with $N = S + I + R$, is homogeneous of degree 1. Let

$$s = \frac{S}{N}, \quad i = \frac{I}{N}, \quad r = \frac{R}{N}. \tag{2.40}$$

Then, we can write a system for the fractional variables (s, i, r) following (2.38), or derive the system by direct differentiation. For instance,

$$\begin{aligned} s' &= \frac{S'}{N} - \frac{S}{N^2} N' = \frac{1}{N}\Big(bN - \frac{\lambda IS}{N} - dS\Big) - \frac{S}{N^2}(b-d)N \\ &= b - \lambda is - ds - s(b-d) = b - \lambda is - bs. \end{aligned}$$

Equations for i and r can be derived similarly. Therefore, we obtain the projected system

$$\begin{aligned} s' &= b - \lambda is - bs \\ i' &= \lambda is - (b+\gamma)i \\ r' &= \gamma i - br, \end{aligned} \tag{2.41}$$

with

$$s + i + r = 1. \tag{2.42}$$

Note that system (2.41) has the same form as system (2.24). We can apply the same phase-plane analysis as in Section 2.3 to arrive at the next threshold result. Let

$$\mathcal{R}_0 = \frac{\lambda}{b+\gamma},$$

and

$$\Gamma = \{(s,i,r) \in \mathbb{R}^3_+ \mid s + i + r = 1\}.$$

Note that Γ is a subset of the hyperplane $s + i + r = 1$ and its interior $\overset{\circ}{\Gamma}$ is also a subset of the hyperplane.

Theorem 2.4.2 *The global dynamics of the projected system* (2.41) *are completely determined by the basic reproduction number* $\mathcal{R}_0$. *More specifically:*

(1) *If* $\mathcal{R}_0 \leq 1$, *the disease-free equilibrium* $P_0 = (1,0,0)$ *is the only equilibrium in the feasible region* Γ, *and it is globally stable in* Γ;

(2) *If* $\mathcal{R}_0 > 1$, *then* P_0 *is unstable and the endemic equilibrium*

$$P^* = \left(\frac{b+\gamma}{\lambda}, \frac{b[\lambda - (b+\gamma)]}{\lambda(b+\gamma)}, \frac{\gamma[\lambda - (b+\gamma)]}{\lambda(b+\gamma)}\right)$$

is globally stable in the interior $\overset{\circ}{\Gamma}$.

With the dynamics of the projected system (2.41) completely determined in Theorem 2.4.2, we can turn to the original system (2.31). First, we note that, at any equilibrium of (2.31), we necessarily have $N'(t) = 0$. If $b \neq d$, this implies $N = 0$, and thus $S = I = R = 0$, which is biologically irrelevant. Therefore, system (2.31) has no biologically relevant equilibria! How do solutions to (2.31) behave? In general, they either exponentially go to zero or exponentially go to infinity, as we see below.

Case I. $b = d$. In this case, $N'(t) = 0$ and thus $N(t)$ is a constant, which can be scaled to 1. Thus (2.31) reduces to (2.41).

Case II. $b < d$. In this case, $N(t) \to 0$ exponentially as $t \to \infty$. Therefore, $S(t), I(t)$, and $R(t)$ converge to 0 exponentially as $t \to \infty$ since $0 \leq S(t), I(t), R(t) \leq N(t)$.

Case III. $b > d$. In this case, $N(t) \to \infty$ exponentially as $t \to \infty$. We consider two subcases.

(IIIa) If $\mathcal{R}_0 < 1$, then, as $t \to \infty$, $\frac{S(t)}{N(t)} = s(t) \to 1$, and thus $S(t) \to \infty$. From the I equation in (2.31) we obtain

$$I'(t) = [\lambda - (d + \gamma)]I + (\frac{S}{N} - 1)I.$$

Since $\frac{S}{N} - 1 \to 0$ exponentially, the behavior of $I(t)$ is determined by the principal part

$$I'(t) = [\lambda - (d + \gamma)]I.$$

Therefore,

(1) $I(t) \to 0$ exponentially if $\mathcal{R}_1 = \frac{\lambda}{d+\gamma} < 1$;

(2) $I(t) \to \infty$ exponentially if $\mathcal{R}_1 > 1$ (while $\frac{I(t)}{N(t)} \to 0$ exponentially).

In case (1), $I(t) \to 0$ exponentially, and thus $R(t)$ is determined by the principal part of the R equation

$$R' = -dR.$$

This implies that $R(t) \to 0$ if $R_1 < 1$. In case (2), there exists $a, \epsilon, T > 0$ such that $I(t) \geq ae^{\epsilon t}$ for $t \geq T$. From the R equation in (2.31),

$$R' = \gamma I - dR$$

we obtain, for $t > T$,

$$\begin{aligned} R(t) &= R(0)e^{-dt} + \gamma e^{-dt} \int_0^t I(\tau) e^{d\tau}\, d\tau \\ &\geq a\gamma e^{dt} \int_T^t e^{(\epsilon+d)\tau}\, d\tau = \frac{a\gamma}{d+\epsilon}\left(e^{\epsilon t} - e^{-d(t-T)+\epsilon T}\right) \\ &\to \infty, \quad \text{as } t \to \infty. \end{aligned}$$

Therefore, $S(t) \to \infty$, $I(t) \to \infty$, and $R(t) \to \infty$ as $t \to \infty$ if $R_1 > 1$.

(IIIb) If $\mathcal{R}_0 > 1$, then, as $t \to \infty$,

$$\frac{S(t)}{N(t)} = s(t) \to s^* = \frac{b+\gamma}{\lambda} > 0, \quad \frac{I(t)}{N(t)} = i(t) \to i^* > 0, \quad \text{and} \tag{2.43}$$

$$\frac{R(t)}{N(t)} = r(t) \to r^* > 0. \tag{2.44}$$

Therefore, $S(t) \to \infty$, $I(t) \to \infty$, and $R(t) \to \infty$ as $t \to \infty$.

Table 2.1: Summary of results for model (2.31). GAS = globally asymptotically stable, US = unstable, and DNE = does not exist.

b, d	$\mathcal{R}_0$[ac]	S, I, R, N		s, i, r	P_0[b]	P^*[c]
$b = d$	$\mathcal{R}_0 \le 1$	$N(t) = N_0$, $S(t) = N_0 s(t)$, $I(t) = N_0 i(t)$, $R(t) = N_0 r(t)$.		$s(t) \to 1$, $i(t) \to 0$, $r(t) \to 0$.	P_0 GAS	P^* DNE
	$\mathcal{R}_0 > 1$			$s(t) \to s^*$, $i(t) \to i^*$, $r(t) \to r^*$.	P_0 US	P^* GAS
$b < d$	$\mathcal{R}_0 \le 1$	$N(t) \to 0$, $S(t) \to 0$, $I(t) \to 0$, $R(t) \to 0$.		$s(t) \to 1$, $i(t) \to 0$, $r(t) \to 0$.	P_0 GAS	P^* DNE
	$\mathcal{R}_0 > 1$			$s(t) \to s^*$, $i(t) \to i^*$, $r(t) \to r^*$.	P_0 US	P^* GAS
$b > d$	$\mathcal{R}_0 \le 1$	$\mathcal{R}_1 \le 1$[d]	$N(t) \to \infty$, $S(t) \to \infty$, $I(t) \to 0$, $R(t) \to \infty$.	$s(t) \to 1$, $i(t) \to 0$, $r(t) \to 0$.	P_0 GAS	P^* DNE
		$\mathcal{R}_1 > 1$	$N(t) \to \infty$, $S(t) \to \infty$, $I(t) \to \infty$, $R(t) \to \infty$.	$s(t) \to s^*$, $i(t) \to i^*$, $r(t) \to r^*$.		
	$\mathcal{R}_0 > 1$	$N(t) \to \infty$, $S(t) \to \infty$, $I(t) \to \infty$, $R(t) \to \infty$.		$s(t) \to s^*$, $i(t) \to i^*$, $r(t) \to r^*$.	P_0 US	P^* GAS

[a] $\mathcal{R}_0 = \frac{\lambda}{(b+\gamma)}$.
[b] $P_0 = (1, 0, 0)$.
[c] $P^* = (s^*, i^*, r^*)$.
[d] $\mathcal{R}_1 = \frac{\lambda}{(d+\gamma)}$.

These results are summarized in Table 2.1. We note that the dynamics of the projected system (2.41) are determined by the basic reproduction number $\mathcal{R}_0$ and the behaviors of solutions of the original system (2.31) are determined by both $\mathcal{R}_0$ and $\mathcal{R}_1$.

To summarize, for model (2.31), disease outcomes are better described in terms of fractional variables, rather than the population size. In particular, we have the following conclusions:

(1) If $\mathcal{R}_0 = \frac{\lambda}{b+\gamma} \leq 1$, then the disease always dies out from the population in the sense that the fraction of the population that is infected (usually called the *disease prevalence*) goes to zero as $t \to \infty$.

(2) If $\mathcal{R}_0 > 1$, then any initial outbreak will lead to an endemic disease because the infectious fraction approaches a positive constant as $t \to \infty$.

Exercises.

(1) A function $x \mapsto f(x) \in \mathbb{R}^n$ defined for $x \in \mathbb{R}^n$ is homogeneous of degree $\delta > 0$ if f satisfies

$$f(\lambda x) = \lambda^\delta f(x), \quad \lambda > 0, \ x \in \mathbb{R}^n. \tag{2.45}$$

Derive the Euler Identity in this case. Give several examples of functions that are homogeneous of degree δ and verify that they satisfy the Euler Identity you have derived.

(2) Let $f : \mathbb{R}^n \to \mathbb{R}^n$ be homogeneous of degree $\delta > 0$. Let $\phi : \mathbb{R}^n \to \mathbb{R}$ be a scalar-valued function that is homogeneous of degree 1. Assume that ϕ is positive definite, namely:

$$\phi(x) \geq 0 \quad \text{and } \phi(x) = 0 \text{ if and only if } x = 0. \tag{2.46}$$

Let $x(t) \neq 0$ be a solution of the differential equation $x' = f(x)$, and

$$y(t) = \frac{x(t)}{\phi(x(t))}.$$

Derive the differential equation satisfied by $y(t)$, which is called the projected equation of $x' = f(x)$ onto the sphere

$$\phi(x) = 1.$$

(3) Using the method described in this section, analyze the models described in Figures 2.12 and 2.13.

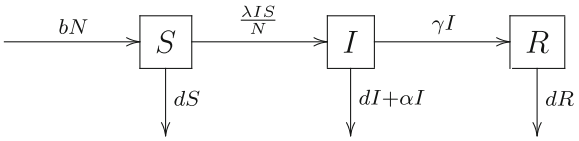

Figure 2.12: Transfer diagram for an SIR model with disease-caused death.

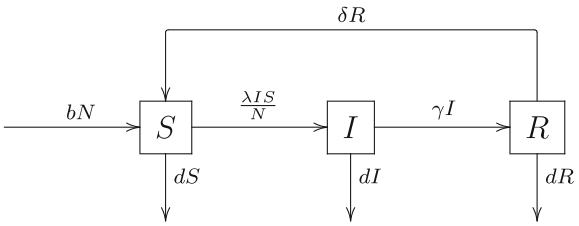

Figure 2.13: Transfer diagram for an SIRS model.

2.5 Ross–MacDonald Model for Malaria: A Monotone System

Malaria is caused by parasitic protozoans of the genus *Plasmodium*. The protozoans are transmitted to people through bites of infected female mosquitoes when they are taking a blood meal. While living in humans and mosquitoes, the protozoans go through long and complex life cycles, each of which is critical for their survival and transmission. Since its transmission critically depends on the disease *vector* mosquitoes, malaria is a typical example of a *vector-borne* disease. The transmission of the Plasmodium protozoans between humans and mosquitoes occurs through mosquito bites: when a healthy (female) mosquito bites an infected human, she takes in the protozoans with the blood and becomes infected; when an infected mosquito bites a healthy

human, a small amount of saliva is injected into the human body from the salivary gland of the mosquito, which malaria protozoans have invaded, and the protozoans enter the human body. In the human body, the protozoans first migrate into the liver where they mature and release their young into the bloodstream; there they will be picked up by mosquitoes taking a blood meal, and the infection cycle continues.

2.5.1 Modeling Malaria Transmission

The earliest work of mathematical modeling of malaria transmission dynamics was done in the early 1900 by R. Ross [52], who later was awarded the Nobel Prize for Medicine for his medical research on malaria. Ross models were further developed by G. MacDonald [42]. To formulate the Ross–MacDonald model for malaria transmission, we consider a human and a mosquito population, and assume, for simplicity, that both populations have a constant size H and V, respectively. Let S_h and I_h denote the susceptible and infectious humans, and S_v and I_v the susceptible and infectious female mosquitoes. Here, we only consider female mosquitoes because only female mosquitoes take blood meals. Important parameters used in the model are listed in Table 2.2.

When applying the model or its variations to malaria control, it is often useful to keep in mind the relative scales of values of the parameters. For instance, γ_v is typically very small since it is known that mosquitoes infected with malaria rarely recover. Also, human birth and death rates μ_h are relatively small compared to other parameters such as human recovery rate γ_h. Typically, the mean life expectancy for humans $1/\mu_h$ is between 60 and 85 years, while the mean recovery time for humans from malaria without serious complications is 1–2 weeks after treatment is given.

Table 2.2: Parameters in the Ross–MacDonald model for malaria transmission.

a:	biting rate (number of humans bitten per mosquito in a unit time)
b_1:	probability of human infection occurring from an infectious bite
b_2:	probability of mosquito infection occurring from an infectious bite
μ_h:	human birth and death rates
μ_v:	mosquitoes birth and death rates
γ_h:	human recovery rate
γ_v:	mosquito recovery rate

The transmission process of malaria between the human and mosquito populations is depicted in Figure 2.14.

The malaria incidence in the human population is calculated as

$$a \cdot b_1 \cdot \frac{S_h}{H} \cdot I_v,$$

which is interpreted as follows: the average number a of infectious bites per unit time multiplies the probability b_1 of an infectious bite will produce a human infection, multiplies the probability $\frac{S_h}{H}$ of a bite is on a susceptible human, and then multiplies the number I_V of infectious female mosquitoes.

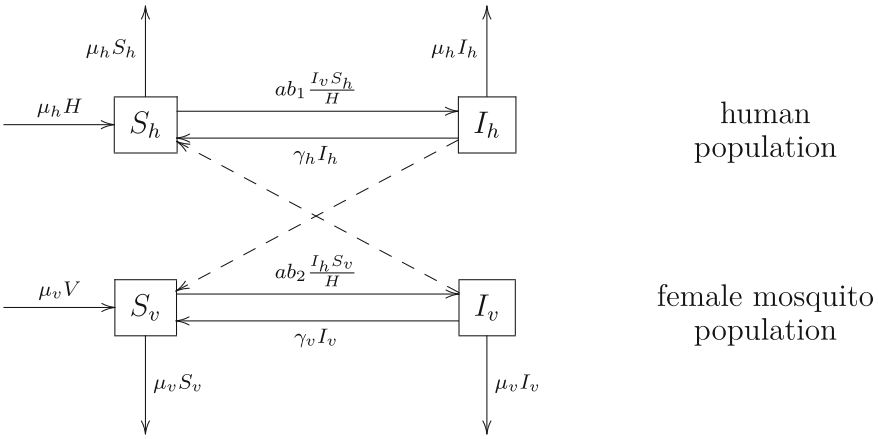

Figure 2.14: Transfer diagram for Ross–MacDonald model. Solid arrows indicate transfer. Dashed arrows indicate cross infection.

To derive the malaria incidence in the mosquito population, let $\tilde{a}$ denote the mosquito biting frequency, namely, the average number of mosquitoes that bit a human within a unit time. Then a and $\tilde{a}$ are related in the relation

$$a\,V \;=\; \tilde{a}\,H. \tag{2.47}$$

Using parameter $\tilde{a}$, the incidence in the mosquito population is given by

$$\tilde{a} \cdot b_2 \cdot \frac{S_v}{V} \cdot I_h.$$

Replacing $\tilde{a}$ by the biting rate a using relation (2.47), we obtain the malaria incidence in the mosquito population

$$a \cdot b_2 \cdot \frac{I_h}{H} S_v.$$

Using the transfer diagram, we can derive the following differential equations:

$$\begin{aligned}
S_h' &= \mu_h H - ab_1 \frac{S_h I_v}{H} - \mu_h S_h + \gamma_h I_h \\
I_h' &= ab_1 \frac{S_h I_v}{H} - \mu_h I_h - \gamma_h I_h \\
S_v' &= \mu_v V - ab_2 \frac{S_v I_h}{H} - \mu_v S_v + \gamma_v I_v \\
I_v' &= ab_2 \frac{S_v I_h}{H} - \mu_v I_v - \gamma_v I_v.
\end{aligned} \tag{2.48}$$

Based on our analysis in the previous section, we see that model (2.48) is a homogeneous system of degree 1. Using fractional variables

$$s_h = \frac{S_h}{H},\; i_h = \frac{I_h}{H},\; s_v = \frac{S_v}{V},\; i_v = \frac{I_v}{V}, \text{and } m = \frac{V}{H},$$

we can derive the following system:

$$\begin{aligned} s_h' &= \mu_h - ab_1 m s_h i_v - \mu_h s_h + \gamma_h i_h \\ i_h' &= ab_1 m s_h i_v - \mu_h i_h - \gamma_h i_h \\ s_v' &= \mu_v - ab_2 s_v i_h - \mu_v s_v + \gamma_v i_v \\ i_v' &= ab_2 s_v i_h - \mu_v i_v - \gamma_v i_v. \end{aligned} \tag{2.49}$$

Since $s_h + i_h = 1$ and $s_v + i_v = 1$, we may choose to keep only two of the four variables, say i_h and i_v, which are the prevalence in the human and mosquito populations, respectively. Let $x = i_h$ and $y = i_v$, then $s_h = 1 - x$ and $s_v = 1 - y$. Substituting into (2.49) we obtain the following equivalent system:

$$\begin{aligned} x' &= amb_1 y(1 - x) - \gamma_1 x \\ y' &= ab_2 x(1 - y) - \gamma_2 y. \end{aligned} \tag{2.50}$$

Here, we have set new parameters $\gamma_1 = \mu_h + \gamma_h$ and $\gamma_2 = \mu_v + \gamma_v$. We consider system (2.50) in the following bounded region:

$$\Gamma = \{(x, y) \in \mathbb{R}_+^2 \mid 0 \le x \le 1,\ 0 \le y \le 1\}. \tag{2.51}$$

By examining the direction of the vector field on the boundary of Γ, we can verify that Γ is positively invariant with respect to system (2.50).

2.5.2 Equilibria and the Basic Reproduction Number

System (2.50) has two possible equilibria: the disease-free equilibrium, $P_0 = (0, 0)$, which corresponds to the absence of infectious individuals in both human and mosquito populations, and an endemic equilibrium $P^* = (x^*, y^*)$, where x^*, y^* are given by

$$x^* = \frac{a^2 mb_1 b_2 - \gamma_1 \gamma_2}{ab_2(amb_1 + \gamma_1)}, \quad y^* = \frac{a^2 mb_1 b_2 - \gamma_1 \gamma_2}{amb_1(ab_2 + \gamma_2)}.$$

We note that $x^*, y^* > 0$ if and only if the following condition holds:

$$\mathcal{R}_0 = \frac{a^2 m b_1 b_2}{\gamma_1 \gamma_2} > 1, \tag{2.52}$$

where $\mathcal{R}_0$ is the basic reproduction number for malaria transmission. Heuristically, it can be interpreted as follows. A primary human case has a recovery rate γ_1, and the average infectious period is $\frac{1}{\gamma_1}$. During this time, the average number of mosquito bites from the susceptible fraction of mosquitoes is $\frac{a}{\gamma_1}$, which gives a total of $\frac{ab_2}{\gamma_1}$ infected mosquitoes. Each of these mosquitoes will survive for an average time $\frac{1}{\gamma_2}$ and produce a total of $\frac{a}{\gamma_2}$ bites, which will lead to a total of $\frac{amb_1}{\gamma_2}$ secondary human infections. Therefore, the average total of secondary human infections from a single primary human case is $\frac{ab_2}{\gamma_1}\frac{amb_1}{\gamma_2}$, giving the basic reproduction number in (2.52).

Local stability analysis can be carried out at each of the two equilibria, using techniques in Section 2.3.2. We arrive at the following result (details of verification are left as an exercise):

Theorem 2.5.1 *Let $\mathcal{R}_0$ be defined in (2.52).*

(1) *If $\mathcal{R}_0 \leq 1$, then system (2.50) has only the disease-free equilibrium $P_0 = (0, 0)$, and P_0 is globally asymptotically stable in Γ.*

(2) *If $\mathcal{R}_0 > 1$, then P_0 is unstable, and a unique endemic equilibrium $P^* = (x^*, y^*)$ exists and is globally asymptotically stable in the interior of Γ.*

2.5.3 Monotonicity and Global Dynamics

The global stability of the disease-free equilibrium P_0 when $\mathcal{R}_0 \leq 1$ and of the endemic equilibrium P^* when $\mathcal{R}_0 > 1$ can be established using the same analysis as in Section 2.3, using a Lyapunov function and the Poincaré–Bendixson theory. In this section, we show that system (2.50) is a monotone system, which allows us to use the machinery developed for monotone systems in Chapter 3 and establish the global stability.

We first show that system (2.50) is a monotone system by the definition in Section 3.8 of Chapter 3. The Jacobian matrix of (2.50) is

$$J(x,y) = \begin{bmatrix} -\gamma_1 - amb_1 y & amb_1(1-x) \\ ab_2(1-y) & -\gamma_2 - ab_2 x \end{bmatrix}.$$

We see that the off-diagonal terms are both positive, and thus $J(x,y)$ is a Metzler matrix. System (2.50) is a monotone system and is irreducible in the interior of Γ, and its solutions preserve the order defined by the positive quadrant.

Next, we verify that system (2.50) is strictly sublinear using the definition in Section 3.8. Let $0 < \lambda < 1$ and

$$F(x,y) = (P(x,y), Q(x,y)) = (amb_1 y(1-x) - \gamma_1 x,\ ab_2 x(1-y) - \gamma_2 y)$$

be the vector field of system (2.50). Then

$$\begin{aligned} P(\lambda x, \lambda y) &= amb_1 \lambda y(1-\lambda x) - \gamma_1 \lambda x \\ &= \lambda[amb_1 y(1-\lambda x) - \gamma_1 x] \\ &> \lambda[amb_1 y(1-x) - \gamma_1 x] = \lambda P(x,y). \end{aligned}$$

Similarly, we can verify that $Q(\lambda x, \lambda y) > \lambda Q(x,y)$, for $(x,y) \in \Gamma$ and $x > 0, y > 0$. This implies that $F(x,y)$ is strictly sublinear. We can thus apply Theorem 3.8.5 to prove the global stability of P_0 when $\mathcal{R}_0 \leq 1$, and that of P^* when $\mathcal{R}_0 > 1$.

2.5.4 Exercises

Gonorrhea is a sexually transmitted infection (STI). Gonorrhea is caused by the bacterium *Neisseria gonorrheae* and spread between people through sexual contact. Individuals who have had gonorrhea and received treatment can get reinfected. The Center for Disease Control and Prevention (CDC) estimated that about 400,000 cases of gonorrhea were reported in the U.S. in 2015. A mathematical model for gonorrhea transmission dynamics was formulated and analyzed in Lajmanovich and Yorke [36]. The model includes cross infections among a finite number of groups.

(1). Since gonorrhea infection yields little immune protection against reinfection, the transmission dynamics fit an SIS model.

(a) Explain the assumptions made in the transfer diagram in Figure 2.15 and use the diagram to derive a single population model for gonorrhea transmission.

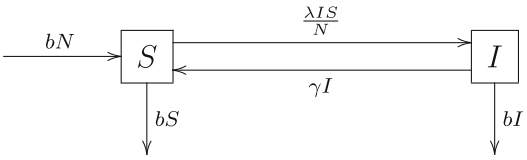

Figure 2.15: Transfer diagram for a single population gonorrhea model.

(b) Show that the total population $N = S + I$ remains a constant.

(c) Derive the system for the fractional variables $s = \frac{S}{N}$ and $i = \frac{I}{N}$.

(d) Discuss the feasible region of the system and its equilibria.

(e) Derive the basic reproduction number $\mathcal{R}_0$ for the system from its biological definition and show that the $\mathcal{R}_0$ you have derived is a threshold parameter: if $\mathcal{R}_0 \leq 1$, the system has only the disease-free equilibrium, and if $\mathcal{R}_0 > 1$, the system has a unique endemic equilibrium.

(f) Using the relation $s + i = 1$, reduce the system of two equations to a single equation for the variable i, and use the phase-line analysis to discuss the local and global stability of each equilibrium. Verify that if $\mathcal{R}_0 < 1$ then the disease-free equilibrium is globally asymptotically stable; if $\mathcal{R}_0 > 1$, then the disease-free equilibrium is unstable, and the endemic equilibrium is globally asymptotically stable.

(2). Sexual contacts within a population are not homogeneous; some people have more sexual partners than others. One way

to model heterogeneous mixing is to divide the population into groups and allow a greater degree of within-group contacts than intergroup contacts.

(a) Explain the assumptions that are made in the transfer diagram shown in Figure 2.16 for a two-group gonorrhea model, and use the transfer diagram to derive the model equations.

(b) Repeat the discussions (b)–(e) in the previous exercise for the new model you have derived.

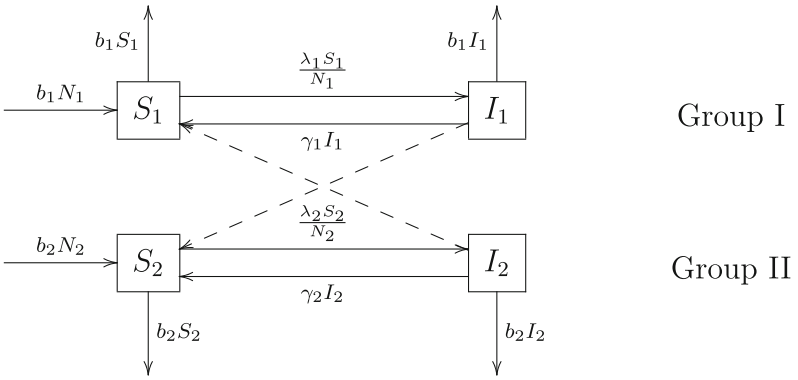

Figure 2.16: Transfer diagram for a two-group gonorrhea model. Here, $\lambda_1 = \lambda_{11}I_1 + \lambda_{21}I_2$ and $\lambda_2 = \lambda_{12}I_1 + \lambda_{22}I_2$. Solid arrows indicate transfer. Dashed arrows indicate cross infection.

(c) Using the relations $s_1 + i_1 = 1$ and $s_2 + i_2 = 1$ for fractional variables $s_k = S_k/N_k$ and $i_k = I_k/N_k$, $k = 1, 2$, reduce the 4-dimensional system to a 2-dimensional system for the prevalence variables i_1 and i_2.

(d) Carry out local stability analysis for each equilibrium using linearization. Verify that the value of $\mathcal{R}_0$ determines the stability of equilibria: if $\mathcal{R}_0 < 1$ then the disease-free equilibrium is locally asymptotically stable; if $\mathcal{R}_0 > 1$, then the disease-free equilibrium is unstable and the endemic equilibrium is locally asymptotically stable.

(e) Prove that the disease-free equilibrium is globally stable in the feasible region when $\mathcal{R}_0 \leq 1$, using the method of Lyapunov functions and the LaSalle Invariance Principle.

(f) Prove that the endemic equilibrium is globally asymptotically stable in the interior of the feasible region when $\mathcal{R}_0 > 1$, using the Poincaré–Bendixson Theorem and the Bendixson–Dulac criteria.

(g) Prove the global stability of the endemic equilibrium (when $\mathcal{R}_0 > 1$) by constructing a global Lyapunov function. **Hint**: you may start by considering $V(I_1, I_2) = c_1(I_1 - I_1^* \log I_1) + c_2(I_2 - I_2^* \log I_2)$, for suitable constants $c_1, c_2 > 0$.

(h) Show that the reduced system for i_1 and i_2 is a monotone system and is sublinear. Prove the global stability of the disease-free equilibrium (when $\mathcal{R}_0 \leq 1$) and of the endemic equilibrium (when $\mathcal{R}_0 > 1$) using the properties of monotone systems.

(3). Draw a transfer diagram for an n-group gonorrhea model, where $n \geq 1$ is an arbitrary integer. Derive a system of differential equations based on your transfer diagram. Derive a system for the fractional variables, and then reduce the system to a system for the n prevalence variables. Try to repeat the discussions in previous exercises on the equilibria and local stability. Can you derive the basic reproduction number $\mathcal{R}_0$? Can you show that, if $\mathcal{R}_0 > 1$, there exists a unique endemic equilibrium? How would you go about proving the global stability of the disease-free equilibrium and the endemic equilibrium? Which of the methods in previous exercises are applicable?

(4). Verify the local stability results for the Ross–MacDonald model in Theorem 2.5.1.

Chapter 3

Basic Mathematical Tools and Techniques

This chapter contains basic concepts and theories for differential equations, focusing on different approaches and methodologies for stability analysis. They provide the mathematical tools needed for model analysis described in earlier chapters. The ideal way to learn the materials in this chapter is through their applications in Chapter 2. For students who are interested in more in-depth reading on the theories of ordinary differential equations and finding more examples, exercises, as well as proofs, classical textbooks of Coddington and Levinson [11], Hale [24], Hartman [25], and Piccinini, Stampacchia and Vidossich [51] are excellent sources.

3.1 Stability of Equilibrium Solutions

Consider an open set D in the phase space $\mathbb{R}^n$, and a function $f \in C^1(D \to \mathbb{R}^n)$, called a *vector field*. A system of differential equations can be defined as

$$x' = f(x). \tag{3.1}$$

A *solution* to (3.1) in an interval $\mathcal{I} \subset \mathbb{R}$ is a differentiable function $\varphi : \mathcal{I} \to \mathbb{R}^n$ such that

$$\varphi'(t) = f(\varphi(t)).$$

M. Y. Li, *An Introduction to Mathematical Modeling of Infectious Diseases*, Mathematics of Planet Earth 2,
https://doi.org/10.1007/978-3-319-72122-4_3

When the vector field $f(x)$ is smooth (C^1), the fundamental theory of differential equations ensures that, for each initial point $x_0 \in D$, a unique solution $x(t, x_0)$ exists in an interval $\mathcal{I} = (-a, a)$ such that $x(0, x_0) = x_0$. We say such a solution starts from the initial point x_0. A solution can be extended to its maximal interval of existence. If a solution $x(t, x_0)$ remains in a compact subset of D throughout its maximal interval of existence (α, ω), then it exists for all $t \in \mathbb{R}$. The orbit of a solution $x(t, x_0)$ is the set

$$\gamma(x_0) = \{x(t, x_0) \ : \ t \in (\alpha, \omega)\}.$$

A solution $x(t)$ is called an *equilibrium*, or steady state, if it is a constant for all t, namely, $x(t) = \bar{x}$ for $t \in \mathbb{R}$. In this case, $\bar{x}$ satisfies $f(\bar{x}) = 0$ since $x'(t) \equiv 0$. A *periodic solution* $x(t)$ of period $T > 0$ satisfies $x(t + T) = x(t)$ for all $t \in \mathbb{R}$, and its orbit $\gamma = \{x(t) \ : \ 0 \le t < T\}$ is a simple closed smooth curve. For this reason, a periodic orbit is also called a closed orbit. For equilibria and periodic solutions, we are interested in their *stability* properties. Intuitively, an equilibrium $\bar{x}$ is stable if any solution starting close to $\bar{x}$ remains close to $\bar{x}$.

Definition. An equilibrium $\bar{x}$ of system (3.1) is

(1) *stable*, if for each ϵ-neighborhood $N(\bar{x}, \epsilon)$ of $\bar{x}$, there exists a δ-neighborhood $N(\bar{x}, \delta)$ of $\bar{x}$ such that $x_0 \in N(\bar{x}, \delta)$ implies $x(t, x_0) \in N(\bar{x}, \epsilon)$ for all $t \ge 0$;

(2) *asymptotically stable*, if $\bar{x}$ is stable and if there exists b-neighborhood $N(\bar{x}, b)$ such that $x_0 \in N(\bar{x}, b)$ implies $x(t, x_0) \to \bar{x}$ as $t \to \infty$.

In the above definition, an asymptotically stable equilibrium $\bar{x}$ is said to attract points in a neighborhood $N(\bar{x}, b)$. The set of points that are attracted by $\bar{x}$ is an open set and is called the *basin of attraction* of $\bar{x}$.

3.2 Stability Analysis by Linearization

A standard method of stability analysis is *linearization*. Let $\bar{x} = 0$ be an equilibrium, namely, $f(0) = 0$, and thus $f(x)$ can be written in Taylor expansion as

$$f(x) = A\,x + F(x), \tag{3.2}$$

where the matrix

$$A = \frac{\partial f}{\partial x}(0)$$

is the Jacobian matrix of f at 0, and

$$F(x) = f(x) - Ax.$$

Therefore $F(0) = 0$ and $\frac{\partial F}{\partial x}(0) = 0$. In the expansion (3.2), Ax is the linearization of f at 0 and $F(x)$ is the higher order term. The linearized system of (3.1) at the equilibrium 0 is

$$y' = Ay. \tag{3.3}$$

The next theorem is a standard result for the method of linearization.

Theorem 3.2.1 *Let A and F be given in (3.2). If $y = 0$ is asymptotically stable for the linearized system (3.3), then the equilibrium $\bar{x}$ is asymptotically stable for the nonlinear system (3.1).*

By Theorem 3.2.1, it is sufficient to investigate the asymptotic stability of an equilibrium for the linearized system.

Theorem 3.2.2 *The solution $y = 0$ is asymptotically stable for the linear system (3.3) if all eigenvalues of A have negative real parts.*

Verifying that an $n \times n$ matrix has n eigenvalues with negative real parts can be a challenging task when n is large, especially if entries of A contain non-numerical parameters. An algorithm by Routh–Hurwitz can be used to derive a set of necessary and sufficient conditions, typically called the Routh–Hurwitz conditions. For $n = 2, 3$, the Routh–Hurwitz conditions are as follows:

(1) All eigenvalues of a 2×2 matrix A have negative real parts if and only if

$$\operatorname{tr}(A) < 0 \quad \text{and} \quad \det(A) > 0. \tag{3.4}$$

(2) All eigenvalues of a 3×3 matrix A have negative real parts if and only if

$$\operatorname{tr}(A) < 0, \quad \det(A) < 0, \quad \text{and} \quad \operatorname{tr}(A)\, a_2 - \det(A) < 0, \tag{3.5}$$

where a_2 denotes the sum of 2×2 principal minors of A.

3.3 Stability Analysis Using Lyapunov Functions

Let $U \subset \mathbb{R}^n$ be a neighborhood of 0 and $V \in C^1(U \to \mathbb{R})$ a real-valued function. The gradient vector of $V(x)$ is

$$\operatorname{grad} V(x) = \left(\frac{\partial V}{\partial x_1}, \cdots, \frac{\partial V}{\partial x_n} \right).$$

Let $f(x)$ be the vector field of system (3.1). The derivative of V in the direction of f is defined as a dot product

$$\overset{*}{V}(x) = \operatorname{grad} V(x) \cdot f(x).$$

$\overset{*}{V}(x)$ is also called the Lyapunov derivative with respect to system (3.1). The function $V(x)$ is called a *Lyapunov function* of system (3.1) near an equilibrium $x = 0$ if $\overset{*}{V}(x) \leq 0$ for $x \in U$. Let $x(t)$ be a solution of system (3.1) that stays in U, then

$$\frac{d}{dt} V(x(t)) = \operatorname{grad} V(x(t)) \cdot x'(t) = \operatorname{grad} V(x(t)) \cdot f(x(t)) = \overset{*}{V}(x(t)) \leq 0.$$

Therefore, $V(x(t))$ decreases along a solution of system (3.1) in a neighborhood of $x = 0$. Theorems 3.3.1–3.3.3 describe a direct method of establishing stability using a Lyapunov function.

Theorem 3.3.1 *Suppose that a function $V(x)$ exists such that*

(1) $V(x) \geq 0$ *for* $x \in U$ *and* $V(x) = 0$ *if and only if* $x = 0$;

(2) $\overset{*}{V}(x) \leq 0$ *for* $x \in U$.

Then the equilibrium $x = 0$ of system (3.1) is locally stable.

Theorem 3.3.2 *Suppose that a function $V(x)$ exists such that*

(1) $V(x) \geq 0$ *for* $x \in U$ *and* $V(x) = 0$ *if and only if* $x = 0$;

(2) $\overset{*}{V}(x) \leq 0$ *for* $x \in U$ *and* $\overset{*}{V}(x) = 0$ *if and only if* $x = 0$.

Then the equilibrium $x = 0$ of system (3.1) is locally asymptotically stable.

A function V satisfying assumption (1) in the above theorems is called *positive definite* at $x = 0$. Similarly, the Lyapunov derivative $\overset{*}{V}(x)$ in the assumption (2) of Theorem 3.3.2 is *negative definite* at $x = 0$. If an equilibrium $\bar{x} \neq 0$, we may consider a change of variables $\tilde{x} = x - \bar{x}$ so that system (3.1) becomes

$$\tilde{x}' = g(\tilde{x}),$$

where $g(\tilde{x}) = f(\tilde{x} + \bar{x})$. Then $g(0) = f(\bar{x}) = 0$ and we have shifted the equilibrium $\bar{x}$ to 0, and Theorems 3.3.1 and 3.3.2 will be applicable. The next result deals with the instability of equilibrium $x = 0$.

Theorem 3.3.3 *Suppose that a function $V(x)$ exists such that*

(1) $V(0) = 0$ *and there exists sequence* $x_n \to 0$ *such that* $V(x_n) < 0$ *for all* n;

(2) $\overset{*}{V}(x) \leq 0$ *for* $x \in U$ *and* $\overset{*}{V}(x) = 0$ *if and only if* $x = 0$.

Then the equilibrium $x = 0$ of system (3.1) is unstable.

Let $G \subset \mathbb{R}^n$ be an open set. A function $V(x)$ is said to be a Lyapunov function with respect to G if

$$\overset{*}{V}(x) \leq 0, \quad \text{for } x \in G.$$

Let K be the largest invariant subset in the set $\{x \in G : \overset{*}{V}(x) = 0\}$. Since $V(x(t))$ decreases along a solution $x(t, x_0)$ of system (3.1), the omega-limit set of the solution,

$$\omega(x_0) = \{x \in G \ : \ \text{there exists } t_n \to \infty \text{ such that } x(t_n, x_0) \to x_1 \text{ as } n \to \infty\},$$

is contained in the set where $\overset{*}{V}(x) = 0$. Since omega-limit sets are invariant, we know $\omega(x_0)$ must be contained in the largest invariant subset K. This is the well-known LaSalle's Invariance Principle.

Theorem 3.3.4 *If a solution $x(t, x_0)$ stays entirely in G for $t \geq 0$, then its omega-limit set $\omega(x_0) \cap G \subset K$.*

Corollary 3.3.5 *If K contains a single point $\bar{x}$, then $\bar{x}$ is an equilibrium and solutions that stay entirely in G for $t \geq 0$ converge to $\bar{x}$ as $t \to \infty$.*

If we also know that $\bar{x}$ is locally stable, and that all solutions starting in G remain in G (in this case, G is said to be positively invariant), then Corollary 3.3.5 implies that $\bar{x}$ is *globally* asymptotically stable in the region G.

3.4 Stability of Periodic Solutions: The Floquet Theory

Let $x = p(t)$ be a nonconstant periodic solution of period T of system (3.1), and

$$\gamma = \{p(t) \ : \ 0 \leq t < T\}$$

be its orbit. Stability analysis of a periodic orbit is more involved than that of an equilibrium. First of all, we make an observation that the notion of Lyapunov stability we gave for equilibria in Section 3.1 is not appropriate for periodic solutions. The phase portrait of a nonlinear pendulum equation

$$x''(t) + \sin x(t) = 0 \tag{3.6}$$

consists of a family of periodic orbits arranged in concentric circles centered at the origin (see Figure 3.1). Each of these orbits should be considered "stable." However, each periodic orbit has a different period. Therefore, for two periodic solutions $p(t), q(t)$ whose orbits are close to each other, $|p(t) - q(t)|$ will not necessarily be small for all t, and thus neither can be stable according to the definition in Section 3.1. This situation necessitates the concept of orbital stability, in the sense that the distance between two orbits remains close while $|p(t) - q(t)|$ may not.

Definition. A periodic solution $x = P(t)$ is said to be

(1) *orbitally stable* if for all $\epsilon > 0$, there exists $\delta > 0$ such that $|x_0 - p(0)| < \delta$ implies $d(x(t, x_0), \gamma) < \epsilon$, where $d(x, \gamma) = \min_{y \in \gamma} |x - y|$ is the distance from x to γ.

(2) *orbitally asymptotically stable* if (a) it is orbitally stable and (b) there exists $\delta_1 > 0$ such that $|x_0 - p(0)| < \delta_1$ implies $d(x(t, x_0), \gamma) \to 0$ as $t \to \infty$. In this case, the periodic orbit is called a *limit cycle*.

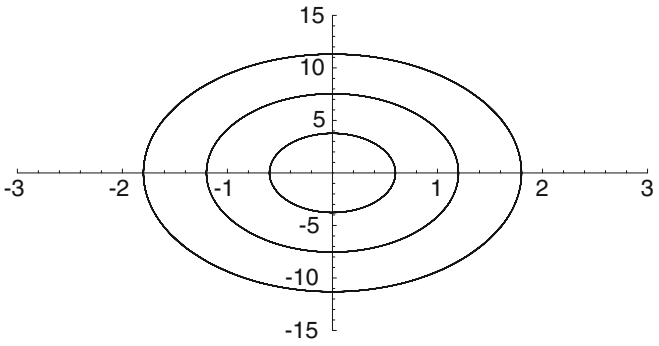

Figure 3.1: A family of nested periodic orbits of the pendulum equation; these orbits all have the same periods if the pendulum equation is linear, but different periods if the pendulum equation is nonlinear, as in equation (3.6).

By these definitions, the periodic orbits in Figure 3.1 are orbitally stable but not orbitally asymptotically stable, since the distance between any two periodic orbits remains a constant as t varies.

To analyze the stability of a periodic solution $x = p(t)$, we also use the method of linearization and consider the linearized system of (3.1) along $x = p(t)$,

$$y'(t) = \frac{\partial f}{\partial x}(p(t))\, y(t). \tag{3.7}$$

We note that system (3.7) is a linear system with periodic coefficients. Structures of the solution space of this type of system are described in the Floquet theory.

Theorem 3.4.1 *(***Floquet Theory***)*

(1) *A fundamental matrix of system (3.7) can be written in the form*

$$Y(t) = P(t)e^{Lt}, \tag{3.8}$$

where $P(t)$ is a $n \times n$ matrix-valued function periodic in t with period T, $P(0) = I_{n\times n}$, and L is a $n \times n$ constant matrix;

(2) *Eigenvalues of L are called Floquet exponents, and eigenvalues of $Y(T) = e^{LT}$ are called Floquet multipliers;*

(3) *System (3.7) has a nonconstant periodic solution of period T if and only if a Floquet multiplier is equal to 1, or equivalently, a Floquet exponent is equal to 0.*

We can verify by direct differentiation that $y(t) = p'(t)$ is a nonconstant periodic solution to system (3.7). Therefore, by Theorem 3.4.1-(3), one of its Floquet multipliers is 1, and we can write all Floquet multipliers of $x = p(t)$ as

$$1,\ \lambda_1,\ \ldots,\ \lambda_{n-1}. \tag{3.9}$$

A fundamental result in the theory of nonlinear differential equations states that $x = p(t)$ is asymptotically stable if the remain-

ing $n-1$ Floquet multipliers, $\lambda_1, \ldots, \lambda_{n-1}$, all have modulus less than 1.

Theorem 3.4.2 *The periodic solution $x = p(t)$ is orbitally asymptotically stable if the Floquet multipliers $\lambda_1, \ldots, \lambda_{n-1}$ in (3.9) have modulus less than* 1.

While Theorem 3.4.2 is a fundamental stability result, we point out that estimation of Floquet multipliers is not an easy task. A method of Poincaré for 2-dimensional systems will be given in Section 3.6. A generalization to higher dimensional systems was developed by J. S. Muldowney [47].

3.5 Global Dynamics of 1-Dimensional Systems: Phase-Line Analysis

Consider a scalar differential equation

$$x' = f(x), \tag{3.10}$$

where $f \in C^1(\mathbb{R} \to \mathbb{R})$ is a real-valued function. Stability analysis of this class of equations can be done using a graphical method called the *phase-line analysis*. Suppose the graph of f is as shown in Figure 3.2. Then, each intersection of the graph with the x-axis is a zero of $f(x)$, and thus is an equilibrium of equation (3.10). If between two consecutive zeros of f, the graph is above the x-axis, and thus $f(x) > 0$, the a solution $x(t, x_0)$ with x_0 in this interval satisfies $x'(t) = f(x(t)) > 0$, and $x(t, x_0)$ is monotonically increasing and converges to the equilibrium on the right as $t \to \infty$. Similarly, if the graph of f is below the x-axis, then $x(t, x_0)$ converges to the equilibrium on the left as $t \to \infty$. Also observe that, if the derivative $f'(\bar{x}) < 0$ at an equilibrium $\bar{x}$, then the slope of the tangent line to the graph at $\bar{x}$ is negative, solutions near $\bar{x}$ will converge to $\bar{x}$, and hence $\bar{x}$ is stable. On the other hand, if $f'(\bar{x}) > 0$, then $\bar{x}$ is unstable since solutions near $\bar{x}$ move away from $\bar{x}$ in this case. These observations are summarized in the next result.

Proposition 3.5.1

(1) *An equilibrium* $\bar{x}$ *of equation* (3.10) *satisfies* $f(\bar{x}) = 0$*;*

(2) *If* $f(x) > 0$ *for* $x \in (a, b)$*, then solutions starting in* (a, b) *monotonically increase; if* $f(x) < 0$ *for* $x \in (a, b)$*, then solutions starting in* (a, b) *monotonically decrease;*

(3) *If* $f'(\bar{x}) < 0$ *then the equilibrium* $\bar{x}$ *is stable; if* $f'(\bar{x}) > 0$ *then* $\bar{x}$ *is unstable.*

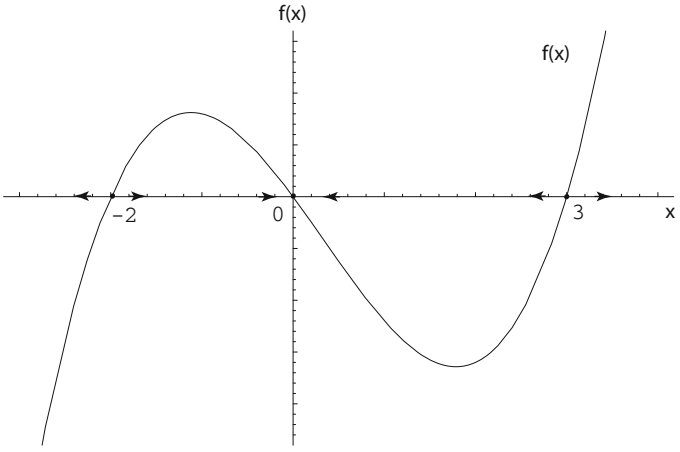

Figure 3.2: A graphical demonstration of phase-line analysis.

As an example, let us consider the logistic equation for population growth

$$N'(t) = rN(t)\left[1 - \frac{N(t)}{K}\right], \tag{3.11}$$

where $r > 0$ is the intrinsic growth rate and K is the carrying capacity. Let

$$f(N) = rN(t)\left[1 - \frac{N(t)}{K}\right].$$

The graph of $f(N)$ intersects the N-axis at two equilibria $N = 0$ and $N = K$. Assume that $r > 0$. Then the graph is above the N-axis between 0 and K, and below the N-axis outside $[0, K]$, see Figure 3.3.

By Proposition 3.5.1, we know that, if $r > 0$ then equilibrium $N = 0$ is unstable and $N = K$ is stable. Furthermore, solutions $N(t, N_0)$ with $0 < N_0 < K$ increase monotonically and converge to $N = K$ as $t \to \infty$, and solutions $N(t, N_0)$ with $N_0 > K$ decrease monotonically and converge to $N = K$ as $t \to \infty$. This allows us to produce the time plots for solutions $N(t, N_0)$ for different N_0, see Figure 3.4.

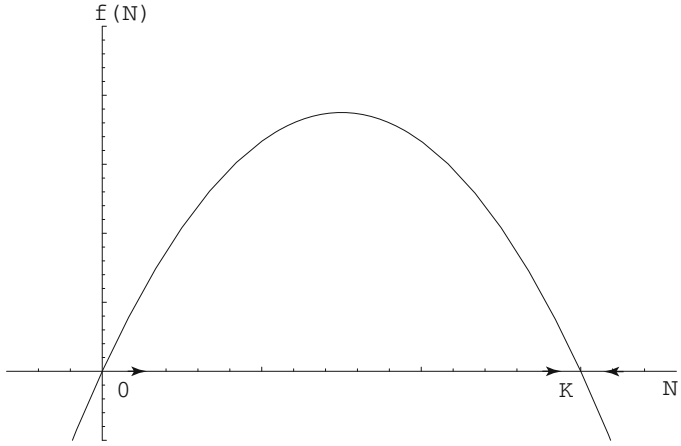

Figure 3.3: Phase-line analysis for the logistic equation when $r > 0$. The equilibrium $N = 0$ is unstable and the equilibrium at the carrying capacity $N = K$ is stable.

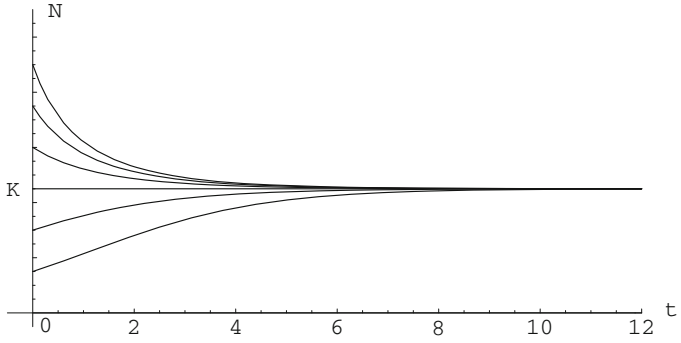

Figure 3.4: Time plots of solutions to the logistic equation when $r > 0$. The equilibrium $N = 0$ is unstable since nearby solutions move away from it, while the equilibrium $N = K$ is asymptotically stable since all nearby solutions converge to it as $t \to \infty$.

3.6 Global Dynamics of 2-Dimensional Systems: Phase-Plane Analysis

We consider a 2-dimensional system of differential equations

$$x' = f(x), \tag{3.12}$$

where $f \in C^1(\mathbb{R}^2 \to \mathbb{R}^2)$. We assume that all solutions to system (3.12) exist for all time $t \geq 0$ and investigate their asymptotic behaviors as $t \to \infty$. We first describe some important concepts:

Definition. Let $x(t, x_0)$ be a solution to system (3.12).

(1) The positive semi-orbit of $x(t, x_0)$ is $\gamma^+(x_0) = \{x(t, x_0) \mid t \geq 0\}$;

(2) The negative semi-orbit of $x(t, x_0)$ is $\gamma^-(x_0) = \{x(t, x_0) \mid t \leq 0\}$;

(3) The orbit of $x(t, x_0)$ is $\gamma(x_0) = \{x(t, x_0) \mid t \in \mathbb{R}\} = \gamma^+(x_0) \cup \gamma^-(x_0)$.

Definition. Limit sets.

(1) The ω-limit set of $x(t, x_0)$ is

$$\omega(x_0) = \{x \mid \text{there exists } t_n \to \infty \text{ such that } x(t_n, x_0) \to x\}; \tag{3.13}$$

(2) The α-limit set of $x(t, x_0)$ is

$$\alpha(x_0) = \{x \mid \text{there exists } t_n \to -\infty \text{ such that } x(t_n, x_0) \to x\}. \tag{3.14}$$

Definition. A subset $K \subset \mathbb{R}^2$ is:

(1) positively invariant, if $x_0 \in K \implies x(t, x_0) \in K$, $t \geq 0$;

(2) negatively invariant, if $x_0 \in K \implies x(t, x_0) \in K$, $t \leq 0$;

(3) invariant, if it is both positively and negatively invariants, namely, $x_0 \in K \implies x(t, x_0) \in K$, $t \in \mathbb{R}$.

Theorem 3.6.1 *Properties of limit sets.*

(1) *A limit set is closed.*

(2) *If $\gamma^+(x_0)$ (or $\gamma^-(x_0)$) is bounded, then $\omega(x_0)$ (or $\alpha(x_0)$) is nonempty, compact, and connected.*

(3) *Limit sets are invariant.*

To investigate asymptotic behaviors of a solution $x(t, x_0)$, we try to characterize its limit sets. Examples of limit sets include a single equilibrium, a periodic orbit, a homoclinic orbit, or a heteroclinic cycle (Figure 3.5). A limit set in higher dimensional systems can also be very complicated: the Lorenz attractor in $\mathbb{R}^3$ is a well-known example and is closely related to chaotic dynamics. The qualitative theory of differential equations aims to classify all limit sets in a given system. In this respect, some of the best theories were developed for 2-dimensional systems, largely due to the work of Poincaré and Bendixson. These results are collectively known as the Poincaré–Bendixson theory.

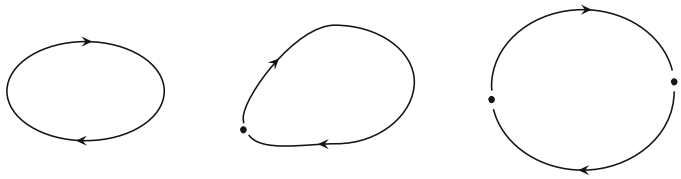

Figure 3.5: A limit set can be a periodic orbit, a homoclinic orbit to an equilibrium, or a heteroclinic cycle consisting multiple equilibria and their connecting orbits.

Theorem 3.6.2 (Poincaré–Bendixson Theorem) *Let $D \subset \mathbb{R}^2$ be open and $f \in C^1(D \to \mathbb{R}^2)$. Assume that*

(1) $\gamma^+(x_0) \subset K \subset D$ *and* K *is compact;*

(2) $\omega(x_0)$ *contains no equilibria.*

Then $\omega(x_0)$ *is a periodic orbit.*

The Poincaré–Bendixson Theorem is often used to prove the existence of periodic orbits.

Corollary 3.6.3 *Assume that*

(1) $K \subset D$ *is compact;*

(2) K *contains no equilibria;*

(3) K *contains a semi-orbit.*

Then K *contains a nonconstant periodic orbit.*

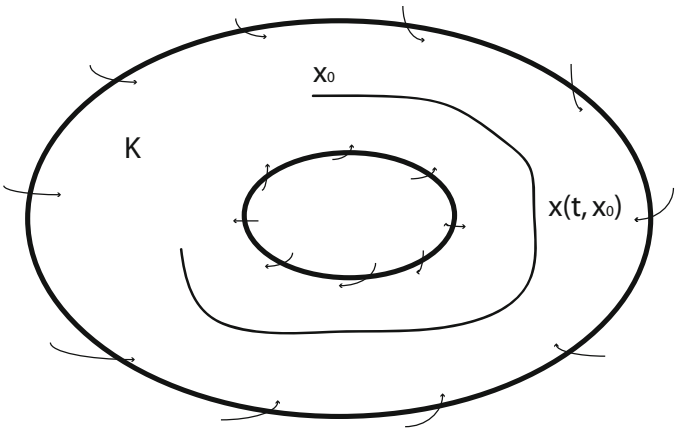

Figure 3.6: A bounded orbit $x(t, x_0)$ in a positively invariant annulus K that contains no equilibria. The omega-limit set of $x(t, x_0)$ is a periodic orbit.

We note that the Poincaré–Bendixson Theorem as stated here does not provide any information on $\omega(x_0)$ if $\omega(x_0)$ contains equilibria. In the case that all equilibria of the system are hyperbolic (therefore isolated), if $\omega(x_0)$ is not a single equilibrium, then it consists of a finite number of equilibria together with their

connecting orbits. See P. Hartman's ODE book [25] for related results. In cases where equilibria are non-hyperbolic, a limit set can contain infinitely many equilibria.

Exercise. Construct a planar system such that:

(a) the unit circle consists entirely of equilibria, and

(b) the omega-limit set of each nonequilibrium positive semi-orbit is the unit circle.

Theorem 3.6.4 (Poincaré's Stability Condition) *Assume that $n = 2$. A T-periodic solution $p(t)$ of system (3.12) is orbitally asymptotically stable if*

$$\int_0^T \operatorname{div} f(p(t))\, dt \; < \; 0. \tag{3.15}$$

Proof. Let $\lambda_1 = 1$ and λ_2 be the two Floquet multipliers of $x = p(t)$, as discussed in Section 3.5. Let $Y(t)$ be the fundamental matrix of the linearized system with respect to $x = p(t)$. Then λ_1, λ_2 are eigenvalues of $Y(T)$. By the Liouville's formula,

$$\lambda_2 = \lambda_1 \lambda_2 = \det Y(T) = e^{\int_0^T \operatorname{tr} \frac{\partial f}{\partial x}(p(t))dt} = e^{\int_0^T \operatorname{div} f(p(t))dt}.$$

Therefore, Poincaré's condition implies $0 < \lambda_2 < 1$, and hence the orbital asymptotic stability of $p(t)$, by Theorem 3.4.2.

Exercise. Suppose that $n = 2$, system (3.12) has only one equilibrium $\bar{x}$, and all solutions are forwardly bounded (for $t \geq 0$). Assume that, for any periodic orbit γ, the condition

$$\oint_\gamma \operatorname{div} f < 0$$

holds.
Show the following:

(a) If $\bar{x}$ is asymptotically stable, then the system has no periodic orbits and $\bar{x}$ is globally stable.

(b) If $\bar{x}$ is unstable, then the system has a unique periodic orbit and it is a limit cycle.

Theorem 3.6.5 (Bendixson's Negative Criterion) *Let $D \subset \mathbb{R}^2$ be a simply connected region. If*

$$\operatorname{div} f(x) < 0, \quad (or > 0) \quad x \in D, \tag{3.16}$$

then no periodic orbits can lie entirely in D.

Proof. Let $x = (u, v)$ and $f(x) = (P(u, v), Q(u, v))$. Suppose a periodic orbit

$$\gamma = \{(u(t), v(t)) \ : \ 0 \leq t < T\} \subset D.$$

Let G be the region enclosed in the interior of γ. Under the right orientation of γ, Green's Theorem implies

$$\begin{aligned} 0 > \iint_G \Big(\frac{\partial P}{\partial u} + \frac{\partial Q}{\partial v}\Big)\, dudv &= \oint_\gamma (Pdv - Qdu) = \int_0^T (Pv' - Qu')dt \\ &= \int_0^T (PQ - PQ)dt = 0, \end{aligned}$$

and the contradiction establishes the theorem.

Remarks.

(a) Bendixson's condition requires that $\operatorname{div}(f)$ does not change sign in D.

(b) From the proof, we can see that Bendixson's condition rules out periodic orbits, homoclinic orbits, and heteroclinic cycles.

Exercise. Construct an example to show that Bendixson's criterion as stated in Theorem 3.6.5 is no longer true in $\mathbb{R}^n$ for $n > 2$, namely, the negative divergence condition may not be able to rule out periodic orbits in dimensions higher than 2.

However, suitable conditions (not necessarily using the divergence) can be derived in higher dimensions that rule out periodic orbits. We refer interested readers to the work of Li and Muldowney [40].

Exercise. Show that if Bendixson's condition holds in an annular region $D \in \mathbb{R}^2$, then D can contain at most one periodic orbit. Can you generalize this result?

Corollary 3.6.6 ***(Dulac's Criteria)*** *Assume that $D \subset \mathbb{R}^2$ is simply connected. If there exists scalar-valued function $\alpha(x)$ such that*

$$\operatorname{div}(\alpha f)(x) < 0 \quad (or > 0) \quad x \in D,$$

then D contains no periodic orbits.

Proof. Follow the same proof of Theorem 3.6.5, apply the Green's Theorem to $(\alpha P, \alpha Q)$.

3.7 Uniform Persistence

Persistence is an important concept in population biology. It captures the longtime survival of a species, even when the population size of the species is quite low at times. For epidemic models, persistence of the model refers to a situation where the disease is endemic in a population. In this section, we formulate the concept of *uniform persistence* and present a theorem for establishing uniform persistence, adapted from the work of J. Hofbauer and J. So [29]. A more general result can be found in [17].

Consider a differential equation in $\mathbb{R}^n$

$$x' = f(x), \quad x \in \mathbb{R}^n. \tag{3.17}$$

We assume that $D \subset \mathbb{R}^n$ is an open subset, and function $f : D \to \mathbb{R}^n$ is such that the solution $x(t, x_0)$ to (3.17) with initial condition $x(0, x_0) = x_0$ exists for $t \geq 0$ and is unique, for $x_0 \in D$.

In the context of population models, we assume D is positively invariant with respect to solutions of (3.17), namely, $x_0 \in D$ implies that $x(t, x_0) \in D$ for $t \geq 0$. Let ∂D denote the boundary of D. Typically, for an epidemic model, $D = \mathbb{R}^n_+$, the nonnegative orthant of $\mathbb{R}^n$, and the boundary ∂D consists of the intersections of the coordinate hyperplanes with $\mathbb{R}^n_+$. The boundary ∂D may not be positively invariant for most epidemic models.

System (3.17) is said to be *uniformly persistent* (see [9, 56, 61]) if there exists constant $\epsilon_0 > 0$ such that all solutions $x(t, x_0)$ with $x_0 \in D$ satisfy

$$\liminf_{t\to\infty} d(x(t,x_0),\partial D) > \epsilon_0. \tag{3.18}$$

Here $d(x,K) = \min\{|x-y| \mid y \in K\}$ denotes the distance from a point x to a subset K. Weaker notions of persistence have been defined and used in the literature of population dynamics (see [61]).

Let $M \subset D$ be a compact invariant set, namely, M is a compact subset of D and $x_0 \in M$ implies that the solution $x(t,x_0)$ stays in M for $t \in \mathbb{R}$. The *stable set* of the set M is defined as

$$W^s(M) = \{x_0 \in D \mid d(x(t,x_0),M) \to 0, \text{ as } t \to \infty\}.$$

A global attractor A in D for system (3.17) is the largest compact invariant set in D.

The next result is a special case of Theorem 4.1 of [29].

Theorem 3.7.1 *Assume that D is positively invariant and contains a global attractor A. Then, system (3.17) is uniformly persistent if and only if*

(1) *the largest compact invariant set M in ∂D is isolated in A, and*

(2) $W^s(M) \subset \partial D$.

As an example, we consider the reduced SIR model (2.25)

$$\begin{aligned} S' &= b - \beta IS - bS \\ I' &= \beta IS - \gamma I - bI. \end{aligned}$$

Its feasible region

$$\Gamma = \{(S,I) \in \mathbb{R}^2_+ \mid 0 \le S + I \le 1\}$$

is bounded and positively invariant. The open set D will be understood as the interior $\overset{\circ}{\Gamma}$ of Γ and its boundary consists of the union of the S-axis, I-axis, and line $S + I = 1$. The definition of uniform persistence given above can be interpreted in this setting as the following: there exists $\epsilon_0 > 0$ such that

$$\liminf_{t\to\infty} S(t) > \epsilon_0, \quad \liminf_{t\to\infty} I(t) > \epsilon_0, \quad \liminf_{t\to\infty} 1 - S(t) - I(t) > \epsilon_0. \tag{3.19}$$

The disease is *endemic* if (2.25) is uniformly persistent, since in this case the infected subpopulation $I(t)$ will remain above a positive level ϵ_0 for all sufficiently large times.

We would like to show that the model is uniformly persistent when $\mathcal{R}_0 > 1$ using Theorem 3.7.1. We note that, being bounded and positively invariant, Γ contains a global attractor $A \neq \emptyset$. The largest compact invariant set on the boundary of Γ is the singleton $\{P_0\}$, which is also isolated, i.e., there is a neighborhood of P_0 that contains no other full orbit. Therefore, the model is uniformly persistent if the stable set $W^s(P_0)$ is contained in the boundary of Γ, or equivalently, if P_0 repels toward the interior of Γ. From Theorem 2.3.2 we know this can only happen if $\mathcal{R}_0 > 1$. This repelling property can be established by showing that the direction of the eigenvector of the Jacobian matrix $J(P_0)$ for the positive eigenvalue (when $\mathcal{R}_0 > 1$) is transversal to the S-axis. Another way to establish this repelling property is to use the same Lyapunov function in Section 2.3.4:

$$L(S, I) = I.$$

Its derivative along a solution $(S(t), I(t))$ of the model, as calculated in Section 2.3.4, is

$$\frac{dL}{dt} = \frac{dI}{dt} = I(\beta S - \gamma - b) = \beta I(S - \frac{1}{\mathcal{R}_0}).$$

Note that $P_0 = (1, 0)$, and $1/\mathcal{R}_0 < 1$ if $\mathcal{R}_0 > 1$. If we take initial conditions (S_0, I_0) in the interior of Γ and sufficiently close to P_0, namely, $I_0 > 0$ and S_0 sufficiently close to 1, we have $S_0 - 1/\mathcal{R}_0 > 0$ and thus $\frac{dL}{dt} > 0$ for small $t > 0$. This implies that $I(t)$ will increase for small $t > 0$ and P_0 repels in the direction of the interior of Γ. This gives the next result.

Theorem 3.7.2 *The SIR model* (2.25) *is uniformly persistent if and only if* $\mathcal{R}_0 > 1$.

3.8 Metzler Matrices and Monotone Systems

Let M be an $n \times n$ real matrix. We say that M is a Metzler matrix if all off-diagonal entries are nonnegative. Metzler matrices were introduced in the economics literature after L. Metzler, whose work provided the essential development of the theory. The importance of Metzler matrices is well recognized in other fields including biology and engineering. Development of Metzler matrices also coincides with that of M-matrices. A matrix M is an M-matrix if and only if $-M$ is Metzler.

For two real matrices $A = (a_{ij})$ and $B = (b_{ij})$, we say that

(a) $A \leq B$ if and only if $a_{ij} \leq b_{ij}$ for all $1 \leq i, j \leq n$.

(b) $A < B$ if and only if $a_{ij} < b_{ij}$ for all $1 \leq i, j \leq n$.

A matrix A is said to be *nonnegative* if $A \geq 0$, and *positive* if $A > 0$. Such a partial order can also be defined for vectors in $\mathbb{R}^n$, and we can define nonnegative vectors and positive vectors in a similar manner.

Letting $\lambda_1, \cdots \lambda_n$ be the eigenvalues of A, the *spectral radius* of A is defined as

$$\rho(A) = \max\{|\lambda_i| \ \mid \ i = 1, \cdots, n\}, \tag{3.20}$$

namely, the largest modulus of eigenvalues of A. The *stability modulus* of A is defined as

$$s(A) = \max\{\mathrm{Re}(\lambda_i) \ \mid \ i = 1, \cdots, n\}, \tag{3.21}$$

namely, the largest real part of eigenvalues of A. If $s(A) < 0$, we say that A is *stable*. In other words, a matrix is stable if all its eigenvalues have negative real parts.

A *permutation matrix* is a binary matrix that has exactly one entry equal to 1 in each row and each column and 0 elsewhere. A permutation matrix P represents a specific permutation of n elements and, when used to multiply another matrix A, can produce the permutation in the rows or columns of A. A nonnegative

matrix A is *reducible* if, for some permutation matrix P,

$$PAP^T = \begin{bmatrix} A_1 & 0 \\ A_2 & A_3 \end{bmatrix},$$

and A_1, A_3 are square matrices. Otherwise, A is *irreducible*. Irreducibility of A can be checked using the directed graph associated with A. The *directed graph* $G(A)$ associated with $A = (a_{ij})$ has vertices $\{1, 2, \cdots, n\}$ with a directed arc (i, j) from i to j if and only if $a_{ij} \neq 0$. It is *strongly connected* if any two distinct vertices are joined by an oriented path. Matrix A is irreducible if and only if $G(A)$ is strongly connected.

The next result is the well-known Perron–Frobenius Theorem.

Theorem 3.8.1 (Perron–Frobenius Theorem) *Let $A \geq 0$ be an $n \times n$ real matrix.*

(1) *The spectral radius $\rho(A)$ is an eigenvalue of A with respect to a nonnegative eigenvector;*

(2) *If A is also irreducible, then $\rho(A)$ is a simple eigenvalue, and the associated eigenvector is positive.*

The next result is the Perron–Frobenius Theorem for Metzler matrices.

Theorem 3.8.2 (Perron–Frobenius Theorem for Metzler Matrices) *Let A be an $n \times n$ Metzler matrix. Then the stability modulus $s(A)$ is an eigenvalue of A with respect to a nonnegative eigenvector. Furthermore, if A is also irreducible, then $s(A)$ is a simple eigenvalue with a positive eigenvector.*

Some useful properties of Metzler matrices are given in the next theorem.

Theorem 3.8.3 *Let A be an $n \times n$ Metzler matrix. Then the following statements are equivalent.*

(1) *A is stable;*

(2) *A is nonsingular and $-A^{-1} \geq 0$;*

(3) *For each* $b > 0$, *there exists* $x > 0$ *such that* $Ax + b = 0$;

(4) *There exists* $x \geq 0$ *such that* $Ax < 0$;

(5) *There exists* $x > 0$ *such that* $Ax < 0$.

Metzler matrices are related to the concept of monotone dynamical systems. A mapping $T : \mathbb{R}^n \to \mathbb{R}^n$ is said to be *monotone* if, for $x, y \in \mathbb{R}^n$,

$$x \leq y \quad \Longrightarrow \quad T(x) \leq T(y).$$

It is *strongly* monotone if, for $x, y \in \mathbb{R}^n$,

$$x \leq y \text{ and } x \neq y \quad \Longrightarrow \quad T(x) < T(y).$$

Let $D \in \mathbb{R}^n$ be a convex subset. Let $f : D \to \mathbb{R}^n$ be a C^1 vector field. Consider a system of differential equations in $\mathbb{R}^n$

$$x' = f(x). \tag{3.22}$$

Let $x(t, x_0)$ be the unique solution to system (3.22) such that $x(0, x_0) = x_0$. The *flow* φ_t generated by system (3.22) is defined as $\varphi_t(x_0) = x(t, x_0)$. System (3.22) is said to be monotone or strongly monotone if its flow φ_t is monotone or strongly monotone, respectively.

Theorem 3.8.4 *Let* f *be a* C^1 *vector field in* $\mathbb{R}^n$ *defined on a convex subset* $D \subset \mathbb{R}^n$. *Then system* (3.22) *is monotone if and only if, for each* $x \in D$, *the Jacobian matrix* $\frac{\partial f}{\partial x}(x)$ *is Metzler. Furthermore, if* $\frac{\partial f}{\partial x}(x)$ *is also irreducible, then* (3.22) *is strongly monotone.*

A mapping $f : \mathbb{R}^n \to \mathbb{R}^n$ is said to be *sublinear* if

$$0 < \lambda < 1, \ x \geq 0 \quad \Longrightarrow \quad f(\lambda x) \geq \lambda f(x),$$

and *strictly sublinear* if

$$0 < \lambda < 1, \ x > 0 \quad \Longrightarrow \quad f(\lambda x) > \lambda f(x).$$

The next theorem is a useful stability result for monotone systems.

Theorem 3.8.5 *Let $f : \mathbb{R}^n \to \mathbb{R}^n$ be a C^1 vector field. Assume*

(a) *The nonnegative orthant $\mathbb{R}^n_+$ is positively invariant with respect to system (3.22).*

(b) *System (3.22) is strongly monotone;*

(c) *$f(x)$ is strictly sublinear;*

(d) *Solutions to system (3.22) are bounded for $t \geq 0$.*

Then:

(1) *If $f(0) = 0$, then either all solutions in $\mathbb{R}^n_+$ tend to the equilibrium 0 or there exists an equilibrium $p > 0$ that is globally asymptotically stable in the region $\mathbb{R}^n_+ \setminus \{0\}$;*

(2) *If $f(0) > 0$, then there exists equilibrium $p > 0$ that is globally asymptotically stable in $\mathbb{R}^n_+$.*

Note: Section 3.8 is adapted from lecture notes of Professor Gauthier Sallet of Université Paul Verlaine, France.

Chapter 4

Parameter Estimation and Nonlinear Least-Squares Methods

In this chapter, we deal with the problem of parameter estimation. We have seen from Chapter 2 that the outcomes of an epidemic model critically depend on the values of the model parameters. While mathematical analysis of models we have discussed in Chapter 2 is very useful for understanding asymptotic behaviors and longtime qualitative outcomes, when models are confronted with disease data the problem is often for finite time, and an accurate estimation of parameter values is essential for reliable quantitative predictions within a finite time interval.

Certain parameters such as birth rates, natural death rates, and recovery rates can be estimated directly from population and epidemiological data. For instance, if the mean life expectancy at birth of the population under study is 70 years, then its natural death rate can be approximated as $d = 1/70 \approx 0.0143$, if the time unit is years. Similarly, if the mean infectious period of the disease is 6 months and the time unit is years, then the recovery rate is $\gamma = 1/0.5 = 2$. The time unit is important in such a conversion. If the time unit is months in these examples, then the natural death rate is $d = 1/(70 \times 12) \approx 0.00119$, and the recovery rate is $\gamma = 1/6 \approx 0.1667$.

Some parameters are not so easily estimated directly from data. Most notable is the transmission coefficient β in the incidence term βIS. If reliable yearly incidence or prevalence data for the disease is available, then we can obtain an estimation of β by best fitting the model outcome to the given data. For simple models,

M. Y. Li, *An Introduction to Mathematical Modeling of Infectious Diseases*, Mathematics of Planet Earth 2,
https://doi.org/10.1007/978-3-319-72122-4_4

this may be done by manually adjusting the values of β to get a satisfactory fit. For more complicated models, or for estimation of multiple parameters, a systematic approach for the fitting is desirable. This is often achieved through the *nonlinear least-squares method*. We will first introduce the classical method of linear least squares for curve fitting, and then examine a nonlinear version of the curve-fitting problem. With a basic understanding of these simple problems, we will then discuss nonlinear least-squares problems associated with parameter estimation of epidemic models.

4.1 Curve-Fitting and Linear Least-Squares Problem

Curve-fitting problems. Given data points (x_1, y_1), $\cdots$, (x_n, y_n), we consider the following curve-fitting problems:

(1) Find a straight line $y = ax + b$ that "best fits" all the data points.

(2) Find a m-th order polynomial

$$y = a_m x^m + a_{m-1} x^{m-1} + \cdots + a_1 x + a_0$$

that "best fits" all data points.

(3) Find a curve of form

$$y = a_0 f_0(x) + a_1 f_1(x) + \cdots + a_m f_m(x)$$

that "best fits" all data points. Here $f_0(x), f_1(x), \cdots, f_m(x)$ are given functions.

We see that Problem (1) is a special case of Problem (2), and Problem (2) is a special case of Problem (3) with $f_i(x) = x^k$, $k = 0, 1, \cdots, m$. For simplicity of presentation, we will use Problem (1) as an example. Problems (2) and (3) can be dealt with the same way.

Least-squares fitting. Suppose that $y = a_1 x + a_0$ is a line of the best fitting, also called a *line of regression*. We need to clarify the

meaning of best fitting. When $n > 2$, there is little hope for a line to pass through more than two data points, or in other words, for all the following equations to hold simultaneously:

$$\begin{aligned} y_1 &= a_1 x_1 + a_0 \\ y_2 &= a_1 x_2 + a_0 \\ &\cdots \\ y_n &= a_1 x_n + a_0. \end{aligned}$$

Instead, we look for a best-fitting line that minimizes the total error

$$d(a_0, a_1) = [y_1 - (a_1 x_1 + a_0)]^2 + \cdots + [y_n - (a_1 x_n + a_0)]^2. \quad (4.1)$$

	data	prediction	error
x_1	y_1	$a_1 x_1 + a_0$	$y_1 - (a_1 x_1 + d_0)$
x_2	y_2	$a_1 x_2 + a_0$	$y_2 - (a_1 x_2 + d_0)$
$\cdots$	$\cdots$	$\cdots$	$\cdots$
x_n	y_n	$a_1 x_n + a_0$	$y_n - (a_1 x_n + d_0)$

Table 4.1: Data, predictions, and errors.

From Table 4.1, we see that $d(a_0, a_1)$ measures the total error between data y_i and prediction $a_1 x_i + a_0$ for $i = 1, \cdots, n$. This problem is also a standard minimization problem: we look for a pair $(\hat{a}_0, \hat{a}_1)$ at which the function $d(a_0, a_1)$ achieves a minimum. The choice of the Euclidean norm for the measure of error gives rise to the term "least squares". It ensures that $d(a_0, a_1)$ is a differentiable function. It also allows the utilization of Euclidean dot product and orthogonal projection.

A mathematical formulation of the least-squares problem. Let

$$b = \begin{bmatrix} y_1 \\ \vdots \\ y_n \end{bmatrix}, \quad A = \begin{bmatrix} 1 & x_1 \\ \vdots & \vdots \\ 1 & x_n \end{bmatrix}, \quad x = \begin{bmatrix} a_0 \\ a_1 \end{bmatrix}.$$

Then a least-squares solution $(\hat{x}) = (\hat{a}_0, \hat{a}_1)^T$ satisfies

$$\|b - A\hat{x}\| \leq \|b - Ax\| \tag{4.2}$$

for all $x \in \mathbb{R}^2$. Here $\|\cdot\|$ denotes the Euclidean norm and the superscript T denotes the transposition of matrices and vectors. The expression in the error term (4.1) is in fact the square of the Euclidean norm $\|b - Ax\|^2$, and we use the fact that $\|b - Ax\|$ is minimized if and only if $\|b - Ax\|^2$ is minimized.

More generally, we allow $A_{m\times n}$ be an $m \times n$ matrix, and $b \in \mathbb{R}^m$. Then $\hat{x} \in \mathbb{R}^n$ is a *least-squares solution* of $Ax = b$ if $\hat{x}$ satisfies

$$\|b - A\hat{x}\| \leq \|b - Ax\| \tag{4.3}$$

for all $x \in \mathbb{R}^n$.

A least-squares solution $\hat{x}$ can be found based on geometrical observations. First we note that the set

$$\text{col}(A) = \{Ax \ : \ x \in \mathbb{R}^n\}$$

is the column space $\text{col}(A)$ of matrix A. Therefore, minimizing $d = \|b - Ax\|$ is equivalent to finding the distance from vector b to the subspace $\text{col}(A)$. From geometry, we know that such distance is achieved at the orthogonal projection of b onto the subspace $\text{col}(A)$,

$$\hat{b} = \text{Proj}_{\text{col}(A)} b.$$

This is illustrated in Figure 4.1. Therefore, the least-squares solution necessarily satisfies

$$A\hat{x} = \hat{b}. \tag{4.4}$$

It would be desirable to find a solution $\hat{x}$ of (4.4) without having to find the projection $\hat{b}$. Again, from geometry, we observe that $b - \hat{b}$ is orthogonal to the subspace $\text{col}(A)$, and thus $(b - A\hat{x}) \perp \text{col}(A)$, see Figure 4.1. In terms of the dot product, we have

$$(b - A\hat{x}) \cdot \text{all columns of } A = 0.$$

Written in matrix form, this relation becomes

$$A^T(b - A\hat{x}) = 0.$$

Based on these observations, we know that a least-squares solution $\hat{x}$ necessarily satisfies the following *normal system*:

$$A^T A\hat{x} = A^T b. \tag{4.5}$$

Theorem 4.1.1 *A least-squares solution $\hat{x}$ satisfies the normal system (4.5).*

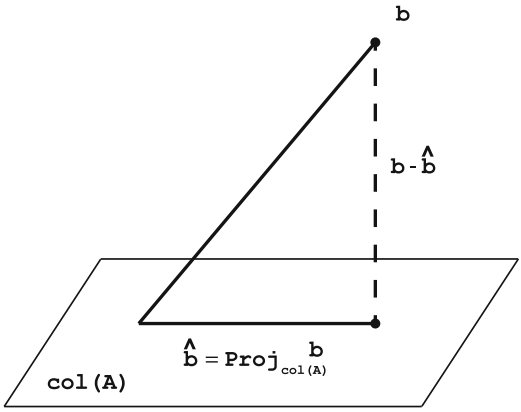

Figure 4.1: A geometric illustration of the least-squares solution.

A least-squares solution $\hat{x}$ may not be unique. However, when solutions to system (4.4) or (4.5) are unique, the least-squares solution must be unique.

Theorem 4.1.2 *The following statements are equivalent.*

(1) *The least-squares solution is unique for each $b \in \mathbb{R}^m$.*

(2) *The columns of A are linearly independent (A has full rank).*

(3) *Matrix $A^T A$ is invertible, and $\hat{x} = (A^T A)^{-1} A^T b$.*

Example 1. Find the line $y = a_0 + a_1 x$ that best fits the data points $(2, 1)$, $(5, 2)$, $(7, 3)$, and $(8, 3)$.

Solution. In this case,

$$A = \begin{bmatrix} 1 & 2 \\ 1 & 5 \\ 1 & 7 \\ 1 & 8 \end{bmatrix}, \quad b = \begin{bmatrix} 1 \\ 2 \\ 3 \\ 3 \end{bmatrix}, \quad x = \begin{bmatrix} a_0 \\ a_1 \end{bmatrix}.$$

The normal system $A^T Ax = A^T b$ becomes

$$\begin{bmatrix} 1 & 1 & 1 & 1 \\ 2 & 5 & 7 & 8 \end{bmatrix} \begin{bmatrix} 1 & 2 \\ 1 & 5 \\ 1 & 7 \\ 1 & 8 \end{bmatrix} \begin{bmatrix} a_0 \\ a_1 \end{bmatrix} = \begin{bmatrix} 1 & 1 & 1 & 1 \\ 2 & 5 & 7 & 8 \end{bmatrix} \begin{bmatrix} 1 \\ 2 \\ 3 \\ 3 \end{bmatrix},$$

namely,

$$\begin{bmatrix} 4 & 22 \\ 22 & 142 \end{bmatrix} \begin{bmatrix} a_0 \\ a_1 \end{bmatrix} = \begin{bmatrix} 9 \\ 57 \end{bmatrix}.$$

Therefore

$$\begin{bmatrix} a_0 \\ a_1 \end{bmatrix} = \begin{bmatrix} 4 & 22 \\ 22 & 142 \end{bmatrix}^{-1} \begin{bmatrix} 9 \\ 57 \end{bmatrix} = \frac{1}{84} \begin{bmatrix} 142 & -22 \\ -22 & 4 \end{bmatrix} \begin{bmatrix} 9 \\ 57 \end{bmatrix} = \begin{bmatrix} \frac{2}{7} \\ \frac{5}{14} \end{bmatrix}.$$

This gives $a_0 = \frac{2}{7}$, $a_1 = \frac{5}{14}$, and the least-squares line

$$y = \frac{2}{7} + \frac{5}{14}x.$$

See Figure 4.2.

Example 2. Find a quadratic curve that best fits the data points

$$(2, 1),\ (-1, 5),\ (6, 2),\ (4, -1).$$

Solution. A quadratic curve has the form

$$y = a_2 x^2 + a_1 x + a_0.$$

We want to find coefficients $(\hat{a}_0, \hat{a}_1, \hat{a}_2)$ such that

$$\begin{aligned} d = {} & [(\hat{a}_0 + 2\hat{a}_1 + 4\hat{a}_2) - 1]^2 + [(\hat{a}_0 + (-1)\hat{a}_1 + \hat{a}_2) - 5]^2 \\ & + [(\hat{a}_0 + 6\hat{a}_1 + 36\hat{a}_2) - 2]^2 + [(\hat{a}_0 + 4\hat{a}_1 + 16\hat{a}_2) - (-1)]^2 \end{aligned}$$

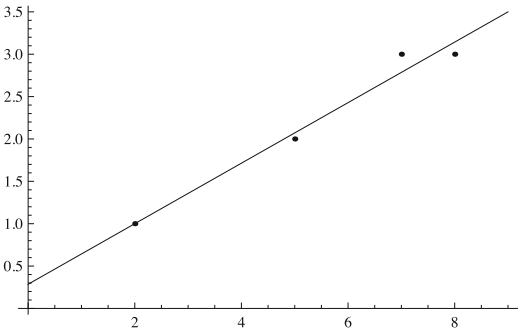

Figure 4.2: The least-squares line for Example 1.

is the smallest among all choices of (a_0, a_1, a_2). Let

$$A = \begin{bmatrix} 1 & x_1 & x_1^2 \\ 1 & x_2 & x_2^2 \\ 1 & x_3 & x_3^2 \\ 1 & x_4 & x_4^2 \end{bmatrix} = \begin{bmatrix} 1 & 2 & 4 \\ 1 & -1 & 1 \\ 1 & 6 & 36 \\ 1 & 4 & 16 \end{bmatrix}, \quad b = \begin{bmatrix} y_1 \\ y_2 \\ y_3 \\ y_4 \end{bmatrix} = \begin{bmatrix} 1 \\ 5 \\ 2 \\ -1 \end{bmatrix}, \quad x = \begin{bmatrix} a_0 \\ a_1 \\ a_2 \end{bmatrix}.$$

Then, the normal system $A^T Ax = A^T b$ becomes

$$\begin{bmatrix} 1 & 1 & 1 & 1 \\ 2 & -1 & 6 & 4 \\ 4 & 1 & 36 & 16 \end{bmatrix} \begin{bmatrix} 1 & 2 & 4 \\ 1 & -1 & 1 \\ 1 & 6 & 36 \\ 1 & 4 & 16 \end{bmatrix} \begin{bmatrix} a_0 \\ a_1 \\ a_2 \end{bmatrix} = \begin{bmatrix} 1 & 1 & 1 & 1 \\ 2 & -1 & 6 & 4 \\ 4 & 1 & 36 & 16 \end{bmatrix} \begin{bmatrix} 1 \\ 5 \\ 2 \\ -1 \end{bmatrix},$$

namely,

$$\begin{bmatrix} 4 & 11 & 57 \\ 11 & 57 & 287 \\ 57 & 287 & 1569 \end{bmatrix} \begin{bmatrix} a_0 \\ a_1 \\ a_2 \end{bmatrix} = \begin{bmatrix} 7 \\ 5 \\ 65 \end{bmatrix}.$$

The system has a unique solution

$$\hat{a}_0 = \frac{4871}{1639} \approx 2.9719, \quad \hat{a}_1 = -\frac{12515}{6556} \approx -1.909, \quad \hat{a}_2 = \frac{1853}{6556} \approx 0.2826,$$

and the unique least-squares quadratic curve for the given data points is

$$y = 0.2826x^2 - 1.909x + 2.9719.$$

See Figure 4.3.

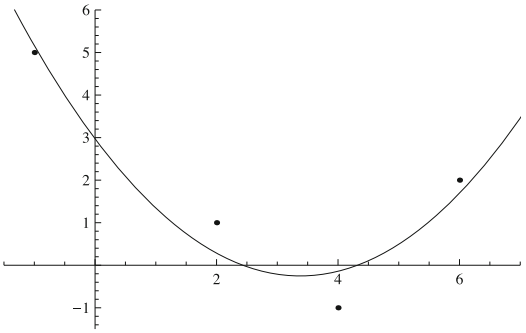

Figure 4.3: The least-squares parabola for Example 2.

We note that, in Example 2, we use nonlinear best-fit functions. Why do we call it a linear least-squares problem? The important characteristic of linear least-squares problems is that a best-fit function takes the form of linear combinations of basis functions, and finding the best-fit function means finding the best choice of coefficients (or parameters). In certain cases when the best-fit function has a nonlinear dependence on parameters, the method for linear least-squares problems can still be applied after a suitable transformation.

Example 3. Find the least-squares function of form

$$x(t) = a_0 e^{a_1 t}, \quad t > 0,\ a_0 > 0$$

for the data points

$$(t_1, x_1),\ (t_2, x_2),\ \cdots, (t_n, x_n), \quad x_1,\ x_2, \cdots, x_n > 0.$$

Solution. Let

$$y(t) = \ln x = \ln a_0 + a_1 t,$$

and

$$b_0 = \ln a_0, \quad b_1 = a_1, \quad y_1 = \ln x_1, \quad \cdots, \quad y_n = \ln x_n.$$

Then, we can first solve the following linear least-squares problem:

Find the least-squares curve of form

$$y(t) = b_0 + b_1 t, \quad t > 0$$

for data points $(t_1, y_1),\ \cdots,\ (t_n, y_n)$.

This problem can be solved using the linear least-squares method as in Example 1 to produce a least-squares solution $(\hat{b}_0, \hat{b}_1)$. The best-fit curve to the original problem is then given by

$$x(t) = \hat{a}_0 e^{\hat{a}_1 t},$$

where $\hat{a}_0 = e^{\hat{b}_0}$, $\hat{a}_1 = \hat{b}_1$.

4.2 Nonlinear Least-Squares Problem

Let $\theta = (\theta_1, \cdots, \theta_m)$ be a multidimensional parameter. Consider a family of scalar-valued curves $y = f(x, \theta)$ that depend on parameter θ.

Nonlinear least-squares fitting: Given data points

$$(x_1, y_1),\ (x_2, y_2),\ \cdots,\ (x_n, y_n),$$

find a parameter value $\hat{\theta}$ such that the curve $y = f(x, \hat{\theta})$ minimizes the squared sum of errors (SSE):

$$\mathrm{SSE}(\theta) = \sum_{i=1}^{n} (y_i - f(x_i, \theta))^2. \tag{4.6}$$

The reader should think about why the method of linear least-squares problems discussed in the previous section will not work for this problem. We will treat $\mathrm{SSE}(\theta)$ as a smooth function of θ and employ multivariable calculus to find its minimum. In fact, a minimum of $\mathrm{SSE}(\theta)$ in $\mathbb{R}^m$ must be achieved at a critical point; namely, where

$$\frac{\partial \text{SSE}(\theta)}{\partial \theta_j} = 0, \quad j = 1, \cdots, m. \tag{4.7}$$

Using the chain rule for differentiation, we rewrite system (4.7) as

$$\sum_{i=1}^{n} [y_i - f(x_i, \theta)] \Big(- \frac{\partial f}{\partial \theta_j}(x_i, \theta) \Big) = 0, \quad j = 1, \cdots, m. \tag{4.8}$$

This system may still be nonlinear in θ through nonlinear dependence in $f(x_i, \theta)$. Numerical schemes are used to find an approximate solution.

Starting from an initial guess $\theta^{(0)}$ of θ, we define a sequence of approximations $\{\theta^{(k)}\}$ inductively, by the process of Newton's method. We expand $f(x_i, \theta)$ by its first-order Taylor polynomial at $\theta^{(k)}$

$$f(x_i, \theta) \approx f(x_i, \theta^{(k)}) + \sum_{s=1}^{n} \frac{\partial f(x_i, \theta^{(k)})}{\partial \theta_s} (\theta_s - \theta_s^{(k)}).$$

Let

$$J = \Big(\frac{\partial f(x_i, \theta^{(k)})}{\partial \theta_j} \Big) = (J_{ij})$$

be the Jacobian matrix at $\theta^{(k)}$. We note that J_{ij} in the above relation depends on k, and for simplicity of notation, we choose to suppress the dependence on k. Then equation (4.8) can be approximated by

$$\sum_{i=1}^{n} \Big[y_i - f(x_i, \theta^{(k)}) - \sum_{s=1}^{m} J_{is} (\theta_s - \theta_s^{(k)}) \Big] [-J_{ij}] = 0, \quad j = 1, \cdots, m. \tag{4.9}$$

Let

$$\Delta y_i = y_i - f(x_i, \theta^{(k)}),$$
$$\Delta \theta_j^{(k+1)} = \theta_j - \theta_j^{(k)}.$$

Then equation (4.9) can be rewritten as

$$\sum_{i=1}^{n}\sum_{s=1}^{m} J_{is}J_{ij}\Delta\theta_s^{(k+1)} = \sum_{i=1}^{n} J_{ij}\Delta y_i, \tag{4.10}$$

from which we can solve for $\Delta\theta^{(k+1)}$ and define

$$\theta^{(k+1)} = \theta^{(k)} + \Delta\theta^{(k+1)}, \quad \text{for } k = 0, 1, 2, \cdots.$$

In matrix form equation (4.10) can be written as

$$J^T J\Delta\theta = J^T\Delta y, \tag{4.11}$$

System (4.11) is called the *normal system.*

The following iteration scheme for the nonlinear least-squares method is called the Gauss–Newton Method:

(1) Choose an initial value $\theta^{(0)}$.

(2) Solve the normal equation (4.11) for $\Delta\theta^{(1)}$.

(3) Update θ by $\theta^{(1)} = \theta^{(0)} + \Delta\theta^{(1)}$.

(4) Repeat the iteration until convergence is achieved (when difference $\theta^{(k+1)} - \theta^{(k)}$ is below margin of error.)

There are many other methods for nonlinear least-squares problems aimed at improving efficiency and rate of convergence.

If $f(x, \theta)$ is a linear function of θ, for example

$$f(x, \theta) = \alpha(x) \cdot \theta,$$

where $\alpha(x) = (\alpha_1(x), \cdots, \alpha_m(x))$ and "$\cdot$" denotes the dot product in $\mathbb{R}^m$, then we would expect that the Gauss–Newton method leads to the linear least-squares method. Indeed,

$$f(x_i, \theta) = \alpha(x_i) \cdot \theta = \sum_{j=1}^{m} \alpha_j(x_i)\theta_i, \quad i = 1, \cdots, n,$$

and

$$\text{SSE}(\theta) = \sum_{i=1}^{n} (y_i - \alpha(x_i) \cdot \theta)^2.$$

Therefore,

$$\begin{aligned}\frac{\partial \text{SSE}}{\partial \theta_j} &= \sum_{i=1}^{n}(y_i - \alpha(x_i)\cdot\theta)(-\alpha_j(x_i)) \\ &= -\sum_{i=1}^{n}\alpha_j(x_i)(y_i - \alpha(x_i)\cdot\theta), \quad j = 1, \cdots, m.\end{aligned} \tag{4.12}$$

Let $A = (\alpha_j(x_i))$. Then equation (4.12) can be written in matrix form as

$$A^T y - A^T A\,\theta = 0,$$

which gives the normal equation

$$A^T A\,\theta = A^T y$$

of the linear least-squares problem.

Example 4. Given data

$$(1, 4.6),\ (2, 8.82),\ (3, 16),\ (4, 31.3),\ (5, 58.5),$$

Find the best-fit curve $x = a_0 e^{a_1 t}$.

Solution 1. Using transformation

$$y = \ln x,\ b_0 = \ln a_0,\ b_1 = a_1,$$

we obtain

$$y = b_0 + b_1 t$$

and the new data set

$$(1, 1.526),\ (2, 2.177),\ (3, 2.773),\ (4, 3.444),\ (5, 4.069).$$

We will apply the linear least-squares method. Let

$$A = \begin{bmatrix} 1 & 1 \\ 1 & 2 \\ 1 & 3 \\ 1 & 4 \\ 1 & 5 \end{bmatrix},\ b = \begin{bmatrix} 1.526 \\ 2.177 \\ 2.773 \\ 3.444 \\ 4.069 \end{bmatrix},\ y = \begin{bmatrix} b_0 \\ b_1 \end{bmatrix}.$$

The normal equation $A^T A y = A^T b$ becomes

$$\begin{bmatrix} 5 & 15 \\ 15 & 55 \end{bmatrix} \begin{bmatrix} b_0 \\ b_0 \end{bmatrix} = \begin{bmatrix} 13.989 \\ 48.32 \end{bmatrix}.$$

Solving this system we obtain

$$\begin{bmatrix} b_0 \\ b_0 \end{bmatrix} = \begin{bmatrix} 5 & 15 \\ 15 & 55 \end{bmatrix}^{-1} \begin{bmatrix} 13.989 \\ 48.32 \end{bmatrix} = \begin{bmatrix} 0.892 \\ 0.635 \end{bmatrix}.$$

This gives

$$a_0 = e^{0.892} = 2.44, \ a_1 = b_1 = 0.635,$$

and the least-squares curve is

$$x = 2.44e^{0.635t}.$$

Solution 2. We will use the Gauss–Newton method to solve the nonlinear least-squares problem directly. Consider the nonlinear function

$$f(t, a) = a_0 e^{a_1 t}, \quad a = (a_0, a_1), \quad x = (1, 2, \cdots, 5)^T.$$

The Jacobian matrix is

$$J(x, a) = \begin{bmatrix} e^{a_1} & a_0 e^{a_1} \\ e^{2a_1} & 2a_0 e^{2a_1} \\ e^{3a_1} & 3a_0 e^{3a_1} \\ e^{4a_1} & 4a_0 e^{4a_1} \\ e^{5a_1} & 5a_0 e^{5a_1} \end{bmatrix}$$

and the normal equation $J^T J \Delta a = J^T \Delta y$ becomes

$$\begin{bmatrix} e^{2a_1} + e^{4a_1} + e^{6a_1} + e^{8a_1} + e^{10a_1} & a_0(e^{2a_1} + 2e^{4a_1} + 3e^{6a_1} + 4e^{8a_1} + 5e^{10a_1}) \\ a_0(e^{2a_1} + 2e^{4a_1} + 3e^{6a_1} + 4e^{8a_1} + 5e^{10a_1}) & a_0^2(e^{2a_1} + 4e^{4a_1} + 9e^{6a_1} + 16e^{8a_1} + 25e^{10a_1}) \end{bmatrix} \begin{bmatrix} \Delta a_1 \\ \Delta a_2 \end{bmatrix}$$

$$= \begin{bmatrix} e^{a_1} & e^{2a_1} & e^{3a_1} & e^{4a_1} & e^{5a_1} \\ a_0 e^{3a_1} & 2a_0 e^{2a_1} & 3a_0 e^{3a_1} & 4a_0 e^{4a_1} & 5a_0 e^{5a_1} \end{bmatrix} \begin{bmatrix} \Delta y_1 \\ \Delta y_2 \\ \Delta y_3 \\ \Delta y_4 \\ \Delta y_5 \end{bmatrix}.$$

Here

$$\begin{bmatrix}\Delta a_1\\ \Delta a_2\end{bmatrix} = \begin{bmatrix}a_0 - a_0^{(k)}\\ a_1 - a_1^{(k)}\end{bmatrix},$$

and

$$\Delta y_i = y_i - a_0^{(k)} e^{a_1^{(k)}}, \quad 1 \le i \le 5.$$

Choosing an initial vector

$$\begin{bmatrix}a_0^{(0)}\\ a_1^{(0)}\end{bmatrix} = \begin{bmatrix}1\\ 1\end{bmatrix}$$

and using the iteration scheme

$$\begin{bmatrix}a_0^{(k+1)}\\ a_1^{(k+1)}\end{bmatrix} = \begin{bmatrix}a_0^{(k)}\\ a_1^{(k)}\end{bmatrix} + (J^T J)^{-1} J^T \Big|_{(a_0^{(k)},\, a_1^{(k)})} \begin{bmatrix} y_1 - a_0^{(k)} e^{a_0^{(k)}} \\ y_2 - a_0^{(k)} e^{a_0^{(k)}} \\ y_3 - a_0^{(k)} e^{a_0^{(k)}} \\ y_4 - a_0^{(k)} e^{a_0^{(k)}} \\ y_5 - a_0^{(k)} e^{a_0^{(k)}} \end{bmatrix}$$

we obtain, for $k = 0$,

$$\begin{bmatrix}a_0^{(1)}\\ a_1^{(1)}\end{bmatrix} = \begin{bmatrix}1\\ 1\end{bmatrix}$$

$$+ \begin{bmatrix}25472.8 & 123383\\ 133383 & 602214\end{bmatrix}^{-1} \begin{bmatrix}2.718 & 7.389 & 20.086 & 54.598 & 148.413\\ 2.718 & 14.778 & 60.257 & 218.393 & 742.066\end{bmatrix} \begin{bmatrix} 1.882 \\ 1.431 \\ -4.086 \\ -23.298 \\ -89.913 \end{bmatrix}$$

$$= \begin{bmatrix}1.386\\ 0.801\end{bmatrix}.$$

Iterating again we obtain, for $k = 1$,

$$\begin{bmatrix} a_0^{(2)} \\ a_1^{(2)} \end{bmatrix} = \begin{bmatrix} 1.386 \\ 0.801 \end{bmatrix}$$

$$+ \begin{bmatrix} 3777.53 & 24873.7 \\ 24873.7 & 166018 \end{bmatrix}^{-1} \begin{bmatrix} 2.228 & 4.965 & 11.064 & 24.653 & 54.934 \\ 3.089 & 13.768 & 46.017 & 136.716 & 380.802 \end{bmatrix} \begin{bmatrix} 1.511 \\ 1.936 \\ 0.661 \\ -2.879 \\ -17.66 \end{bmatrix}$$

$$= \begin{bmatrix} 2.104 \\ 0.651 \end{bmatrix}.$$

Subsequent iterations can be calculated in the same way to obtain

$$\begin{bmatrix} a_0^{(3)} \\ a_1^{(3)} \end{bmatrix} = \begin{bmatrix} 2.428 \\ 0.635 \end{bmatrix}, \quad \begin{bmatrix} a_0^{(4)} \\ a_1^{(4)} \end{bmatrix} = \begin{bmatrix} 2.431 \\ 0.636 \end{bmatrix}, \quad \begin{bmatrix} a_0^{(5)} \\ a_1^{(5)} \end{bmatrix} = \begin{bmatrix} 2.431 \\ 0.636 \end{bmatrix}, \quad \dots .$$

We see that if the margin of error is three decimal points, then we have achieved the required accuracy at the 4th iteration and obtain

$$a_0 \approx 2.431, \quad a_1 \approx 0.636.$$

Comparing with the answers in Solution 1, we see that they agree up to the first decimal point. The resulting curves are shown in Figure 4.4. The two curves are virtually indistinguishable.

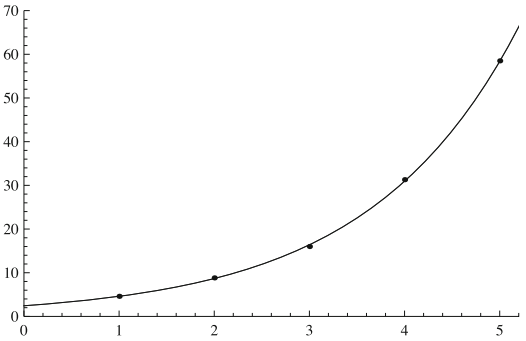

Figure 4.4: The least-squares curve for Example 4.

4.3 Parameter Estimation for Epidemic Models

Suppose that our epidemic model is described by the initial value problem of a system of differential equations:

$$\begin{aligned} &x' = f(x,\theta), \quad x \in \mathbb{R}^d,\ t \in [0, t_{\max}], \\ &x(0) = x_0. \end{aligned} \tag{4.13}$$

Here, $\theta \in \mathbb{R}^m$ is an m-dimensional parameter, and $[0, t_{\max}]$ is the finite time interval in which we investigate the epidemic. The disease data is often given at discrete observation time points $t_1, t_2, \cdots, t_p \in [0, t_{\max}]$ in the form

$$(t_1, g(x^{(1)})),\ (t_2, g(x^{(2)})),\ \cdots,\ (t_p, g(x^{(p)})), \quad x^{(i)} \in \mathbb{R}^d. \tag{4.14}$$

The function $g(x) : \mathbb{R}^d \to \mathbb{R}^n$ represents measurable quantities of the state variable x, also called the *observables*. To fit with data, it is natural that we only consider values of the solution $x(t,\theta)$ at these observational time points:

$$x(t,\theta) \approx (x(t_1,\theta), x(t_2,\theta), \cdots, x(t_p,\theta))^T.$$

From the fundamental theory of differential equations we know that, if the vector field $f(x,\theta)$ is a smooth function (having continuous partial derivatives) with respect to (x,θ), then the solution $x(t,\theta)$ has a dependence on θ with the same order of smoothness as f. In the above notation, the dependence of the solution on initial condition x_0 is understood and suppressed. In the following discussion, we will keep x_0 fixed and discuss fitting the parameter θ. In many applications, the initial conditions are not always known and need to be fitted. Since the solution $x(t, x_0, \theta)$ is a diffeomorphism with respect to the initial conditions x_0, we can consider x_0 as part of the parameter θ. We denote the data points as

$$y = (g(x^{(1)}), g(x^{(2)}), \cdots, g(x^{(p)})), \quad x^{(i)} \in \mathbb{R}^d.$$

Then the squared sum of errors (SSE) between our solution and the data can be measured by

$$\mathrm{SSE}(\theta) = d(g(x(t,\theta)), y)^2 = \sum_{i=1}^{p} ||g(x(t_i,\theta)) - g(x^{(i)})||^2. \quad (4.15)$$

We note here that in the above expression, it is important to measure differences in quantities of the same type. Since the data is given as the observable quantities $g(x)$, we need to compare the observable part of the model solution $g(x(t,\theta))$ with the data. This is often referred to as "comparing apples to apples, and oranges to oranges." We also note that $||g(x) - g(y)||$ in the above expression denotes the Euclidean norm of the n-dimensional vector $g(x) - g(y)$, namely,

$$||g(x) - g(y)||^2 = \sum_{i=1}^{n} |g_i(x) - g_i(y)|^2.$$

In the least-squares fitting, we look for a value $\hat{\theta}$ of model parameter θ such that $\mathrm{SSE}(\theta)$ is the minimum. Such a problem is clearly a nonlinear least-squares problem, since the dependence of a solution $x(t,\theta)$ on the parameter θ is through a highly nonlinear system of differential equations.

We can apply the Gauss–Newton method to the least-squares parameter fitting problem. The differential equations can be discretized to give a system of difference equations for the solution. The normal equation for the difference equation can be derived and then solved by Gauss–Newton iteration. When the number of equations in (4.13) is large, this requires too much human effort for code writing. An alternative to this approach is to take advantage of the powerful direct search routines of mathematical software packages such as Matlab, Maple, and Mathematica. We will explain this approach using a simple SIR model as an example, together with the Matlab codes for each step.

Several Matlab functions can be used for parameter estimation. Matlab function *lsqcurvefit* requires the following inputs: the

model equation, an initial guess for the parameters to be fitted, and the time points and data points. It then solves the nonlinear least-squares problem directly. Matlab function *nlinfit* is another nonlinear regression routine that uses an iterative least-squares estimation with an initial value for the parameters. Matlab function *fminsearch* is commonly used for parameter estimation. We first define the sum of squares of errors $\mathrm{SSE}(\theta)$ between the model output and data. With an initial guess θ_0 of the unknown parameters, the epidemic model can be numerically solved to produce a value for $\mathrm{SSE}(\theta_0)$. The *fminsearch* routine takes the least-squares error function $\mathrm{SSE}(\theta)$ and an initial guess of the parameter value, and uses a direct search routine to find a minimum value of least-squares error. To ensure the minimum value returned by *fminsearch* is not just a local minimum, the process can be repeated with several choices of initial guess.

4.3.1 An Example of Using Matlab for Parameter Estimation

We will use the Kermack–McKendrick SIR model for demonstration:

$$\begin{aligned} S' &= -\lambda IS \\ I' &= \lambda IS - \gamma I \\ R' &= \gamma I. \end{aligned} \tag{4.16}$$

Our objective is to estimate the parameters λ and γ by fitting the model to disease data.

The first step is to input the model equation into Matlab by defining a function, SIRModel, to be called on later for fitting. The function takes three inputs: the time variable $t \in \mathbb{R}$, state variable $y \in \mathbb{R}^3$, and parameter vector $par \in \mathbb{R}^2$.

```
function f=SIRmodel(t,y,par)
%  Label the parameters and variables
        lambda = par(1);
        gamma = par(2);
        S=y(1);
        I=y(2);
        R=y(3);
        N=S+I+R;
% Input the differential equations
        Sdot=-lambda*I*S;
        Idot=lambda*I*S-gamma*I;
        Rdot=gamma*I;
        f=[Sdot Idot Rdot]';
end
```

We use the ODE Solver ODE45 of Matlab to solve the differential equation for a given set of initial conditions (IC), by defining a function SIRSol.

```
function sol=SIRSol(par,IC,t)
% disp(num2str(par))
        DeHandle=@(t,y) SIRModel(t,y,par);
        [~, Y]=ode45(DeHandle,t,IC);
        sol=Y';
end
```

The second step is create the data. For demonstration purposes, we will artificially generate data at 20 time points from the model with prescribed parameter values, and add random noise to the generated data. To mimic real disease situations, we assume that only data from the infected population I (prevalence) and the total population $N = S + I + R$ are given.

First take 20 randomly chosen time points:

```
numpts=20;
tdata=[0 sort(20*rand(1,numpts))];
```

Then we generate normally distributed noise:

```
width=0.1;
ndataSIR=20*[ 0 normrnd(0,width,[1,numpts]);
          0 normrnd(0,width,[1,numpts]);
          0 normrnd(0,width,[1,numpts])];
```

We add the noise term to the model outputs with $\lambda = 0.01$ and $\gamma = 0.1$ and initial conditions $S(0) = 50$, $I(0) = 1$, and $R(0) = 0$ to produce a set of artificial data:

```
lambda=0.01;
gamma=0.1;
par=[lambda gamma];
IC=[50 1 0];
SIRData=SIRSol(par, IC, tdata)+ndataSIR;
```

We will only use the data for $I(t)$ and $N(t)$:

```
SIRData=[0 1 0 ; 1 1 1]*SIRData;
```

We can visualize the data (shown in Figure 4.5) for $I(t)$ and $N(t)$:

```
figure;
plot(tdata,SIRData(1,:), 'r*');
hold on;
plot(tdata,SIRData(2,:), 'o');
```

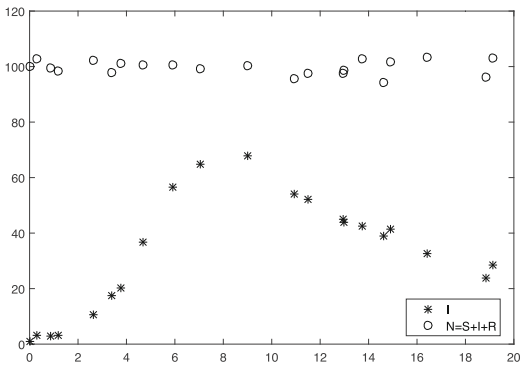

Figure 4.5: Data on I and $N = S + I + R$ that are artificially created by adding noise to solution curves.

In the last step, we define least-squares error terms:

```
SIRparSol= @(par,t) [0 1 0 ; 1 1 1]*SIRSol([par(1) par(2)],
    IC, t);
SumSquaresSIR = @(par) sum(sum((SIRparSol(par,tdata)-SIRData
    ).^2));
```

and call *fminsearch* with an initial guess for the parameter values $\lambda = 8, \gamma = 0.02$:

```
[SIRtheta,fval,exitflag] = fminsearch (SumSquaresSIR,[8
    0.02]);
SIRsol=SIRparSol(SIRtheta,tsol);
```

Then we visualize the solutions in comparison to data, as shown in Figure 4.6, using:

```
figure;
plot(tdata,SIRData,'.');
hold on;
plot(tsol,SIRsol,'--');
```

The results of the best-fit values for the parameters are $\lambda = 0.0099658$ and $\gamma = 0.10063$, which are very close to the preassigned values $\lambda = 0.01$ and $\gamma = 0.1$. Fitting results can be visualized in Figure 4.6. Solutions to the model with the best-fit parameter values are shown in Figure 4.7.

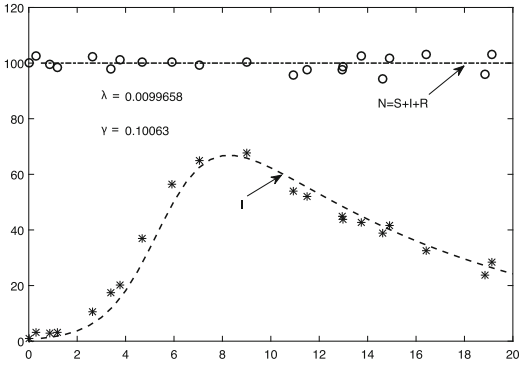

Figure 4.6: Fitting results of solutions $I(t)$ and $N(t) = S(t) + I(t) + R(t)$ to the artificial data.

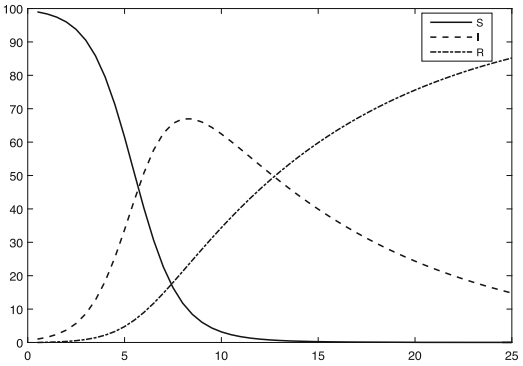

Figure 4.7: Solutions $(S(t), I(t), R(t))$ of the model using best-fit parameter values.

Exercises.

(1) Try out the Matlab codes in the example and reproduce the best-fit parameter values and the graphics. You may want to choose a different set of values for λ and γ to generate the data and see what results you get. Another good practice is to pick several initial guesses for the *fminsearch* to repeat the fitting process, and see if you obtain the same set of best-fit parameters.

(2) Suppose that we only have data for $I(t)$ available for us. How would you modify the least-squares error term to reflect this change? Can you modify the Matlab codes and fit the best-fit parameter values for both λ and γ?

Chapter 5

Special Topics

In this chapter, we select some materials for further study. In Section 5.1, an SEIR model for measles is presented and analyzed. This is an example of higher dimensional models, models having more than two modeling equations. For the local stability analysis, we demonstrate how the Routh–Hurwitz conditions can be used to show that the eigenvalues of a 3×3 matrix have negative real parts. The proof of global stability of the endemic equilibrium using a Lyapunov function is adapted from the work of Korobenikov and Maini [34].

In-host models describe the infection of different cell types by viruses, bacteria, and other pathogens in the body, typically in the peripheral blood. Whereas these models describe infections on a microscopic level, the modeling equations strongly resemble epidemic models we have derived in earlier chapters. As a result, the machinery we have learned in this book can also be applied to analyze this type of models. In Section 5.2, we present a simple in-host model for the infection of $CD4^+$ T cells by the Human T-cell Lymphotropic Virus type I (HTLV-I) in the peripheral blood. This is one of the simplest disease models that have the phenomenon of backward bifurcation. We will explain how a backward bifurcation occurs, its difference from the forward bifurcation we have discussed in Section 2.3.3, as well as its implications for the infection process and disease control.

M. Y. Li, *An Introduction to Mathematical Modeling of Infectious Diseases*, Mathematics of Planet Earth 2,
https://doi.org/10.1007/978-3-319-72122-4_5

5.1 Higher Dimensional Models: SEIR Models

Let us consider an infectious disease that has latency and causes a permanent immunity in its host, and whose transmission is described by the transfer diagram in Figure 5.1.

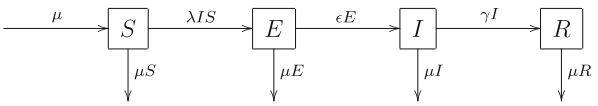

Figure 5.1: Transfer diagram for an SEIR model.

As usual, S, E, I, and R denote the subpopulations that are susceptible, exposed, infectious, and recovered, respectively. As we have seen in Section 1.4.4, this type of model is called an SEIR model. One of the diseases that can be described by an SEIR model is measles, whose latent period is typically about two weeks. The parameters ϵ and γ are understood in such a way that $1/\epsilon$ and $1/\gamma$ are the mean latent and infectious period, respectively. The parameter μ denotes the natural birth rate, which we assume to be equal to the natural death rate to keep the total population constant.

5.1.1 SEIR Models

Let $S(t), E(t), I(t)$, and $R(t)$ denote the number of hosts in the corresponding compartments. Based on our assumptions and the transfer diagram, we can derive the following system of differential equations for the model:

$$\begin{aligned} S' &= \mu - \lambda IS - \mu S \\ E' &= \lambda IS - (\epsilon + \mu)E \\ I' &= \epsilon E - (\gamma + \mu)I \\ R' &= \gamma I - \mu R. \end{aligned} \tag{5.1}$$

We investigate solutions with initial conditions $S(0) = S_0 \geq 0$, $E(0) = E_0, I(0) = I_0$, and $R(0) = R_0$.

First, we show that the total population remains a constant. If we add all four equations in (5.1) we obtain

$$(S + E + I + R)' = \mu - \mu(S + E + I + R).$$

If we let $N(t) = S(t) + E(t) + I(t) + R(t)$ and $N_0 = S_0 + E_0 + I_0 + R_0$, then $N(t)$ satisfies

$$(1 - N)' = -\mu(1 - N),$$

which can be solved to yield

$$1 - N(t) = (1 - N_0)e^{-\mu t}, \quad t \in \mathbb{R}.$$

We can draw two conclusions based on this relation:

(1) If $N_0 = 1$ then $N(t) = 1$ for all t, and thus the total population remains a constant 1.

(2) If $N_0 \neq 1$ then $N(t) \to 1$ exponentially as $t \to \infty$.

Based on these conclusions, we can deduce that all the limit sets (as $t \to \infty$) of solutions to (5.1) are contained in the hyperplane $S + E + I + R = 1$, which is also invariant. If we are interested in the limiting behaviors of solutions, it suffices to restrict our attention to the invariant plane $S + E + I + R = 1$. The invariance of the plane means that the total population $N(t)$ remains 1 for all t if $N(0) = 1$. As we have seen in Chapter 2, the constant total population N has been scaled to 1 for simplicity.

The conservation of the total population, $S + E + I + R = 1$, allows us to simplify system (5.1) by reducing the number of variables by 1. For instance, we can substitute

$$R(t) = 1 - S(t) - E(t) - I(t) \tag{5.2}$$

into the system and only consider the equations for S, E, and I. Once the behaviors of $S(t), E(t)$, and $I(t)$ are understood, the behaviors of $R(t)$ can readily be obtained from the linear

relation (5.2). In fact, for system (5.1), since the first three equations do not contain the variable R, we may simply first ignore the R equation and consider the following 3-dimensional system of differential equations:

$$\begin{aligned} S' &= \mu - \lambda IS - \mu S \\ E' &= \lambda IS - (\epsilon + \mu)E \\ I' &= \epsilon E - (\gamma + \mu)I. \end{aligned} \tag{5.3}$$

In the rest of the section, we focus our mathematical analysis on system (5.3). Our results can be readily translated to those for system (5.1).

We first derive the natural feasible region of system (5.3). We note that the nonnegative orthant of $\mathbb{R}^3$,

$$\mathbb{R}^3_+ = \{(S, E, I) \mid S \geq 0, E \geq 0, I \geq 0\},$$

is positively invariant for system (5.3). This can be checked by verifying that the vector field of (5.3) on the boundary of $\mathbb{R}^3_+$ is either tangential to the boundary or pointing to the interior of $\mathbb{R}^3_+$. Similarly, we can show that the nonnegative orthant $\mathbb{R}^4_+$ is positively invariant for system (5.1). Biologically speaking, the positive invariance of $\mathbb{R}^4_+$ is equivalent to the following statement: nonnegative initial conditions give rise to nonnegative solutions for $t \geq 0$, a required property considering that $S(t), E(t), I(t), R(t)$ all represent numbers of individuals and should be nonnegative. In this sense, we say that the model is well-posed.

As it turns out, there is no need to consider all initial conditions in $\mathbb{R}^3_+$. Noting that $S(t) + E(t) + I(t) + R(t) = 1$ and $R(t) \geq 0$, we know that

$$S(t) + E(t) + I(t) \leq 1 \quad \text{for all } t.$$

Therefore we only need to consider initial conditions in the bounded region

$$\Gamma = \{(S, E, I) \in \mathbb{R}^3_+ \mid S + E + I \leq 1\}. \tag{5.4}$$

By considering the direction of the vector field on the plane $S + E + I = 1$, we can verify that Γ is positively invariant for system (5.3) and solutions starting in Γ will remain in Γ. We will investigate system (5.3) in the feasible region Γ.

5.1.2 Equilibria and the Basic Reproduction Number

The coordinates of an equilibrium (S, E, I) of system (5.3) satisfy the following equations:

$$\begin{aligned} \mu - \lambda IS - \mu S &= 0 \\ \lambda IS - (\epsilon + \mu)E &= 0 \\ \epsilon E - (\gamma + \mu)I &= 0. \end{aligned} \tag{5.5}$$

The disease-free equilibrium $P_0 = (1, 0, 0)$ always exists. An endemic equilibrium $P^* = (S^*, E^*, I^*)$, with $S^*, E^*, I^* > 0$, satisfies

$$S^* = \frac{(\epsilon + \mu)(\gamma + \mu)}{\lambda\epsilon}, \quad E^* = \frac{\gamma + \mu}{\epsilon} I^*, \quad I^* = \frac{\mu(1 - S^*)}{\lambda S^*}. \tag{5.6}$$

We note that equilibrium P^* does not always belong to the feasible region Γ, especially its interior $\overset{\circ}{\Gamma}$, since the relations $0 \leq S^*, E^*, I^* \leq 1$ have to be satisfied. It is then clear that

$$P^* \in \overset{\circ}{\Gamma} \quad \Longleftrightarrow \quad S^* < 1 \iff \quad \frac{\lambda\epsilon}{(\epsilon + \mu)(\gamma + \mu)} > 1.$$

Using the interpretation of the basic reproduction number in Section 1.4.9, we see that

$$\mathcal{R}_0 = \frac{\lambda\epsilon}{(\epsilon + \mu)(\gamma + \mu)} \tag{5.7}$$

is the basic reproduction number for model (5.3). We arrive at the next proposition.

Proposition 5.1.1

(1) *If* $\mathcal{R}_0 \leq 1$, *then system* (5.3) *has only the disease-free equilibrium* $P_0 = (1, 0, 0)$ *in* Γ.

(2) *If* $\mathcal{R}_0 > 1$, *then system* (5.3) *has two equilibria: the disease-free equilibrium* P_0 *and a unique endemic equilibrium* $P^* = (S^*, E^*, I^*)$, *whose coordinates are given in* (5.6).

5.1.3 Local Stability Analysis

In the previous section, we have seen that the basic reproduction number serves as a threshold parameter in determining the number of equilibria in system (5.3). We will show in this section that $\mathcal{R}_0$ also determines the local stability of the equilibria.

Theorem 5.1.2

(1) *If* $\mathcal{R}_0 < 1$, *then the disease-free equilibrium* $P_0 = (1, 0, 0)$ *is locally asymptotically stable in* Γ.

(2) *If* $\mathcal{R}_0 > 1$, *then the disease-free equilibrium* P_0 *becomes unstable and the endemic equilibrium* P^* *is asymptotically stable.*

We will apply the method of linearization to the stability analysis in both cases.

Proof. The Jacobian matrix of system (5.3) at $P_0 = (1, 0, 0)$ is

$$J(P_0) = \begin{bmatrix} -\mu & 0 & -\lambda \\ 0 & -\epsilon - \mu & \lambda \\ 0 & \epsilon & -\gamma - \mu \end{bmatrix}.$$

The characteristic equation $\det(pI_{3\times 3} - J(P_0)) = 0$ is a cubic equation

$$(p + \mu)[p^2 + (\epsilon + \gamma + 2\mu)p + (\epsilon + \mu)(\gamma + \mu) - \lambda\epsilon] = 0.$$

Therefore, one eigenvalue is $p_1 = -\mu < 0$. The remaining two eigenvalues p_2 and p_3 satisfy

$$p^2 + (\epsilon + \gamma + 2\mu)p + (\epsilon + \mu)(\gamma + \mu) - \lambda\epsilon = 0.$$

Since

$$\begin{aligned} p_2 + p_3 &= -(\epsilon + \gamma + 2\mu) < 0, \\ p_2 p_3 &= (\epsilon + \mu)(\gamma + \mu) - \lambda\epsilon) = (\epsilon + \mu)(\gamma + \mu)(1 - \mathcal{R}_0), \end{aligned}$$

we know that, if $\mathcal{R}_0 < 1$, then $p_2 p_3 > 0$, and p_2 and p_3 are either both real numbers of the same sign, or complex numbers that are conjugates of each other. The condition $p_2 + p_3 < 0$ implies that they are either both negative real numbers or complex numbers with negative real parts. Therefore P_0 is asymptotically stable by Theorems 3.2.1 and 3.2.2 in Chapter 3. If $\mathcal{R}_0 > 1$, then $p_2 p_3 < 0$, and thus p_2 and p_3 have opposite signs, and P_0 is unstable.

Assume that $\mathcal{R}_0 > 1$ so that $P^* \in \overset{\circ}{\Gamma}$. The Jacobian matrix at P^* is

$$J(P^*) = \begin{bmatrix} -\lambda I^* - \mu & 0 & -\lambda S^* \\ \lambda I^* & -\epsilon - \mu & \lambda S^* \\ 0 & \epsilon & -\gamma - \mu \end{bmatrix}.$$

The characteristic equation of $J(P^*)$ is more complicated than that of $J(P_0)$. We will use the Routh–Hurwitz conditions in Section 3.2 of Chapter 3.

It is easy to see that $\operatorname{tr}(J(P^*)) = -\lambda I^* - \epsilon - \gamma - 3\mu < 0$. Direct calculation gives

$$\begin{aligned} \det(J(P^*)) &= -(\lambda I^* + \mu)(\epsilon + \mu)(\gamma + \mu) - \lambda I^* \lambda S^* \epsilon + (\lambda I^* + \mu)\epsilon\lambda S^* \\ &= -(\lambda I^* + \mu)(\epsilon + \mu)(\gamma + \mu) + \mu\epsilon\lambda S^* \\ &= -(\lambda I^* + \mu)(\epsilon + \mu)(\gamma + \mu) + \mu(\epsilon + \mu)(\gamma + \mu) \\ &= -\lambda I^*(\epsilon + \mu)(\gamma + \mu) < 0. \end{aligned}$$

The sum of 2×2 principal minors of $J(P^*)$ is

$$\begin{aligned} a_2 &= (\lambda I^* + \mu)(\epsilon + \mu) + (\lambda I^* + \mu)(\gamma + \mu) + (\epsilon + \mu)(\gamma + \mu) - \lambda\epsilon S^* \\ &= (\lambda I^* + \mu)(\epsilon + \gamma + 2\mu), \end{aligned}$$

since $(\epsilon + \mu)(\gamma + \mu) - \lambda\epsilon S^* = 0$. Therefore,

$$\begin{aligned} \operatorname{tr}(J(P^*)) \cdot a_2 &= -(\lambda I^* + \epsilon + \gamma + 3\mu)(\lambda I^* + \mu)(\epsilon + \gamma + 2\mu) \\ &< -\lambda I^*(\epsilon + \mu)(\gamma + \mu) = \det(J(P^*)). \end{aligned}$$

We have verified all the Routh–Hurwitz conditions and proved that P^* is asymptotically stable when $\mathcal{R}_0 > 1$.

Remark. Careful readers might have noticed that, in Theorem 5.1.2, we have neglected the case $\mathcal{R}_0 = 1$. We note that, when $\mathcal{R}_0 = 1$, $E^* = I^* = 0$ and the two equilibria P_0 and P^* coincide. Furthermore, the two eigenvalues p_2, p_3 of $J(P_0)$ satisfy $p_2 p_3 = (\epsilon + \mu)(\gamma + \mu)(1 - \mathcal{R}_0) = 0$, and thus at least one eigenvalue of $J(P_0)$ is zero. In this case, P_0 is not a hyperbolic equilibrium, and the method of linearization will not directly yield a nonlinear stability result of P_0. As we will see in the next section, the stability of P_0 when $\mathcal{R}_0 = 1$ can be established using a Lyapunov function.

5.1.4 The Global Stability of the Disease-Free Equilibrium When $R_0 \leq 1$: LaSalle's Invariance Principle

Theorem 5.1.3 *The disease-free equilibrium* $P_0 = (1, 0, 0)$ *of* (5.3) *is globally asymptotically stable in* Γ *if* $\mathcal{R}_0 \leq 1$.

Proof. Consider function $L = \epsilon E + (\epsilon + \mu) I$. Then the derivative of L along a solution $(S(t), I(t), R(t))$ is

$$\begin{aligned} L' &= I\,[\,\lambda\epsilon S - (\epsilon + \mu)(\gamma + \mu)\,] \\ &= (\epsilon + \mu)(\gamma + \mu)\, I\,[\,\mathcal{R}_0 S - 1\,] \leq 0 \quad \text{since } S \leq 1. \end{aligned} \tag{5.8}$$

If $L' = 0$ then either $I = 0$ or $\mathcal{R}_0 S = 1$. If $\mathcal{R}_0 = 1$, then the second relation implies $S = 1, E = I = 0$. The set $G = \{\,(S, E, I) \in \Gamma \,|\, L' = 0\,\} \subset \{\,(S, E, I) \in \Gamma \,|\, I = 0\,\}$. A solution $(S(t), E(t), I(t))$ that stays in G satisfies equation $S' = \mu - \mu S$, and thus $S(t) \to 1$ as $t \to \infty$. It follows that $E(t), I(t) \to 0$ as $t \to \infty$ since $S(t) + E(t) + I(t) \leq 1$. The largest invariant set in G is then the singleton $\{P_0\}$. The global asymptotic stability of P_0 when $\mathcal{R}_0 \leq 1$ follows from LeSalle's Invariance Principle (Theorem 3.3.4 and Corollary 3.3.5, Chapter 3).

5.1.5 Uniform Persistence and Endemicity of a Disease When $R_0 > 1$

In this section, we show that a disease persists and becomes endemic in the host population when the basic reproduction number $R_0 > 1$. This is done by establishing that system (5.3) is uniformly persistent in the feasible region Γ when $\mathcal{R}_0 > 1$. System (5.3) is said to be *uniformly persistent* if there exists a constant $0 < \epsilon_0 < 1$ such that any solution $(S(t), E(t), I(t))$ with $(S(0), E(0), I(0)) \in \overset{\circ}{\Gamma}$ satisfies:

$$\begin{aligned} &\liminf_{t\to\infty} S(t) > \epsilon_0, \quad \liminf_{t\to\infty} E(t) > \epsilon_0, \quad \liminf_{t\to\infty} I(t) > \epsilon_0, \\ &\liminf_{t\to\infty} 1 - S(t) - E(t) - I(t) > \epsilon_0. \end{aligned} \tag{5.9}$$

The disease is endemic if (5.3) is uniformly persistent, since in this case the infected subpopulations $E(t)$ and $I(t)$ will remain above a positive level $\epsilon_0 > 0$ after a long time. Weaker notions of persistence have been defined and used in the literature of population dynamics (see [61]). One may choose to define endemicity of the disease using one of the weaker notions of persistence. However, as the following result shows, persistence of (5.3) in any reasonable sense is equivalent to the uniform persistence as defined above.

Proposition 5.1.4 *System* (5.3) *is uniformly persistent in* Γ *if and only if* $\mathcal{R}_0 > 1$.

Proof. The necessity of $\mathcal{R}_0 > 1$ follows from Theorem 5.1.3 and the fact that the asymptotic stability of P_0 precludes persistence. To establish sufficiency of the condition $\mathcal{R}_0 > 1$, we will apply the uniform persistence result Theorem 3.7.1, from Chapter 3. Using the same argument as in the proof of Theorem 3.7.2 in Section 3.7, we see that the maximal invariant set M on the boundary $\partial\Gamma$ is the singleton $\{P_0\}$ and is an isolated invariant set. To show that, when $\mathcal{R}_0 > 1$, the disease-free equilibrium P_0 repels in the direction of the interior of Γ, we use the Lyapunov function L and relation (5.8) in the preceding section:

$$L' = (\epsilon + \mu)(\gamma + \mu)\, I\, (\, \mathcal{R}_0 S - 1\,).$$

Here we see that, when $\mathcal{R}_0 > 1$, $L' > 0$ for (S, E, I) in the interior of Γ if S is sufficiently close to 1. As a result, solutions in the interior of Γ starting sufficiently close to P_0 leave a neighborhood of P_0. This verifies the condition of Theorem 3.7.1 and system (5.3) is uniformly persistent in Γ when $\mathcal{R}_0 > 1$.

Theorem 5.1.3 and Proposition 5.1.4 establish the basic reproduction number $\mathcal{R}_0$ as a sharp threshold parameter; if $\mathcal{R}_0 \leq 1$ the disease always dies out irrespective of initial conditions, and if $\mathcal{R}_0 > 1$ the disease remains endemic in the population as long as it is initially present.

5.1.6 The Global Stability of the Endemic Equilibrium When $R_0 > 1$

Theorem 5.1.5 *Suppose that $\mathcal{R}_0 > 1$. Then the unique endemic equilibrium P^* is globally asymptotically stable in the interior of Γ.*

Proof. Let $P^* = (S^*, E^*, I^*)$ be the endemic equilibrium. Consider a function

$$V(S,E,I) = (S - S^*) - S^* \log \frac{S}{S^*} + (E - E^*) - E^* \log \frac{E}{E^*} + \frac{\epsilon + \mu}{\epsilon}\left((I - I^*) - I^* \log \frac{I}{I^*}\right).$$

We first show that $V(S, E, I) \geq 0$ in the interior of Γ and $V(S, E, I) = 0$ only at P^*. For $x^* > 0$, let $f(x) = x - x^* - x^* \log \frac{x}{x^*}$. Then $f(x^*) = 0$ and $f'(x) = 1 - x^*/x$. Therefore $f'(x) < 0$ if $x < x^*$ and $f'(x) > 0$ if $x > x^*$. This implies that $f(x)$ has an absolute minimum 0 at $x = x^*$ in the interval $(0, \infty)$. This property shows that $V(S, E, I)$ is positive definite with respect to point P^*.

The Lyapunov derivative of V along solutions of (5.3) is

$$\begin{aligned}\dot{V} &= S' - \frac{S^*}{S}S' + E' - \frac{E^*}{E}E' + \frac{\epsilon+\mu}{\epsilon}\Big(I' - \frac{I^*}{I}I'\Big)\\ &= \mu - \mu S - \frac{S^*}{S}(\mu - \lambda IS - \mu S) - (\epsilon+\mu)E - \frac{E^*}{E}(\lambda S - (\epsilon+\mu)E)\\ &\qquad + \frac{\epsilon+\mu}{\epsilon}(\epsilon E - (\gamma+\mu)I) - \frac{\epsilon+\mu}{\epsilon}\frac{I^*}{I}(\epsilon E - (\gamma+\mu)I)\\ &= \mu - \mu S - \mu\frac{S^*}{S} - \lambda IS^* - \mu S^* - \frac{\lambda ISE^*}{E} + (\epsilon+\mu)E^* - \frac{(\epsilon+\mu)(\gamma+\mu)}{\epsilon}I\\ &\qquad - (\epsilon+\mu)\frac{EI}{I^*} + \frac{(\epsilon+\mu)(\gamma+\mu)}{\epsilon}I^*.\end{aligned}$$

While the expressions in $\dot{V}$ seem complex, we can simplify them using the equilibrium relations satisfied by P^*:

$$\mu = \lambda I^*S^* + \mu S^*, \quad \lambda I^*S^* = (\epsilon+\mu)E^*, \quad \epsilon E^* = (\gamma+\mu)I^*. \tag{5.10}$$

These relations are obtained by setting the derivatives in system (5.3) to 0. Substituting (5.10) into $\dot{V}$, we obtain

$$\begin{aligned}\dot{V} &= \mu - \mu S - \frac{\mu S^*}{S} + \mu S^* + \lambda I^*S^*\frac{S}{S^*}\frac{E^*}{E}\frac{I}{I^*} - (\epsilon+\mu)E^*\frac{E^*}{E}\frac{I}{I^*}\\ &\qquad + (\epsilon+\mu)E^* + \frac{(\epsilon+\mu)(\gamma+\mu)}{\epsilon}I^*\\ &= \mu S^*\Big[2 - \frac{S}{S^*} - \frac{S^*}{S}\Big] + \lambda I^*S^*\Big[3 - \frac{S^*}{S} - \frac{S}{S^*}\frac{E^*}{E}\frac{I}{I^*} - \frac{E}{E^*}\frac{I^*}{I}\Big]\\ &\le 0, \quad \text{for all } (S,E,I) \text{ in the interior of } \Gamma.\end{aligned}$$

The last inequality follows from the inequality for the arithmetic and geometric means, and the same inequality implies that we must have $S = S^*$, $E/E^* = I/I^*$ if $\dot{V} = 0$. Letting $S = S^*$ in the first equation of system (5.3), we obtain $I = I^*$, and thus $E = E^*$. This implies that $\dot{V}$ is negative definite with respect to P^*. This proves the global stability of P^* when it exists.

5.2 In-host Models and Backward Bifurcation

We have seen in previous chapters how mathematical models can be used to describe disease transmission on the scale of an epidemic. We will show in this section that the same modeling approach can also be applied to describe disease processes at a microscopic level, such as the spread of a viral infection among a population of target cells. The resulting models are commonly called *in-host* models. It is interesting to note that, although the in-host models are intended for processes at a very different scale from that of epidemic models, the resulting differential equations are very similar. This allows us to apply the mathematical machinery and our modeling intuitions developed in previous chapters to the analysis of in-host models.

Just as an understanding of infectious disease epidemiology is important for modeling epidemics, a sufficient understanding of cell biology, cell physiology, and immunology is crucial for in-host modeling. It often requires an extensive study of medical literature on the molecular biology and pathogenesis of the infection process we set out to model. A good place to start is often recent review articles on the subject in medical journals.

In this section, we will use the infection of CD_4 T cells by Human T-cell Lymphotropic Virus Type 1 (HTLV-I) as an example. HTLV-I was the first retrovirus linked to human diseases and consequently one of the most studied retroviruses in medical literature. We will show that a 2-dimensional model for HTLV-I infection can demonstrate a very interesting phenomenon of *backward bifurcation*. This presentation is adapted from the publication [19]. For further readings on this topic, we refer the reader to the book of Nowak and May [49] and research papers of the author and his collaborators [20, 37, 39].

At the time this book is written, in-host modeling is one of the most active areas of research in mathematical biology, and there are many opportunities for interdisciplinary collaborations between modelers and medical researchers.

5.2.1 Infection of T Cells by HTLV-I

Human T-cell Lymphotropic Virus Type 1 (HTLV-I) infection is responsible for several diseases such as Adult T-cell Leukemia/Lymphoma (ATL) and HTLV-I Associated Myelopathy (HAM). As a retrovirus, HTLV-I uses a viral protein called reverse transcriptase to synthesize DNA segments (provirus) that integrate into the host DNA. The main target for the viral infection is the $CD4^+$ T-lymphocyte population. HTLV-I shares the same target cells and replication mechanism as Human Immunodeficiency Virus Type 1 (HIV-1), which causes Acquired Immune Deficiency Syndrome (AIDS). There are many differences between HTLV-I and HIV-I. Unlike HIV-1, which can break free from host cells and infect other T cells, cell-free HTLV-I does not trigger infection. Cell-to-cell contact is normally required to transmit the infection between $CD4^+$ T cells. Like other retroviruses, the HTLV-I provirus can also be vertically transmitted to the daughter cells of an infected cell during mitosis.

The proportion of provirus-containing cells in HTLV-I infection is remarkably high; typically between 0.1% and 10% of peripheral blood mononuclear cells harbor HTLV-I provirus. It requires a considerable level of viral replication to obtain such a proviral load. During mitotic division, proviruses in an HTLV-I infected T cell are replicated by the host DNA polymerase and the rate of mutation is very low. In contrast, the action of viral reverse transcriptase is error-prone and accumulates sequence variations rapidly. HTLV-I exhibits an extraordinary genetic stability, while HIV-1 is known to be highly mutative. This apparent discrepancy between a high proviral load and low genetic variability suggests that mitotic transmission may play a crucial role in the persistence of the HTLV-I infection. For more detailed discussions on the biology of the HTLV-I infection and transmission, we refer the reader to selected medical studies [3, 4, 10, 21, 46] and books on modeling viral dynamics [49, 65].

We will derive a mathematical model to describe HTLV-I infection among a population of $CD4^+$ T cells based on biological

assumptions, and investigate the role of mitotic transmission in viral persistence.

5.2.2 An In-host Model for HTLV-I Infection

To model the HTLV-I infection of $CD4^+$ T cells, we partition the $CD4^+$ T-cell population into uninfected and infected classes. Let $x(t)$, $y(t)$ denote the number of uninfected and infected cells at time t, respectively. We assume that the growth of T cells through mitotic division obeys the law of logistic growth, and is described by $\nu_1 x(t)[1-(x(t)+y(t))/K]$, where ν_1 is the growth rate constant and K is the level at which mitotic division of $CD4^+$ T cells stops. Infected cells retain most of the cellular functionalities. Their division is assumed to be similar to that of the uninfected cells: $\nu_2 y(t)[1-(x(t)+y(t))/K]$, with a growth rate constant ν_2. The horizontal transmission of HTLV-I occurs through cell-to-cell contact between infected and uninfected cells. Since we are modeling the infection process in the peripheral blood, where the cells are sufficiently mixed, a bilinear incidence form $\beta x(t)y(t)$ is commonly used, where β is the transmission coefficient. Newly infected $CD4^+$ T cells face a strong immune response by antibodies and cytotoxic lymphocytes. We crudely incorporate the effects of immune responses into the model by assuming that only a fraction σ of cells newly infected by direct contact escape the immune system actions. Here $0 \le \sigma \le 1$. We assume that the body generates $CD4^+$ T cells at a constant rate λ and newly generated cells are uninfected. The removal rate of uninfected $CD4^+$ T cells is a constant μ_1, and may include loss due to natural death and from other sources. The removal rate for infected cells, μ_2, may include loss due to natural causes and immune responses.

The model is described by the following system of differential equations:

$$\begin{aligned} x' &= \lambda + \nu_1 x\left(1-\frac{x+y}{K}\right) - \mu_1 x - \beta xy \\ y' &= \sigma\beta xy + \nu_2 y\left(1-\frac{x+y}{K}\right) - \mu_2 y. \end{aligned} \tag{5.11}$$

Adding the two equations and using $N = x + y$, we obtain

$$(x+y)' \le \lambda + \nu(x+y)\left(1 - \frac{x+y}{K}\right) - \mu(x+y),$$

where $\nu = \max\{\nu_1, \nu_2\}$ and $\mu = \min\{\mu_1, \mu_2\}$. It follows that

$$\limsup_{t\to\infty}(x(t) + y(t)) \le \overline{N},$$

where $N = \overline{N}$ is the positive root of the quadratic equation

$$\lambda + (\nu - \mu)N - \frac{\nu}{K}N^2 = 0.$$

Thus a feasible region for (5.11) is

$$\Gamma = \{(x, y) \in \mathbb{R}^2_+ \mid x + y \le \overline{N}\}. \tag{5.12}$$

It can be shown that Γ is positively invariant with respect to (5.11).

We present a detailed mathematical analysis of the bifurcation and global dynamics of (5.11) in Γ. Since the system is 2-dimensional, the phase-plane analysis in Chapter 3 can be applied for the mathematical analysis. We will use graphical method to demonstrate the occurrence of the backward bifurcation: multiple stable equilibria exist for an open set of parameter values when the basic reproduction number is below one.

5.2.3 Equilibria and Backward Bifurcation

Bifurcation analysis can be done by first examining the changes in the number of equilibria as we vary a model parameter. An equilibrium (x, y) of model (5.11) satisfies

$$\begin{aligned} 0 &= \lambda + \nu_1 x\left(1 - \frac{x+y}{K}\right) - \mu_1 x - \beta xy \\ 0 &= \sigma\beta xy + \nu_2 y\left(1 - \frac{x+y}{K}\right) - \mu_2 y. \end{aligned} \tag{5.13}$$

The *infection-free equilibrium* $P_0 = (x_0, 0)$ exists for all parameter values, where $x_0 > 0$ is the positive root of the polynomial

$$f_1(x) = \lambda + (\nu_1 - \mu_1)x - \frac{\nu_1}{K}x^2. \tag{5.14}$$

A *chronic-infection equilibrium* $\overline{P} = (\overline{x}, \overline{y})$ satisfies (5.13) with $\overline{y} > 0$. From the second equation of (5.13) we obtain

$$\overline{y} = \frac{K}{\nu_2}\left[(\sigma\beta - \frac{\nu_2}{K})\overline{x} + (\nu_2 - \mu_2)\right]. \tag{5.15}$$

Substituting (5.15) into the first equation of (5.13), we conclude that a chronic-infection equilibrium satisfies

$$f_1(\overline{x}) = f_2(\overline{x}),$$

where f_1 is defined in (5.14) and

$$f_2(x) = \frac{1}{\nu_2}\left(\frac{\nu_1}{K} + \beta\right)\left[(\sigma K\beta - \nu_2)\ x + K(\nu_2 - \mu_2)\right]\ x. \tag{5.16}$$

The number of chronic-infection equilibria can be analyzed geometrically by examining intersections of the graphs of f_1 and f_2. System (5.11) can have more than one chronic-infection equilibrium only if f_2 is concave down and has a positive root. This happens if and only if the following condition holds:

$$\sigma K\beta < \nu_2 \quad \text{and} \quad \mu_2 < \nu_2. \tag{5.17}$$

Since our primary interest is to explore the occurrence of backward bifurcation in system (5.11), we will assume condition (5.17) holds throughout the section. Evidence from medical research literature can be used to show that the parameter range defined by (5.17) is biologically sound.

To ensure that the graphs of f_1 and f_2 intersect, we require the following technical condition:

$$(\nu_1 + \beta K)^2 \left(1 - \frac{\mu_2}{\nu_2}\right)^2 > (\nu_1 - \mu_1)^2 + 4\lambda \frac{\nu_1}{K}, \tag{5.18}$$

which is derived from the condition $f_2'(x_0) > f_1'(x_0)$, see Figure 5.2 (d).

Define

$$\sigma_0 = \frac{4\lambda\beta\nu_2^2 - [(\nu_1 - \mu_1)\nu_2 - (\nu_1 + K\beta)(\nu_2 - \mu_2)]^2}{4\lambda\beta\nu_2(\nu_1 + K\beta)} \tag{5.19}$$

and

$$\sigma_c = \frac{\nu_2}{K\beta} - \frac{(\nu_2 - \mu_2)}{\beta x_0}. \tag{5.20}$$

As parameter σ varies, the number of chronic equilibria changes and the changes can be summarized in the following four cases:

(1) If $0 < \sigma < \sigma_0$, the graphs of f_1 and f_2 do not intersect and there is no chronic-infection equilibrium. See Figure 5.2 (a).

(2) If $\sigma = \sigma_0$, the graphs of f_1 and f_2 are tangent and there is a unique chronic-infection equilibrium. See Figure 5.2 (b).

(3) If $\sigma_0 < \sigma < \sigma_c$, there are two chronic-infection equilibria, $P_* = (x_*, y_*)$ and $P^* = (x^*, y^*)$, $x_* < x^*$. These are the two intersections of graphs of f_1 and f_2 in the first quadrant. See Figure 5.2 (c).

(4) If $\sigma \geq \sigma_c$ there is a unique chronic-infection equilibrium $P_* = (x_*, y_*)$ in the feasible region Γ. In this case, graphs of f_1 and f_2 have only one intersection in the first quadrant. The value σ_c is such that $x^* = x_0$. Also the condition (5.18) implies that $|f_1'(x_0)| < |f_2'(x_0)|$ when $\sigma = \sigma_c$, so that the graph of f_2 is above that of f_1 to the left of and close to x_0. See Figure 5.2 (d).

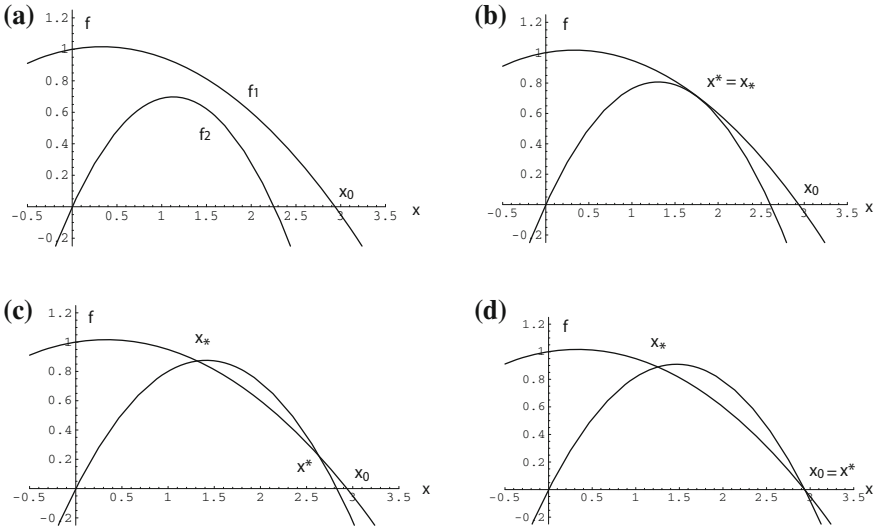

Figure 5.2: A geometric analysis of changes in the number of equilibria as parameter σ is varied. (a) $0 < \sigma < \sigma_0$, (b) $\sigma = \sigma_0$, (c) $\sigma_0 < \sigma < \sigma_c$, and (d) $\sigma \geq \sigma_c$.

Results of the preceding analysis are summarized in the next result. The corresponding bifurcation diagram is shown in Figure 5.3.

Theorem 5.2.1 *System (5.11) always has the infection-free equilibrium $P_0 = (x_0, 0)$. Assume that conditions (5.17) and (5.18) are satisfied. Then the number of chronic-infection equilibria is determined by σ. More specifically,*

(1) *If $0 < \sigma < \sigma_0$, there are no chronic-infection equilibria.*

(2) *If $\sigma = \sigma_0$, there is a unique chronic-infection equilibrium.*

(3) *If $\sigma_0 < \sigma < \sigma_c$, there are two chronic-infection equilibria P_* and P^*.*

(4) *If $\sigma \geq \sigma_c$, there is a unique chronic-infection equilibrium P_*.*

Similar to the basic reproduction number for epidemics, the basic reproduction number for HTLV-I infection is the average number of secondary infections caused by a single infected $CD4^+$

T cell introduced in an entirely susceptible $CD4^+$ T-cell population, over its entire infectious period $1/\mu_2$. For model (5.11), the basic reproduction number $\mathcal{R}_0$ is given as follows:

$$\mathcal{R}_0 = \mathcal{R}_0(\sigma) = \frac{1}{\mu_2}\left[\sigma\beta x_0 + \nu_2\left(1 - \frac{x_0}{K}\right)\right]. \tag{5.21}$$

Here we emphasize the dependence of $\mathcal{R}_0(\sigma)$ on the HTLV-I parameter σ. The first term in the brackets describes the per-unit-time secondary infections through cell-to-cell contact, and the second term those through mitotic division. From its definition, we see that $\mathcal{R}_0(\sigma)$ is an increasing function of σ. Furthermore, $\mathcal{R}_0(\sigma_c) = 1$ by (5.20) and (5.21).

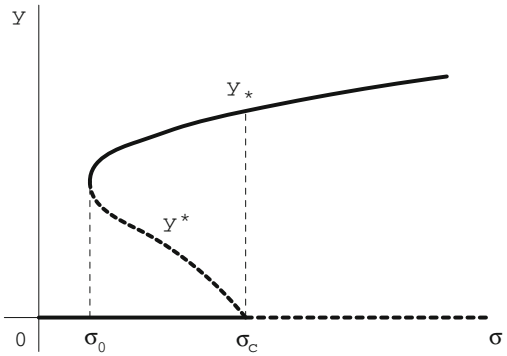

Figure 5.3: Bifurcation diagram for backward bifurcation.

The bifurcation diagram in Figure 5.3 shows the standard features of a *backward bifurcation*: multiple chronic-infection equilibria exist when the basic reproduction number is below unity. Such a bifurcation possesses certain catastrophic behaviors:

(1) When $\mathcal{R}_0$ increases through 1, the number of infected cells has a sudden jump. This may result in a sudden explosion of the infected cell population.

(2) When $\mathcal{R}_0$ decreases through 1, the level of chronic-infection remains high.

This is in sharp contrast to the standard forward bifurcation in virus-host and epidemic models. A serious complication associated with a backward bifurcation is the following: lowering the basic production number $\mathcal{R}_0$ below unity may no longer be a viable control measure, hence different prevention and control measures may have to be considered.

5.2.4 Stability of Equilibria

Proposition 5.2.2 *The infection-free equilibrium $P_0 = (x_0, 0)$ is locally asymptotically stable if $\mathcal{R}_0(\sigma) < 1$ and is unstable if $\mathcal{R}_0(\sigma) > 1$.*

Proof. The Jacobian matrix of (5.11) at $P_0 = (x_0, 0)$ is

$$J(P_0) = \begin{pmatrix} \nu_1\left(1 - \frac{x_0}{K}\right) - \frac{\nu_1 x_0}{K} - \mu_1 & -\frac{\nu_1 x_0}{K} - \beta x_0 \\ 0 & \mu_2(R_0(\sigma) - 1) \end{pmatrix}.$$

One of the eigenvalues is $\nu_1\left(1 - \frac{x_0}{K}\right) - \frac{\nu_1 x_0}{K} - \mu_1 = f_1'(x_0) < 0$, by (5.14) and the graph of f_1. The other is $\mu_2(R_0(\sigma) - 1)$, which has the same sign as $\mathcal{R}_0(\sigma) - 1$. This establishes the proposition.

Proposition 5.2.3

(1) *If $\sigma_0 < \sigma < \sigma_c$, then P_* is locally asymptotically stable whereas P^* is a saddle.*

(2) *If $\sigma > \sigma_c$, then P_* is locally asymptotically stable.*

Proof. The Jacobian matrix $J(\overline{P})$ of (5.11) at a chronic-infection equilibrium point $\overline{P} = (\overline{x}, \overline{y})$ is

$$\begin{pmatrix} \nu_1(1 - \frac{\overline{x}+\overline{y}}{K}) - \frac{\nu_1 \overline{x}}{K} - \mu_1 - \beta\overline{y} & -\frac{\nu_1 \overline{x}}{K} - \beta\overline{x} \\ (\sigma\beta - \frac{\nu_2}{K})\overline{y} & \sigma\beta\overline{x} + \nu_2(1 - \frac{\overline{x}+\overline{y}}{K}) - \frac{\nu_2 \overline{y}}{K} - \mu_2 \end{pmatrix}.$$

By the equilibrium equation (5.13),

$$\begin{aligned} \operatorname{tr} J(\overline{P}) = {} & \nu_1\left(1 - \tfrac{\overline{x}+\overline{y}}{K}\right) - \tfrac{\nu_1 \overline{x}}{K} - \mu_1 - \beta\overline{y} \\ & + \sigma\beta\overline{x} + \nu_2\left(1 - \tfrac{\overline{x}+\overline{y}}{K}\right) - \tfrac{\nu_2 \overline{y}}{K} - \mu_2 = -\tfrac{\lambda}{\overline{x}} - \tfrac{\nu_1 \overline{x}}{K} - \tfrac{\nu_2 \overline{y}}{K} < 0. \end{aligned}$$

Thus $\operatorname{tr} J(\overline{P}) < 0$ for both $\overline{P} = P_*$ and $\overline{P} = P^*$. Also, using the definition of f_1 and f_2 in (5.14) and (5.16), respectively, we obtain

$$\begin{aligned}\det J(\overline{P}) &= \left(f_1'(\overline{x}) - \left(\tfrac{\nu_1}{K} + \beta\right)\overline{y}\right)\left(-\tfrac{\nu_2 \overline{y}}{K}\right) + \left(\tfrac{\nu_1}{K} + \beta\right)\left(\sigma\beta - \tfrac{\nu_2}{K}\right)\overline{x}\overline{y} \\ &= \overline{y}\left[-\tfrac{\nu_2}{K} f_1(\overline{x}) + \tfrac{\nu_2}{K}\left(\tfrac{\nu_1}{K} + \beta\right)\overline{y} + \left(\tfrac{\nu_1}{K} + \beta\right)\left(\sigma\beta - \tfrac{\nu_2}{K}\right)\overline{x}\right] \\ &= \overline{y}\left[\tfrac{\nu_2}{K} f_1'(\overline{x}) + \left(\tfrac{\nu_1}{K} + \beta\right)(\nu_2 - \mu_2) + 2\left(\tfrac{\nu_1}{K} + \beta\right)\left(\sigma\beta - \tfrac{\nu_2}{K}\right)\overline{x}\right] \\ &= \overline{y}\tfrac{\nu_2}{K}\left(f_2'(\overline{x}) - f_1'(\overline{x})\right).\end{aligned}$$

Note that $f_2'(x) - f_1'(x) > 0$ when $x = x_*$ and $f_2'(x) - f_1'(x) < 0$ when $x = x^*$. We know that P_* is locally asymptotically stable whenever it exists, and P^* is a saddle whenever it exists. This establishes Proposition 5.2.3.

The stability properties of equilibria are indicated in the bifurcation diagram in Figure 5.3, where solid lines indicate stable equilibria, and dotted lines indicate unstable equilibria. Note that $\mathcal{R}_0 = \mathcal{R}_0(\sigma)$ increases with σ and $\mathcal{R}_0(\sigma_c) = 1$. Thus $\sigma_0 < \sigma < \sigma_c \iff \mathcal{R}_0(\sigma_0) < \mathcal{R}_0(\sigma) < 1$, and $\sigma > \sigma_c \iff \mathcal{R}_0(\sigma) > 1$. We see that $\mathcal{R}_0(\sigma)$ still behaves as a threshold parameter in that if $\mathcal{R}_0(\sigma) < 1$, the infection-free equilibrium P_0 is stable, whereas if $\mathcal{R}_0(\sigma) > 1$, P_0 becomes unstable and a unique chronic-infection equilibrium P_* is stable. However, the peculiarity of the backward bifurcation as shown in Figure 5.3 is that a stable chronic-infection equilibrium coexists with the stable infection-free equilibrium P_0 when $\mathcal{R}_0(\sigma)$ is in the parameter range $\mathcal{R}_0(\sigma_0) < \mathcal{R}_0(\sigma) < 1$, or equivalently when $\sigma_0 < \sigma < \sigma_c$.

5.2.5 Global Dynamics

The coexisting local attractors P_0 and P^* established by the stability analysis in the previous section and their basins of attraction are further described in the next result, which establishes the global dynamics of (5.11).

Theorem 5.2.4 *Assume that conditions* (5.17) *and* (5.18) *are satisfied. Then*

(1) *When* $0 < \mathcal{R}_0 < \mathcal{R}_0(\sigma_0)$, *the infection-free equilibrium* P_0 *is globally asymptotically stable in* $\overline{\Gamma}$;

(2) *When* $\mathcal{R}_0(\sigma_0) < \mathcal{R}_0 < 1$, *system (5.11) has two attractors in* $\overline{\Gamma}$, *the infection-free equilibrium* P_0 *and the chronic-infection* P_*. *Their basins of attraction in* $\overset{\circ}{\Gamma}$ *are separated by the stable manifolds of the saddle point* P^*;

(3) *When* $\mathcal{R}_0 > 1$, *the unique chronic-infection equilibrium* P_* *is globally asymptotically stable in* $\overset{\circ}{\Gamma}$.

Proof. We first rule out periodic orbits in $\overset{\circ}{\Gamma}$ using Dulac's criteria (Corollary 3.6.6 in Chapter 3). We choose a Dulac multiplier $\alpha(x, y) = 1/xy$. Let $(P(x, y), Q(x, y))$ denote the right-hand side of (5.11). We have

$$\frac{\partial(\alpha P)}{\partial x} + \frac{\partial(\alpha Q)}{\partial y} = -\left(\frac{\lambda}{x^2 y} + \frac{\nu_1}{Ky} + \frac{\nu_2}{Kx}\right) < 0,$$

for all $x > 0, y > 0$. Thus (5.11) has no periodic orbits in $\overline{\Gamma}$. By the Poincaré–Bendixson Theorem (Theorem 3.6.2, Chapter 3), we conclude that all solutions in $\overline{\Gamma}$ converge to a single equilibrium. This establishes the claims in the theorem.

A phase portrait of (5.11) for case (2) of Theorem 5.2.4 is numerically generated using *Mathematica* and shown in Figure 5.4. Three equilibria are marked as dots, with P_0 on the x-axis and P_* sitting between P^* and P_0. The heteroclinic orbits from P_* to P^* and P_0 are clearly identifiable, as are the basin boundaries, which are the stable manifolds of the saddle point P_*. In this case, $\mathcal{R}_0(\sigma) < 1$, but the fate of an initial infection critically depends on the initial conditions. If the initial point lies in the basin of attraction of P_0, then the infection will clear, whereas the infection will persist if the initial point lies in the basin of attraction of P_*. This behavior does not occur in virus-host models that have only forward bifurcation.

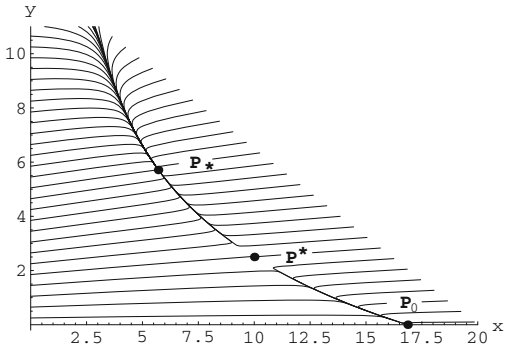

Figure 5.4: Phase portrait showing the coexistence of two stable equilibria when $\mathcal{R}_0(\sigma_0) < \mathcal{R}(\sigma) < 1$.

5.2.6 Simulation Results

We would like to interpret the mathematical results in previous sections in the biological context of HTLV-I infection.

Clinical evidence has led to the hypothesis that HTLV-I infection consists of two steps: a transient phase of reverse transcription and a phase of persistent multiplication of infected $CD4^+$ T cells. When an infected T cell multiplies, proviruses can be passed to the genome of the daughter cells as a form of vertical transmission. This two-step process is proposed as an explanation for the observed high proviral load and low genetic variability in HTLV-I infected T cells [46].

Model (5.11) for the infection of $CD4^+$ T cells by HTLV-I is derived based on the biological assumptions of the two-step process hypothesis. The model incorporates both horizontal transmission through cell-to-cell contact and vertical transmission through mitotic division of infected T cells. We also assume that a fraction σ of the infected cells survives the immune system attack after the error-prone reverse transcription process. The genetic stability of HTLV-I suggests that the fraction σ should be very low ($\sigma \ll 1$). Also, the high proviral load in HTLV-I infection suggests that the rate of mitotic division should be high ($\nu_2 > \mu_2$). The bifurcation diagram of model (5.11) predicts persistent infection for an

extended range of the basic reproduction number $\mathcal{R}_0 > \mathcal{R}_0(\sigma_0)$. This verifies the hypothesis on the two-step process.

What might come as a surprise is that the same bifurcation diagram shows that the model undergoes a backward bifurcation as σ increases: a stable chronic-infection equilibrium P_* exists when the basic reproduction number $\mathcal{R}_0(\sigma)$ is below unity for an open range of parameter values. The global dynamics for the corresponding parameter range show that P_* and the infection-free equilibrium P_0 are coexisting attractors whose basins of attraction partition the feasible region. Even when the basic reproduction number $\mathcal{R}_0(\sigma) < 1$, whether an infection persists or dies out critically depends on if the initial point lies in the basin of attraction of P_* or that of P_0, respectively. This clearly demonstrates that the catastrophic behavior accompanies the backward bifurcation.

Clinical data in the literature can be used to show that the parameter region for backward bifurcation defined by (5.17) and (5.18) is realistic for human HTLV-I infection. According to [50], the human body produces $CD4^+$ T cells at a rate of $\lambda = 25$ cells/mm^3 and $CD4^+$ T cells have a natural death rate $\mu_2 \approx \mu_1 \approx 0.03$ day^{-1}. In the absence of HTLV-I infection, the number of $CD4^+$ T cells is expected to be constant and has a normal value around 1000/mm^3 ([50]), and a carrying capacity constant $K = 1150$/mm^3. This gives us $x_0 \approx 1000$/mm^3, or $f_1(1000) \approx 0$. Using (5.14) we can then estimate the proliferation constant for the $CD4^+$ T cells as $\nu_2 \approx \nu_1 \approx 0.038$ day^{-1}. To get an estimate of β, we use the data in Hoshino et al. [31] on 10 cell lines derived from ATL patients. It was reported in [31] that in a culture of 5×10^6 cells/ml, within 243 days 47% of the total cell population showed significant amounts of retroviral genetic materials. This information allows a rough estimate of $\beta \approx 1.03 \times 10^{-3}$ mm^3/cells/day. One can verify that, with these parameter values, condition (5.18) holds, and condition (5.18) gives a range (0, 0.032) of σ for backward bifurcation to occur. Furthermore, $\sigma_c = 0.024$, $\sigma_0 = 0.00007$, and $\mathcal{R}_(\sigma_0) = 0.169$. Therefore, infection is able to persist at steady state if $\mathcal{R}_0 > 0.169$. Numerical simulations of the model using these parameter values

are carried out using *Mathematica*, see Figure 5.5. The simulations show that persistent infection will produce a proviral load in the range of 10–20%, which is consistent with the clinical data.

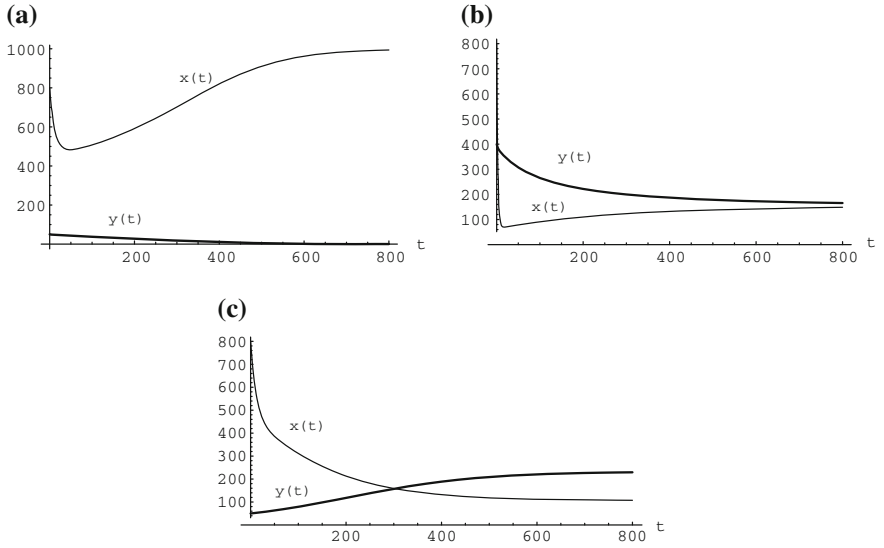

Figure 5.5: Mathematica simulations with parameter values $\mu_1 = \mu_2 = 0.03$, $\nu_1 = \nu_2 = 0.038$, $\lambda = 25$, $K = 1150$, $\beta = 0.00103, x_0 = 1000$. (a) and (b) show that, when $\sigma = 0.015$ and $\mathcal{R}_0 = 0.68$, the fate of the infection depends on the initial condition due to the bistability. (c) shows that, when $\sigma = 0.03$ and $\mathcal{R}_0 = 1.17$, infection persists even when $y(0) = 50$. The persistent infection shows a proviral load level of 16%.

5.2.7 Biological Interpretations

Several biological mechanisms have been shown to lead to backward bifurcation in epidemic models, see [12, 16, 22, 23, 35, 43, 58]. These include imperfect immunity, a vaccine that is leaky, and behavioral responses to perceived disease risk. In many of these models, backward bifurcation occurs due to an asymmetry among different contact groups, multiple routes for transmission,

or density dependence in disease incidence. The results in this section indicate that backward bifurcation can be a byproduct of the two-step process of HTLV-I infection.

In a standard forward bifurcation, when $\mathcal{R}_0$ passes through 1, the level of chronic infection remains low. In contrast, as demonstrated in the bifurcation diagram in Figure 5.3, a backward bifurcation results in the following catastrophic effects:

(1) When $\mathcal{R}_0$ increases through 1, the infected T-cell population may experience a sudden explosion.

(2) When $\mathcal{R}_0$ decreases through 1, the level of chronic-infection remains high.

As a result, the standard infection-control measure of lowering $\mathcal{R}_0$ to below 1 is no longer viable; $\mathcal{R}_0$ needs to be below $\mathcal{R}_0(\sigma_0)$ to achieve infection control, which may be very difficult. Other infection-control measures need to be investigated. Based on our model and analysis, such measures may include:

(1) Lowering the level of chronic infection y_* to safe levels;

(2) Increasing the value $\mathcal{R}_0(\sigma_0)$ to be close to 1, thus reducing the parameter range for backward bifurcation to occur.

(3) Identifying basin of attractions and basin boundaries as shown in Figure 5.4. This may help to design tests to screen for development of chronic infection.

In conclusion, outcomes of modeling studies in this section suggest that backward bifurcation may be intrinsic to HTLV-I infection dynamics.

Bibliography

1. H.I. Abrash, C.M. Gulberg, Studies concerning affinity. J. Chem. Ed. **63**, 1044–1047 (1986)
2. R.M. Anderson, R.M. May, *Infectious Diseases of Humans: Dynamics and Control* (Oxford University Press, Oxford, 1991)
3. C.R.M. Bangham, The immune response to HTLV-I. Curr. Opin. Immunol. **12**, 397–402 (2000)
4. C.R.M. Bangham, S.E. Hall, K.J.M. Jeffery, A.M. Vine, A. Witkover, M.A. Nowak, K. Usuku, M. Osame, Genetic control and dynamics of the cellular immune response to the human T-cell leukemia virus, HTLV-I. Philos. Trans. R. Soc. Lond. B Biol. Sci. **354**, 691–700 (1999)
5. M. Begon, J.L. Harper, C.R. Townsend, *Ecology: Individuals, Populations, and Communities*, 3rd edn. (Blackwell Science, Cambridge, 1996)
6. M. Begon, M. Bennett, R.G. Bowers, N.P. French, S.M. Hazel, J. Turner, A clarification of transmission terms in host-microparasite models: numbers, densities and areas. Epidemiol. Infect. **129**, 147–153 (2002)
7. F. Brauer, C. Castillo-Chavez, *Mathematical Models in Population Biology and Epidemiology* (Springer, New York, 2001)
8. S. Busenberg, K.L. Cooke, *Vertically Transmitted Diseases, Biomathematics*, vol. 23 (Springer, Berlin, 1993)
9. G.J. Butler, P. Waltman, Persistence in dynamical systems. Proc. Am. Math. Soc. **96**, 425–430 (1986)
10. A.J. Cann, I.S.Y. Chen, Human T-cell leukemia virus types I and II, in *Fields Virology*, 3rd edn., ed. by B.N. Fieds, D.M. Knipe, P.M. Howley, et al. (Lippincott-Raven Publishers, Philadelphia, 1996), pp. 1849–1880
11. E.A. Coddington, N. Levinson, *Theory of Ordinary Differential Equations* (McGraw-Hill Education, New York, 1985)
12. R. de Boer, M.Y. Li, Density dependence in disease incidence and its impacts on transmission dynamics. Can. Appl. Math. Q. **19**, 195–218 (2011)

M. Y. Li, *An Introduction to Mathematical Modeling of Infectious Diseases*, Mathematics of Planet Earth 2,
https://doi.org/10.1007/978-3-319-72122-4

13. M.C.M. de Jong, O. Diekmann, H. Heesterbeek, How does transmission of infection depend on population size? in *Epidemic Models: Their Structure and Relation to Data*, ed. by D. Mollison, Publications of the Newton Institute, vol. 5 (Cambridge University, Cambridge, 1995), pp. 84–94
14. O. Diekmann, J.A.P. Heesterbeek, *Mathematical Epidemiology of Infectious Diseases* (Wiley, New York, 2000)
15. O. Diekmann, J.A.P. Heesterbeek, J.A.J. Metz, On the definition and computation of the basic reproduction ratio R_0 in models for infectious diseases in heterogeneous populations. J. Math. Biol. **28**, 365–382 (1990)
16. J. Dushoff, W. Huang, C. Castillo-Chávez, Backwards bifurcations and catastrophe in simple models of fatal diseases. J. Math. Biol. **36**, 227–248 (1998)
17. H.I. Freedman, M.X. Tang, S.G. Ruan, Uniform persistence and flows near a closed positively invariant set. J. Dyn. Differ. Equ. **6**, 583–600 (1994)
18. L.Q. Gao, H.W. Hethcote, Disease transmission models with density dependent demographics. J. Math. Biol. **30**, 717–731 (1992)
19. H. Gomez-Acevedo, M.Y. Li, Backward bifurcation in a model for HTLV-I infection of CD4+ T cells. Bull. Math. Biol. **67**, 101–114 (2005)
20. H. Gomez-Acevedo, M.Y. Li, S. Jacobson, Multi-stability in a model for CTL response to HTLV-I infection and its implications to HAM/TSP development and prevention. Bull. Math. Biol. **72**, 681–696 (2010)
21. C. Grant, K. Barmak, T. Alefantis, J. Yao, S. Jacobson, B. Wigdahl, Human T cell leukemia virus type I and neurologic disease: Events in bone marrow, peripheral blood, and central nervous system during normal immune surveillance and neuroinflammation. J. Cellular Phys. **190**, 133–159 (2002)
22. D. Greenhalgh, O. Diekmann, M.C.M. de Jong, Subcritical endemic steady states in mathematical models for animal infections with incomplete immunity. Math. Biosci. **165**, 1–25 (2000)
23. K.P. Hadeler, P. van den Driessche, Backward bifurcation in epidemic control. Math. Biosci. **146**, 15–35 (1997)
24. J.K. Hale, *Ordinary Differential Equations* (Dover Publications, New York, 2009)
25. P. Hartman, *Ordinary Differential Equations*, Classics in Applied Mathematics, Society for Industrial and Applied Mathematics, 2nd edn. (2002)
26. J.A.P. Heesterbeek, The law of mass-action in epidemiology: a historical perspective, in *Ecological Paradigms Lost: Routes of Theory Change*, ed. by B.E. Beisner, (Elsevier Academic Press, Amsterdam, 2005), pp. 81–104
27. H.W. Hethcote, The mathematics of infectious diseases. SIAM Rev. **42**, 599–653 (2000)

28. M.W. Hirsch, Systems of differential equations which are competitive or cooperative IV: structural stability in three dimensional systems. SIAM J. Math. Anal. **21**, 1225–1234 (1990)
29. J. Hofbauer, J. So, Uniform persistence and repellers for maps. Proc. Am. Math. Soc. **107**, 1137–1142 (1989)
30. C.S. Holling, Some characteristics of simple types of predation and parasitism. Can. Entomol. **91**, 385–398 (1959)
31. H. Hoshino, H. Esumi, M. Miwa, M. Shimoyama, K. Minato, K. Tobinai et al., Establishment and characterization of 10 cell lines derived from patients with adult T-cell leukemia. Proc. Nat. Acad. Sci. USA **80**, 6061–6065 (1983)
32. M. Iannelli, Mathematical Theory of Age-Structured Population Dynamics, Appl. Math. Monogr. C.N.R., vol. 7, Giardini Editori e Stampatori, Pisa (1995)
33. H. Inaba, Threshold and stability results for an age-structured epidemic model. J. Math. Biol. **28**, 411–434 (1990)
34. A. Korobeinikov, P.K. Maini, A Lyapunov function and global properties for SIR and SEIR epidemiological models with nonlinear incidence. Math. Biosci. Eng. **1**, 57–60 (2004)
35. C.M. Kribs-Zaleta, J. Velasco-Hernández, A simple vaccination model with multiple endemic states. Math. Biosci. **164**, 183–201 (2000)
36. A. Lajmanovich, J.A. Yorke, A deterministic model for gonorrhea in a nonhomogeneous population. Math. Biosci **28**, 221–236 (1976)
37. J. Lang, M.Y. Li, Stable and transient periodic oscillations in a mathematical model for CTL response to HTLV-I infection. J. Math. Biol. **65**, 181–199 (2012)
38. J.P. LaSalle, *The Stability of Dynamical Systems*. Regional Conference Series in Applied Mathematics (SIAM, Philadelphia, 1976)
39. M.Y. Li, A. Lim, Modelling the role of tax expression in HTLV-I persistence in vivo. Bull. Math. Biol. **73**, 3008–3029 (2011)
40. Y. Li, J.S. Muldowney, On Bendixson's criterion. J. Differ. Equ. **106**, 27–39 (1994)
41. E.W. Lund, Guldberg and Waage and the law of mass action. J. Chem. Ed. **42**, 548–550 (1965)
42. G. MacDonald, *The Epidemiology and Control of Malaria* (Oxford University Press, London, 1957)
43. M. Martcheva, H.R. Thieme, Progression age enhanced backward bifurcation in an epidemic model with super-infection. J. Math. Biol. **46**, 385–424 (2003)
44. L. Michaelis, M.L. Menten, Die kinetik der invertinwirkung. Biochem. Z **49**, 333–369 (1913)
45. J. Monod, The growth of bacterial cultures. Ann. Rev. Microbiol. **3**, 371–394 (1949)
46. F. Mortreux, A.-S. Gabet, E. Wattel, Molecular and cellular aspects of HTLV-I associated leukemogenesis in vivo. Leukemia **17**, 26–38 (2003)

47. J.S. Muldowney, Compound matrices and ordinary differential equations. Rocky Mountain J. Math. **20**, 857–872 (1990)
48. J.D. Murray, *Mathematical Biology: I. An Introduction*, 3rd edn. (Springer, New York, 2002)
49. M.A. Nowak, R. May, *Virus Dynamics: Mathematical Principles of Immunology and Virology* (Oxford University Press, Oxford, 2001)
50. P.W. Nelson, J.D. Murray, A.S. Perelson, A model of HIV-1 pathogenesis that includes an intracellular delay. Math. Biosci. **163**, 201–215 (2000)
51. L.C. Piccinini, G. Stampacchia, G. Vidossich, *Ordinary Differential Equations in* $\mathbb{R}^n$ (Springer, New York, 1984)
52. R. Ross, *The Prevention of Malaria* (John Murray, London, 1910)
53. H.L. Smith, *Monotone Dynamical Systems, An Introduction to the Theory of Competitive and Cooperative Systems* (American Mathematical Society, Providence, 1995)
54. H.L. Smith, Periodic orbits of competitive and cooperative systems. J. Differ. Equ. **65**, 361–373 (1986)
55. H.L. Smith, P. Waltman, *The Theory of the Chemostat: Dynamics of Microbial Competition* (Cambridge University Press, Cambridge, 1995)
56. H.R. Thieme, Epidemic and demographic interaction in the spread of potentially fatal diseases in growing populations. Math. Biosci. **111**, 99–130 (1992)
57. H.R. Thieme, *Mathematics in Population Biology* (Princeton University Press, Princeton, 2003)
58. P. van den Driessche, J. Watmough, A simple SIS epidemic model with a backward bifurcation. J. Math. Biol. **40**, 525–540 (2000)
59. P. Waage, C.M. Guldberg, *Studies concerning affinity*, Forhandlinger: Videnskabs - Selskabet i Christinia (Norwegian Academy of Science and Letters): 35 (1864)
60. P. Waltman, *Deterministic Threshold Models in the Theory of Epidemics*. Lecture Notes in Biomathematics, vol. 1 (Springer, Berlin, 1974)
61. P. Waltman, A brief survey of persistence, in *Delay Differential Equations and Dynamical Systems*, ed. by S. Busenberg, M. Martelli (Springer, New York, 1991)
62. L. Wang, M.Y. Li, D. Kirschner, Mathematical analysis of the global dynamics of a model for HTLV-I infection and ATL progression. Math. Biosci. **179**, 207–217 (2002)
63. G.F. Webb, *Theory of Age Dependent Population Dynamics* (Marcel Dekker, New York, 1985)
64. P. van den Driessche, J. Watmough, Reproduction numbers and subthreshold endemic equilibria for compartmental models of disease transmission. Math Biosci. **180**, 29–48 (2002)
65. D. Wodarz, M.A. Nowak, C.R.M. Bangham, The dynamics of HTLV-I and the CTL response. Immun. Today **20**, 220–227 (1999)
66. J. Zhou, H.W. Hethcote, Population size dependent incidence in models for diseases without immunity. J. Math. Biol. **32**, 809–834 (1994)

Index

M. Y. Li, *An Introduction to Mathematical Modeling of Infectious Diseases*, Mathematics of Planet Earth 2,
https://doi.org/10.1007/978-3-319-72122-4